1-1-2015

Climate Driven Changes to Malaria Transmission Patterns in Ethiopian Highlands

Amir Said Siraj
University of Denver

CLIMATE DRIVEN CHANGES TO MALARIA TRANSMISSION PATTERNS IN ETHIOPIAN HIGHLANDS

A Dissertation

Presented to

The Faculty of Natural Sciences and Mathematics

University of Denver

In Partial Fulfillment

of the Requirements for the Degree

Doctor of Philosophy

---

by

Amir S. Siraj

August 2015

Advisor: Dr. Paul C. Sutton

Author: Amir S. Siraj
Title: CLIMATE DRIVEN CHANGES TO MALARIA TRANSMISSION PATTERNS IN ETHIOPIAN HIGHLANDS:
Advisor: Dr. Paul C. Sutton
Degree Date: August 2015

ABSTRACT

In the highlands of East Africa, the most populated regions in Africa, temperature is assumed to be intimately connected to the patterns of malaria both in time and space. A large section of the Ethiopian population in this region has historically been shielded from the disease mainly due to the altitudes in the highland regions that have remained free of the disease. However, the region has also seen a large part of its population being affected by malaria in epidemic outbreaks that seem to follow climatic anomalies, especially those of inter-annual increases in temperature. This project examines the inter-annual variability in the distribution of disease incidence over space and explores how changes in these distributions correlate to corresponding climate variability. By using extensive records of disease cases at high spatial resolution, it explores how population at the high end of the disease transmission range is affected by inter-annual climate variability. It further examines factors at play in the persistence of the disease in these low-transmission highland fringes to draw lessons for better targeting of interventions. With lessons learnt from the micro-scale investigations of associations between spread of the disease and generalizable factors, especially climatic factors, the project scales up to the national level to explore the risk of malaria transmission among the Ethiopian population, and how these risks have changed with the observed climatic factors in the last few decades. Finally, it quantifies the potential impacts of climate change on the

spatial spread and intensity of malaria incidence and risks in a country whose population has doubled in the last 30 years.

In chapter two, at a micro-scale and with high resolution disease and climate data, we examine the impact of inter-annual climate variation on the spatial distribution of malaria incidence over time. With the looming climate change in mind, we examine and infer what this could mean for the future. The impact of global warming on insect-borne diseases and on highland malaria in particular remains controversial. Temperature is known to influence transmission intensity through its effects on the population growth of the mosquito vector and on pathogen development within the vector. Spatio-temporal data at a regional scale in the highlands of Ethiopia provide an opportunity to examine how the spatial distribution of the disease changes with the interannual variability of temperature. We provide evidence for an increase in altitude of the malaria distribution in warmer years. This implies that climate change will, without mitigation, result in an increase of the malaria burden in the densely populated highlands of Africa and other regions with similar conditions.

In chapter three, we stay at the same scale as in Paper II, and explore factors that explain the persistence of malaria in this low transmission epidemic prone region. A better understanding of malaria's persistence in highly seasonal environments such as highlands and desert fringes requires identifying the factors behind the spatial and temporal reservoir of the pathogen in the low transmission season. In these 'unstable' malaria regions, such reservoirs play a critical role during the low transmission season by allowing persistence between seasonal outbreaks. In the highlands of East Africa, the

most populated epidemic regions in Africa, temperature is expected to be intimately connected to spatial persistence because of pronounced altitudinal gradients. It is not clear, however, that variation in altitude is in itself sufficient to explain persistence of the disease during the low season, and that other environmental and demographic factors, in particular population density are not also major factors. We address this question with an extensive spatio-temporal data set of confirmed monthly *Plasmodium falciparum* cases from 1995 to 2005 that finely resolves space in an Ethiopian highland. Using a Bayesian approach for parameter estimation and a generalized linear mixed model that includes a spatially-structured random effect, we demonstrate that population density is important to disease persistence during the low transmission season. As malaria risk usually decreases in more urban environments with increased human densities, this counter-intuitive finding identifies novel control targets during the low transmission season in African highlands. It also underscores limitations of current coupled vector-host models of the population dynamics of the disease, which do not typically incorporate an explicit effect of population density.

In chapter four, we scale-up to the national level and explore the use of climate factors to quantify spatially explicit malaria risk for Ethiopia. Climate suitability for malaria transmission has been used to account for Africa's continental distribution of the disease and to estimate the potential effects of climate change. So far, the limited application of the standard suitability index on smaller spatial scales, and the coarse resolution of future climate scenarios, which can overestimate malaria suitability, have hampered adequate estimation of the regional impact of global warming in the highly

populated African highlands. In this chapter we intend to validate the existing African malaria Suitability index for Ethiopian conditions in order to study potential shifts in the epidemiology of malaria with past and predicted warming. With a modified suitability index for Ethiopia, we estimate that since the 1970s 12% of the rural population has become exposed to the disease, and 7% of the rural population who live in areas above 1000m. shifted into the ”stable” malaria category. These figures reflect less than 1 degrees of warming that have occurred between 1975 and 2010. With 2 and 3 degrees of additional warming possible in the 21th century, the proportion of Ethiopia’s population safe from malaria is likely to decrease to 10% and 5% respectively from 31% in the pre-1990 baseline assessment. At the same time, endemic stable malaria is predicted to affect 51% and 64% of the population respectively compared to 22% pre-1990s. With a shifting uphill burden of malaria, epidemic risk will occur in vulnerable populations without previous disease exposure. This risk will materialize in exceptionally warm years that can now be forecasted with reasonable accuracy; epidemic warning and timely intervention should be able to avoid severe morbidity and mortality. However, the populations that are shifted into the stable malaria category due to warming will have to rely on the continuation of assistance that has alleviated Ethiopia’s malaria burden in the last decade, and future scientific progress to improve malaria control and keep ahead of developing drug and insecticide resistance. Despite applying a 50% reduction in malaria caused mortality to account for the reported progress achieved in Africa since 2000, we conservatively estimate that 2521 children and 1646 adults (above 15 years of age) die in Ethiopia each year from warming that has occurred so far. At current levels of

technology, control effort and population in Ethiopia, a 3 degree increase in temperature would result in an eight fold increase in these figures.

ACKNOWLEDGEMENTS

I would foremost like to thank my advisor, Dr. Paul Sutton, for his continual academic support without which this thesis would not have been possible. Paul was always there to answer questions and made timely revisions to my work. I am truly and deeply grateful to Dr. Mercedes Pascual, who has continuously supported, encouraged and nurtured my pursuit of this research. She has remained steadfast and patient in her support and mentoring through my professional challenges. I would also like to thank members of my committee Drs Dale Rothman, Andrew Goetz, and Kristopher Kuzera, for their careful examination of my dissertation draft. In particular, I wish to thank Dr. Rothman for his close follow-up and support. It would not have been possible to complete this dissertation without the encouragement and support of Dr. Menno Bouma. I will never forget the extra miles you went. I would also like to thank Drs. Barry Hughes and Jonathan Moyer and all my co-workers at the Pardee Center for International Futures. I am grateful to Madeline Thomson and Stephen Connor for their encouragement and support. I am indebted to the Oromia Regional Bureau for allowing me to use the malaria data, especially to Damtew, Abiy, Asnakew and all Debre Zeit malaria control staffs. I would like to acknowledge the support of Center for National Health Development in Ethiopia and its Directors Drs. Awash Teklehaimanot; and. Yemene Ye-ebiyo. Finally, I will always be grateful to my father Said Siraj and my mother Mebrat Tikue, my brothers and sisters and their families, for their unreserved support. My wife Semira, for your love and sacrifices in support of my research, I hope I can repay the debt. My sons, Awad and Ayub, have also sacrificed time for my research. I dedicate this dissertation to them.

TABLE OF CONTENTS

LIST OF TABLES

LIST OF FIGURES

CHAPTER ONE: INTRODUCTION

1.1 Background

Malaria is a vector borne disease that occurs when blood is infected with plasmodium parasites through infective *Anopheles* mosquito bites. The disease results from a complex interaction between the parasite, the mosquito vector, the human host and the broader environment (social and ecological). Globally, four species of plasmodium are primarily responsible for malaria morbidity and mortality: *Plasmodium falciparum*, *Plasmodium vivax*, *Plasmodium malariae* and *Plasmodium ovale*, with their spread and significances varied in different regions across the world. *P. falciparum*, which is responsible for the deadly type of malaria, is most prevalent in Sub-Sahara Africa while *P. vivax* is most common in Asia.

The vector is female mosquito of the genus Anopheles. Forty different species of anopheles mosquito are known to transmit the disease. Like in the case of the parasites, the vectors are also diverse in their geographic coverage and their efficiency of transmitting malaria. The African continent hosts several species of anopheles including Anophelus arabiensis, Anophelus funestus, and Anophelus gambiae s.s, the latter known for its affinity to human hosts and associated efficiency in transmitting malaria (Sinka *et al*., 2010; Kiszewski *et al*., 2004).

The parasite's reproductive cycle starts when male and female sexual parasites (gametocytes), ingested by the mosquito during blood meal, meet inside the mosquito's guts and produce fertile eggs (zygotes). The zygotes in turn develop and invade the guts of the mosquito where they further grow, rupture, and release immature parasites (sporozoites) which make their way to the mosquito's salivary glands, causing the mosquito to become infective - capable of transmitting malaria to non-infected persons. This reproductive cycle is termed sporogonic cycle (Clement, 1992). The parasite undergoes further asexual reproduction inside the human host before making a full circle and getting picked up by another mosquito bite. In this last process, the parasite causes a lot of suffering and possibly death to the human host.

1.2 Public health burden

According to the World Health Organization's estimates, 500 million clinical malaria cases and more than a million deaths were reported annually in the early 2000s. Africa, where the deadly *Plasmodium falciparum* is wide spread, is disproportionately affected by malaria, accounting for an estimated 60 to 85 percent of the clinical malaria cases and 90 percent of malaria caused deaths (WHO, 2005; WHO, 2013). Children are particularly affected by the disease with 75 percent of malaria caused deaths occurring among the under five year age group (WHO, 2013). Recent WHO estimates indicate a significantly lower malaria burden, with 37 percent decrease in clinical cases and 47 percent decreases in malaria caused deaths from the year 2000 to 2014 (WHO, 2014).

1.3 Malaria prevention and control

Since the recognition of malaria as a public health priority in the mid-20th century, several interventions that target the transmission of the disease and/ or managing disease cases have been practiced at district, country, regional and global levels. These interventions are broadly classified as (i) vector control including indoor residual spraying of houses with insecticides such as dichlorodiphenyltrichloroethane (DDT) (Najera *et al*., 2011; Mabaso *et al*., 2004; Tanser *et al.,* 2007) (ii) halting or reducing human-vector contacts which include using of insecticide treated bed nets (Lindblade *et al*., 2015; Choi *et al*., 1995) and as a residual effect of improved housing (Lindsay *et al*., 2002; Bradley *et al*., 2013) (iii) treating of malaria cases with chloroquine and other efficacious drugs such as Arthemecinin Combination Therapy (ACT) (Visser *et al.*, 2014) and (iv) vector source reduction through environmental management such are clearing or draining of swamps (Yohannes *et al.*, 2005), and or larviciding (Maheu-Giroux and Castro, 2013).

It has however been recognized that even in regions where the disease has been eliminated, the biological and operational obstacles to maintain the situation are very high (Bruce-Chwatt 1987; Najera *et al*., 2011). Widespread drug (Phillips *et al.*, 1996; Trape, 2001; Murphy *et al*, 1993) and insecticide (Karunaratne and Hemingway, 2001) resistance are among the major challenges facing global public health efforts. In addition, the disease is highly resurgent and a slowdown in the control efforts has been enough to enable the disease's re-emergence often with devastating outcomes (Mendis *et al*., 2009; Sharma & Mehrotra 1986; Mouchet, 1998). Finally, despite many decades of

intense research and development effort, there is currently no commercially available malaria vaccine.

1.4 Malaria and climate

The fact that malaria involves an interaction of three species: the parasite, the vector and the host, has given rise to numerous opportunities for external factors to influence its transmission dynamics. First, the vector's choice of habitat is related to environmental and climatic conditions.

Second, development of the plasmodium parasite inside the vector can be constrained or sped up by the prevailing climatic conditions. In this section, we review scientific evidences on the influence of environmental factors on the different components of the disease transmission dynamics. We explore how these factors affect the dynamics and look at field studies that corroborate these hypotheses.

1.4.1 The vector

Sub-Saharan Africa, the prime region affected by malaria, is inhabited by seven species of anopheles vectors with varying geographic coverage and efficiency[1] of transmitting the disease: *An. arabiensis*, *An. funestus, An. gambiae s.s., An. nili, An. moucheti, An. melas and An. merus* (Sinka *et al.*, 2010, Kiszewski *et al*., 2004). These vector species have varied preferences for breeding habitat and exhibit different feeding behaviors. For instance, among the gambiae sibling species of the *An. gambiae s.s*. and

[1] Vector efficiency is usually expressed in terms of their feeding frequency and their degree to which they prefer to feed on humans (anthropophily) and in domestic settings (endophily)

An. arabiensis - two of the most efficient species, the latter predominates in hotter, drier areas (Kirby and Lindsay, 2004).

Ambient temperature is one of the major extrinsic factors that affect rates of vector growth and development (Clements, 1992). Increasing temperature shortens the generation time of vectors hence increasing the growth rate. The development and survival of the vector occur within a temperature range that is defined by a lower developmental threshold and an upper lethal temperature (Craig *et al.*, 1999). Moreover, while this temperature range varies with species, the rate of growth and development within the range is positively correlated with temperature (Molineaux, 1998, Anderson and May, 1992).

During the vector's immature stage, development rate peaks at around 27°C for *An. gambiae ss* and *An. Arabiensis*, while no adult vector comes out of the immature stage at or below 18°C temperature. At the high end of the temperature limits, immature mosquitoes will not develop into adults when the air temperature is in the range 34-37°C or above (Clements, 1992; Martens *et al.*, 1997; Bayou and Lindsay, 2003; Kirby and Lindsay, 2004).

Anopheles larvae characteristically live at the air/water interface. Larvae of the most prevalent mosquito species in Africa live in fresh, less saline water habitat (Clements, 1992). However, mosquitoes adapt to changes to available water types. For instance, *An. arabiensis* and *An. stephensi* - a vector common in India, have adapted to changes in the type of surface water available in urban areas (Molineaux, 1988). Rainfall

affects the availability of these breeding habitats by creating pools most preferred by the species of *An. arabiensis* and *An. gambiae s.s.* (Molineaux, 1998). At the same time excessive rainfall may cause flooding which could wash out the larvae population in stagnant river pools.

The longevity of mosquito vectors decreases with rising temperature, while it increases with rising relative humidity of the air (Molineaux, 1998). There is also some evidence that humidity affects the rate of digestion in mosquitoes. Observations on several Anopheles species showed that during days of low relative humidity, digestion of blood took longer than during high relative humidity days (Clements, 1992). Another study observed that when relative humidity went below 60%, it shortened the survival of the vector leading to a situation where there was no malaria transmission (Pampana, 1969). However, due to the fact that relative humidity is closely related to temperature it is difficult to prove the specific effect of relative humidity.

1.4.2 The parasite

Four species of plasmodium are primarily responsible for malaria morbidity and mortality: *Plasmodium falciparum*, *Plasmodium vivax*, *Plasmodium malariae* and *Plasmodium ovale*. Many studies have focused on the most prevalent two species: *P. falciparum* – responsible for the deadly type of malaria, and *P. vivax*. *P. falciparum* is the most prevalent species in the African continent, being responsible for 80-90% of cases. While *P. vivax* is common among Asian patients accounting for 70-90% of cases, there are parts of Africa that have significant *P. vivax* cases reported. Ethiopia, the subject of this thesis, attributes about 40% of malaria cases to *P. vivax* (MOH, 2001).

Temperature is among the principal extrinsic factors that affect the length of the sporogonic cycle, the stage during which the parasite develops inside the mosquito gut. As the temperature increases, the length of the sprogonic cycle decreases for a given species of malaria parasite. The sporogonic cycle lasts for 8-9 days at an ambient temperature of 27°C and increases to between 20-30 days as temperature drops to around 20°C (MacDonald, 1957; Detinova, 1962; Pampana, 1969). With adult mosquito's life time limited to about 30 days at most, the length of sporogony is thus key to the probability of a mosquito biting a malaria positive person and ending up being capable of transmitting the disease to healthy individuals.

The duration of sporogony increases exponentially with decreasing environmental temperatures to a point where parasite development ceases. This critical temperature varies by parasite species; for *P. falciparum* laboratory studies have estimated it to be in the range16-19°C (MacDonald, 1957; Detinova, 1962; Craig *et al.*, 1999). Field observations agree with these findings. In India, Gill (1923) observed that a monthly mean temperature of 16.7 °C was required for malaria transmission (Gills, 1923).

In summary, the availability and type of the aquatic habitat, the level of ambient temperature together with relative humidity constitute important limiting factors in the vector population, a key factor in the disease's transmission dynamics. Moreover, for transmission of malaria to occur the ambient temperature levels have to be high enough to make sporogony fast enough for the vector’s lifespan, larval development fast enough to sustain the reproductive process; and not too high or too low so as to threaten the mosquito’s survival. This relationship between the physical environment and the vector

population also suggest that seasonal shifts in ambient temperature and/ or rainfall could either suppress or boost transmission of the disease.

1.5 Epidemiological regions

Several human biological, social, economic and behavioral factors have been identified as contributing to the transmission of malaria. As non-immune humans get infected they begin to acquire some immunity during from their previous infections. This process, when repeated over time, leads to an immune adult population with resilience to the clinical symptoms (Molineaux, 1998). Children and pregnant women are the exceptions who are always at risk of getting disease symptoms.

Such preferential effects of the disease on human population create variations among regions based on the disease's endemicity in those regions. In areas of stable transmission, where parasitamea in the population is stable, immunity is acquired over time. However, the disease still causes a heavy burden of illness and death especially among children and pregnant women. In contrast, in areas of unstable or periodic transmission, the population lacks "herd" immunity and hence will have increased risk among all age groups.

Geographic differences in malaria transmission patterns are usually characterized by the transmission's intensity, frequency and length. Broadly, regions can be defined as: (1) stable – where conditions are always suitable for transmission; (2) seasonal – where conditions become suitable for a short season every year; (3) epidemic – where long-term variation in climate renders conditions suitable for transmission on an irregular basis (with a potential of epidemic malaria); and (4) malaria-free – where conditions are

always unsuitable (Craig *et al*, 1999). These regions correspond to the disease's effect on the population with stable region having its adult population acquiring herd immunity.

1.6 Climate change

The global mean surface temperature has increased by about 0.74^{o}C since 1905. The rate of warming over the last 50 years is almost double that rate of warming over the last 100 years, and this rate is expected to increase in the future (Parry *et al*., 2007). In response to these global changes, the geographic ranges of species are expected to move upward in altitude and through mid-latitude towards the poles. In the current global scenarios warm isotherms will shift pole-wards and vector-borne diseases follow in the same direction (Parry *et al*., 2007).

Consideration of the relationship between climatic factors and malaria transmission also suggests that warmer temperatures are likely to increase favorability for malaria transmission in many cooler and moderately warmer areas. Indeed, several studies have indicated that malaria transmission could shift its geographical area of transmission in response to climate change (Patz *et al*., 2005, Mc Michael *et al.,* 1996). Other statistical models backed by vectorial capacity models demonstrate the potential for it to spread to regions of higher elevations (Martens *et al*., 1997, Martins *et al*., 1995).

Efforts to establish relationships between environmental change and spread of malaria have been marred by uncertainties because (i) the causal links are often indirect, displaced in space and/or time, and dependent on a number of modifying forces (ii) the complexity of the climate system as well as the effect of other non-climate factors on large scale disease patterns; and (iii) the chronic lack of multiple decades of

epidemiological data (Barry *et al*, 2007). However, a great deal could be learned about these causal relationships by examining the past patterns at multiannual and longer time scales, provided data that can resolve small scale differences in both climatic and disease patterns are available.

Projected effects of climate change on malaria transmission relies on understanding the historical associations, where we examine how climate variability or /change have played a role in changing the disease transmission patterns. Such associations, along with projected climate estimates are then used to estimate future health impacts. Studies have provided evidence of the impact of climate variability/ change in last few decades in the East African highland, indicating a warming climate increasing the intensity of malaria transmission (Patz *et al.,* 2002; Zhou, *et al*, 2004; Pascual *et al*., 2006; Chaves and Koenraadt, 2010; Omumbo *et al.*, 2011). This evidence, however has led to a debate with scientists who attributed the observed increases in the intensity of malaria to non-climate factors such as drug- resistance and a slowing down of control efforts (Hay *et al*., 2002a, 2002b). However, this counter argument was criticized for using satellite data that could have biased their analyses (Pascual *et al*., 2006).

One reason for such debates is related to the fact that these two arguments were based on a single location and it was always going to be difficult to disentangle the effect of climate change from all other possible confounders. One way to overcome this problem is to use a process based model that provides a complete representation of all factors at play, which then leads to quantifying the contribution of each factor. Another and perhaps less difficult approach is by looking at several relatively similar locations at

the same time and examining differences not just over time but also over space. For the latter to happen however, there needs to be a record of climate and disease incidence data for several locations at high spatial and temporal resolution and for a period long enough to see long term trends, which unfortunately have been missing for many regions, especially in the African continent.

This thesis aims to fill this scientific gap by utilizing high resolution climate and disease incidence data for more than 150 locations in Ethiopian highlands for over a decade. By assessing historic associations between climate factors and disease incidence, both in time and space, we explore the potential impact future increases in temperature could bring about, assuming similar levels of interventions against the disease. The recent decline in disease burden across Africa and the world is welcome news (WHO, 2013). However, as has happened in the past, these improvements need a concerted effort to sustain them at the current level or better. It is therefore imperative that we are aware of the consequences of not maintaining these high coverage interventions, while also reminding the scientific community and policy makers to work towards providing alternative solutions in the face of the multi-faceted challenges humanity has experienced with the deadly old foe.

1.7 Study area

This thesis studies Ethiopia (see Fig. 1,1) at two scales (i) at a micro scale covering four districts (ii) and at national scale. In this section I provide a succinct introduction to the country, while specific chapters will cover the corresponding study areas they address.

Figure 1.1: Map of Ethiopia and the horn of Africa. Souces: GIS files for country and provincial boundaries from Esri, DeLorme, HERE, MapmyIndia, TomTom, OpenStreetMap contributors, and the GIS user community; for lakes and rivers sources ESRI, NASA, WWF, USGS EROS, Global Runoff Data Centre, GeoNames, Commonwealth of Australia Bureau of Meteorology, USGS, EPA.

1.7.1 Climate

Ethiopia has diverse topography and greatly contrasting climate. The northeastern and southeastern parts of Ethiopia are dry lowlands regions with annual rainfall as low as 250 mm. In contrast, the southwestern parts, which include tropical rainforest, cover a wet and humid region that receives up to 2000 mm in annual

precipitation (NMSA 2001). In general, rainfall decreases northwards and eastwards from the Southwestern peaks, which benefits from its proximity to the Inter-tropical Tropical Convergence Zone (ITCZ) (Korecha, 2013).

Seasonal rainfall in Ethiopia is driven mainly by the migration of the ITCZ. The position of the ITCZ changes over the course of the year, oscillating across the equator from its northern most position over northern Ethiopia in July and August, to its southern most position over southern Kenya in January and February. Three seasons are associated with high rainfall in different parts of Ethiopia: the *Kiremt* (June-September), *Bega* (October-December) and *Belg* (February-May). *Kiremt,* when the ITCZ is in its northernmost position, provides much of the rainfall in the northern half of Ethiopia. The eastern half of Northern Ethiopia has a second rain season during the *Belg*, a less intense and more sporadic rainfall season (see Fig 1.2, A and B).

The southern regions of Ethiopia experience two distinct wet seasons which occur as the ITCZ passes through this more southern position. The *Belg* season is the main rainfall season, followed by the *Bega*, a lesser rainfall season (see Fig 1.2, C).

Studies have divided Ethiopia into different homogenous rainfall regimes. Gissila *et al.* (2004) divided the country into five homogeneous *Kiremt* rainfall zones. Similarly, Diro *et al.* (2010) classified the country into five *Kiremt* rainfall zones but with different boundaries. The difference between these two was primarily due to the number of stations each used (Diro *et al*., 2010). In addition, Diro *et al.* (2008) developed a rainfall regime based on the *Belg* rains which included five regions, again with different

boundaries (Diro *et al*., 2008). In contrast, the National Meteorological Agency (NMA) has been using eight homogeneous rainfall regimes for its forecast (Korecha and Sorteberg, 2013). These variations in the number of homogeneous and locations of rainfall regimes are mainly due to the season they were based on and the temporal disparities in the representation of different geographic regions in the meteorological records the regimes are based on.

A more recent work that applied Principal Component Analysis (PCA) to monthly rainfall data revealed that 67% of the total variance in Ethiopian rainfall is accounted for by three major regimes, which resemble the seasonality based regimes described above (Korecha and Sorteberg, 2013).

In chapter four of this thesis, we use the three broad regimes that have been commonly identified based on their annual cycles (see Fig.1.2) (NMSA, 2013). Figure 1.2 also shows the annual rainfall cycles based on stations data in the three rainfall regimes (our analysis).

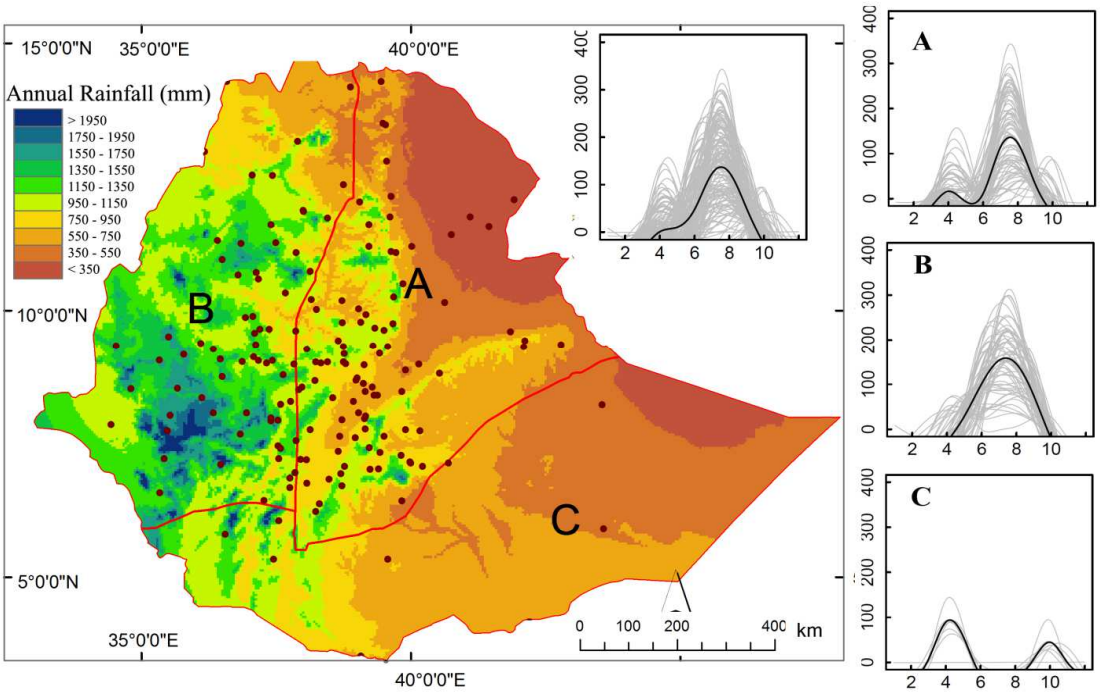

Figure 1.2: Average annual rainfall based on 1961-1990 monthly station data for Ethiopia and its three rainfall regimes. The three major rainfall regimes are outlined in red. Smaller plots on the right show seasonal rainfall patterns for 149 stations in region A, B and C, with regional average (black line). Dots on the map are location of meteorological stations which provided the monthly rainfall, minimum and maximum temperature data for the period 1961-2010. Not all started in 1961. The number of stations reporting data in 1960s, 1970s, 1980s, 1990s and 2000s were 31, 57, 110, 150 and 160 respectively. Source: Rainfall regime boundaries digitized from the World Meteorological Organization website, http://www.wmo.int/pages/prog/wcp/wcdmp/documents/Ethiopia.pdf (accessed Jan 30, 2015)

Regime A, comprising of the central and eastern parts of the country, has two rainy periods: *Belg* and *Kiremt*. This includes large areas in Eastern Oromia, Eastern Amhara, Eastern Tigray and Afar regions of the country. A total population of 55 million (55%) reside in this regime at an estimated density of 116 people per sq. km (our estimate based on GPW3 after calibration using UNPDWPP 2000 data and growth rates).

Regime B, in the western part of the country has a mono-modal rainfall cycle relying on the *Kiremt* rains. This regime includes areas in Western Oromia, Western Amhara, Western Tigray, Northwestern of SSNP, Benishangul Gumuz and Gambela regions. Regime B's population is about 37 million (37% of the national total), distributed at an estimated density of 50 people per sq. km.

Regime C in the south and southeast has two distinct rainy periods: *Belg,* and the shorter *Bega* season. This regime includes most of Somali region, southern Oromia and South SNNP region. At a sparse density of 18 people per sq. km, and with limited rainfall (see Fig. 1.2C), most of the 7.5 million people living in this regime are nomadic and dependent on livestock herding.

Temperature in Ethiopia is greatly associated with altitude although there are seasonal variations in regions. Three broad classifications of regions have been widely used to identify regions by their average temperatures, namely: *Dega* (temperate and cool climate -highlands lying above 2500m.), *Weina dega* (warm- 1500-2500m), and *Kola* (hot and arid type, less than 1500m in altitude) (see Fig. 1.3).

Majority of Ethiopia's 98 million population lives in regions that are categorized as Woina dega (61%) where the average monthly temperature ranges from 15^{o}C to 23^{o}C. Another 15 percent live in areas above 2,500 meters with average monthly temperatures ranging from near freezing to 17^{o}C. The remaining 24 percent live in areas below 1,500 meters where average monthly temperature ranges from 24^{o}C to 34^{o}C (our estimates based on GPW3 and interpolated monthly station data for 1961-1990).

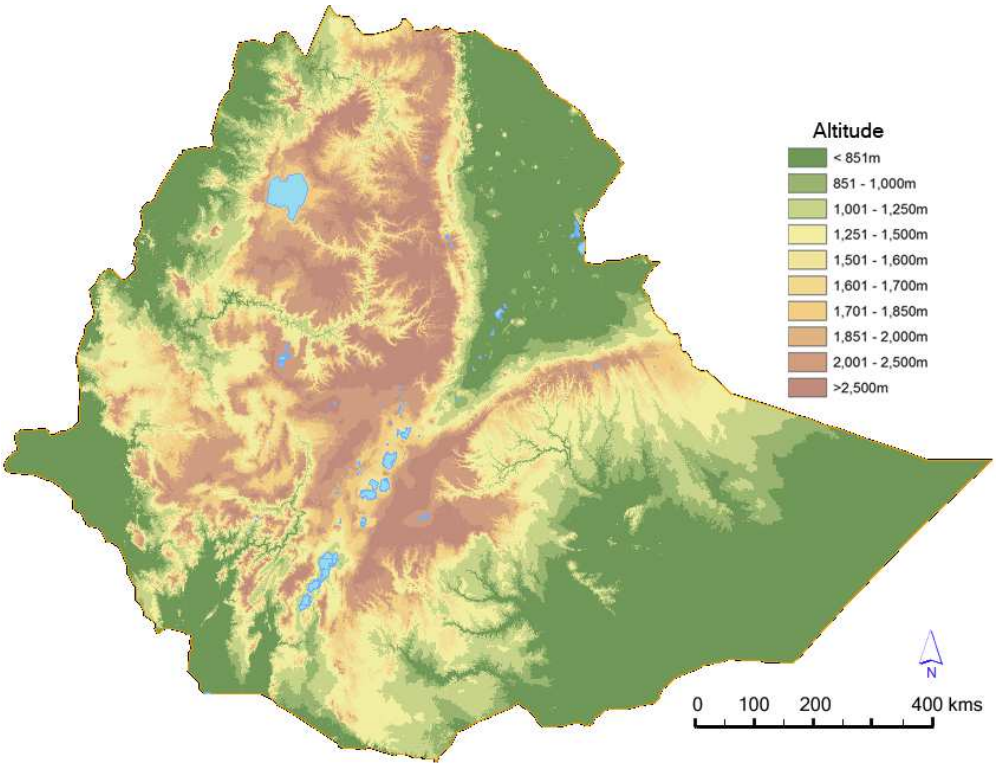

Figure 1.3: Relief map of Ethiopia. Source: Gridded altitude data at a resolution of 30m x30m downloaded from USGS website http://earthexplorer.usgs.gov/ (accessed on 14 March 2011).

A large part of the inter-annual variability of *Kiremt rainfall* is governed by systems related to the ENSO phenomenon. Other secondary forcings acting at the regional level, especially Indian Oceans Sea-Surface Temperatures (SST), play a modulating role (Korecha and Barnston, 2006, Goddard *et al.*, 2001). Overall, dry conditions in *Kiremt* tend to occur during *El Niño* (ENSO Warm Phase), while wet conditions correspond to La Niña (ENSO Cool Phase) years. Time series data of the last four decades confirm a strong El Niño signal in the seasonal precipitation in Ethiopia, though some years had relatively less ENSO influence as a result of other modulating factors in the tropical ocean basins, particularly the Indian Ocean's delayed warming response to the abnormally warm tropical Pacific (Goddard *et al*. 2001).

The *Belg season rainfall* exhibits large annual variability in term of its amount as well as times of onset and secession. *Belg* rainfall weakens when La Nina situations prevail and increases during El Nino situations. In addition, warmer than normal South Western Indian ocean SST, Atlantic ocean SST and Mediterranean SST correspond with better than normal *Belg* rains in Ethiopia (NMSA 2009a).

1.7.2 Malaria in Ethiopia

P. falciparum accounts for 60 percent of malaria cases while *P. vivax* accounts for the remainder (40%). The main malaria vector in Ethiopia is *Anopheles arabiensis (*White, 1980). For the most part, malaria in Ethiopia is more of a seasonal problem, in addition to intermittent epidemics outbreaks. In areas above the altitude of 1500m anomalous climatic conditions are often associated with malaria epidemics (MOH, 1999). Since population in epidemic prone regions has low level of herd immunity, and due to the relatively higher population density in those regions of Ethiopia, epidemic outbreak are often marked with significant higher mortality and morbidity among all age groups. .

Recurrent epidemics have been reported from these densely populated highlands since the 1930s (Melville *et al*. 1945; Corradetti, 1938, 1940). In 1958 many regions in the central highland regions were devastated by an epidemic that caused an estimated three million cases and 150 thousand deaths (Fontain *et al* 1961). Cyclic epidemics of various sizes were reported from highland areas in subsequent years between 1965 and the end of 1980s at a frequency of 5-8 years. In more recent years, widespread and severe epidemics occurred in 1992, 1998 and 2003 (Bosman, 1993; Teklehaimanot, 1999; Negash *et al* 2005). The most recent epidemic in 2003 affected more than three thousand

villages and 200 districts across the country causing more than two million clinical cases and three thousand deaths (Negash *et al* 2005)

1.7.3 The Debre Zeit Sector

When Ethiopia launched its malaria control program in the 1970s, it was organized into sectors that covered about two to five districts each or 75,000 to 150,000 people. Each malaria sector had the responsibility of running a malaria detection and treatment post which collected data on microscopically confirmed cases from self-reporting patients. In addition, sectors managed indoor residual spraying (IRS) operations in their constituent districts. Sector malaria control offices had been set up under a vertical administrative structure before they were decentralized and reorganized under regional administrations of Ethiopia in 1993. Despite these changes, the sector malaria control offices provide examination and treatment services to patients free of charge, as well as carrying out IRS operations, for the entire duration covered by our data.

Initially, four malaria sectors were established in the East Shoa zone, in the central part of the rift valley, at Bishoftu, Metehara, Adama, and Zeway towns (see Fig. 1.4 and Fig. 1.5). Later in 1998 and 2002, two additional health centers in Shashemene and Meki towns respectively were reorganized to carry out malaria detection and treatment services. In all malaria detection and treatment services, blood specimen from patients are spread as smear, stained with Giemsa, and examined under microscope. At the time of data collection, positive cases were treated with Chloroquine for *P. vivax* and Sulfadoxine/pyrimethamine (Fansidar) for *P. falciparum*. Each health facility is managed and run by laboratory technicians specifically trained on malaria detection and treatment.

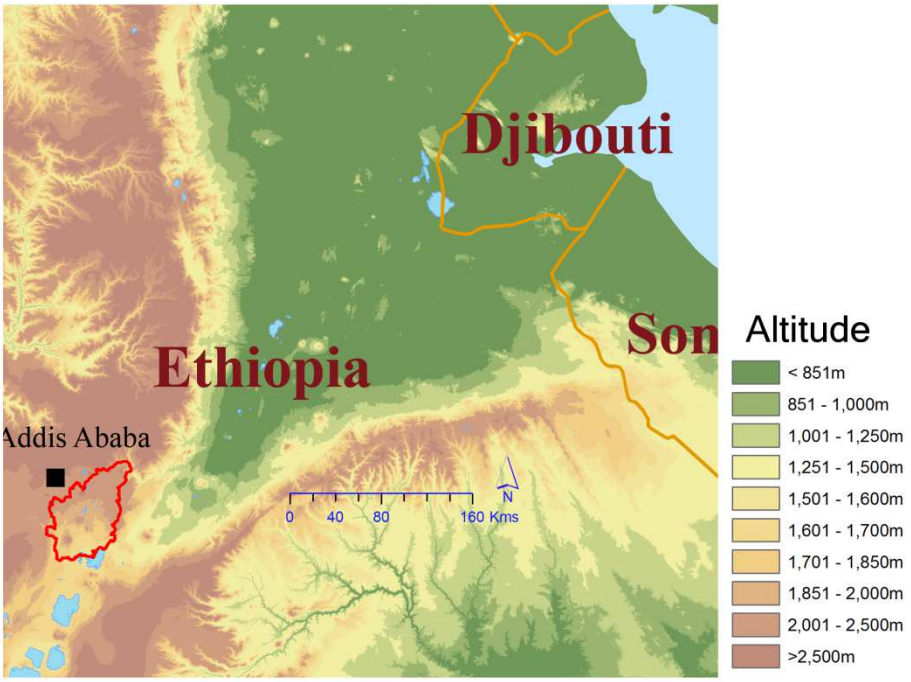

Figure 1.4: Geographic location of the Debre Zeit study area. The Debre Zeit sector in the central part of Ethiopia has an area of 3620 sq. km. Its altitude ranges between 1600m and 2500m. Source: Gridded altitude data downloaded from USGS website http://earthexplorer.usgs.gov/ (accessed on 14 March 2011); lakes from ESRI, NASA, WWF, USGS EROS, Global Runoff Data Centre, GeoNames, Commonwealth of Australia Bureau of Meteorology, USGS, EPA.

Debre Zeit sector, East of the capital city of Addis Ababa, serves four districts in the East Shoa zone, namely, Ad'a Liben Chukala, Gimbichu, Akaki and Lume, and a total population of 572 thousand, of which 75% are rural[2] (2005 estimate based on CSA 1996; CSA, 2008). These districts are further subdivided into smaller administrative units called *kebeles* (n=159). On average, a *kebele* has a population of 3600 population and an area of 23 sq. km, and is further subdivided into one to four sub-units. The sub-units were formerly *kebeles* before a redistricting in the early 1990s that merged many

[2] This section uses the definition of urban used by the Central Statistical Agency (CSA). Accordingly, urban center was defined as a locality with 2,000 or more inhabitants. All administrative capitals (Region, Zone and Wereda), and localities in which urban dwellers' associations were established were also considered as urban centers, irrespective of the population size. (CSA, 1996)

old *kebeles*. Indeed, the 1994 population census of Ethiopia reported population , s at the old *kebeles* (sub-units) level.

The Debre Zeit malaria detection and treatment center is located at Bishoftu town (also called Debre Zeit). Most people in the constituent *kebeles* walk for hours to get to the center for examination and treatment, while a smaller proportion, especially of those from towns outside Bishoftu, uses transportation mean. Half of the patients come from rural areas (51%) usually walking for an average of 14km (one-way aerial distance), while the remaining proportion comes from the five towns (including Bishoftu). The vast majority of cases, however, come from rural *kebeles* (74% for *P. falciparum*).

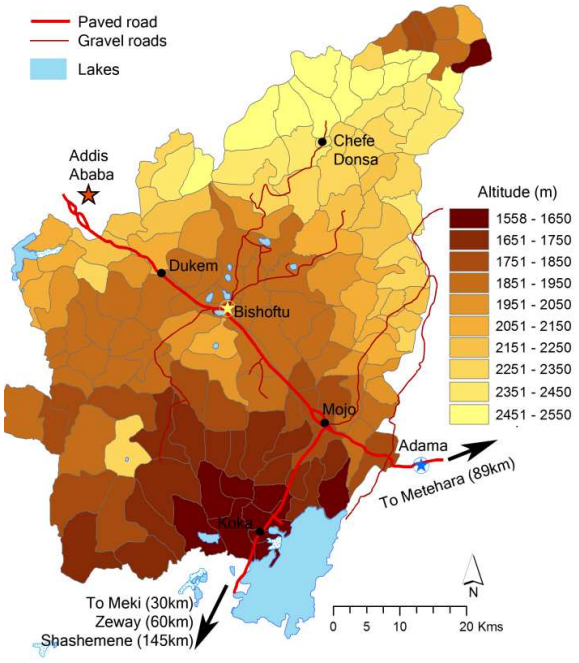

Figure 1.5: Map of *kebeles* and towns in the Debre Zeit study area. *Kebele* boundaries digitized from administrative sketch maps. Source: Lakes from ESRI, NASA, WWF, USGS EROS, Global Runoff Data Centre, GeoNames, Commonwealth of Australia Bureau of Meteorology, USGS, EPA; Roads from ESRI, HERE, DeLorme, USGS, Intermap, iPC, NRCAN, Esri Japan, METI, Esri China (Hong Kong), Esri (Thailand), MapmyIndia, TomTom, OpenStreetMap contributors, and the GIS User Community.

The town of Bishoftu (also called Debre Zeit) accounts for 68 percent the urban population and 68 percent of urban cases, followed by Mojo town which accounts for 20 percent of the urban population and 23 percent of urban cases. Road distance to Debre zeit malaria detection and treatment center for the four towns (outside Bishoftu) ranges from just 11km (Dukem) to 41km (Koka). The most inaccessible town is Chefe Donsa which has a distance of 35km distance from Bishoftu town on gravel roads. The towns of Mojo and Koka might find it closer to Adama malaria detection and treatment center (17km and 36km road distance respectively) than to Bisohftu (22km and 41km road distance respectively).

The Debre Zeit Malaria cases record is organized by *kebeles* on a weekly basis. Patients report their address (district and *kebele*) when registering for blood examination. Daily patient data are then manually summarized at weekly level by *kebele*, number examined, and number of cases by species of malaria. These records cover the period between September 1993 and August 2002. Beginning September 2002, patient data is registered prospectively both on paper and in a computerized registry system the moment patients are registered for examination. The computerized registry and reporting system was designed to help the malaria detection and treatment centers (including those at Shashemene and Meki health centers) to automate their information system and enhance the existing disease surveillance system in the zone. The prospective data registry covers the period between September 2002 and March 2007.

To enable analysis of the weekly surveillance data since 1993, the Oromia Regional Bureau of Health digitized weekly paper records from all four sectors in the

zone (and since 1998 for Shashemene health center). These weekly records were then merged with the prospective data records for the four detection and treatment centers and the two health centers at Shashemene and Meki, to generate a weekly record of *kebele* level species specific cases data.

Once the data from the facilities was compiled into a central repository system, it was aggregated by weeks and *kebeles*. Note that patients living in Debre Zeit sector's districts may have been diagnosed at a neighboring sector's detection and treatment center, though such cases are very few (less than 2% of all cases for Debre Zeit sector). In addition, the regional bureau of health collected data on Geographic Positioning System (GPS) coordinates of approximate central locations (in terms of population distribution) of the old *kebeles* (sub-units). In this study, we use the *kebele* level merged and aggregated cases data for the Debre Zeit sector and sub-unit coordinates along with sub-unit population obtained from the 1994 population census (CSA, 1996).

Beginning 2005, Ethiopia scaled up antimalarial interventions with the approval and free provision of Artemisinin-bases combination therapy (ACT) at malaria detection and treatment posts, and distribution of Long Lasting insecticide-treated nets (LLINs) to household in areas at risk of malaria transmission. To avoid confounding our data with the effect of these interventions, we excluded data after September 2005, a period when the first ACT drugs were used in the zone. All analysis in this project is based on monthly aggregated P.*falciparum* cases disaggregated at *kebele* level.

CHAPTER TWO: ALTITUDINAL CHANGES IN MALARIA INCIDENCE IN HIGHLANDS OF ETHIOPIA

2.1 Introduction

The impact of warming temperatures on highland malaria remains a subject of debate (Hay *et al*., 2002a; Zhou *et al*., 2004; Patz and Olson, 2006; Lindsay and Birley, 1996; Chaves and Koenraadt, 2010; Stern *et al*., 2011; Bouma *et al.*, 2011). Because the etiological agent has a complex life-cycle requiring an insect vector, malaria is a multifactorial disease and the factors that regulate its distribution and abundance are diverse and complex (Molineaux, 1988). Despite the expectation that global warming should lead to an increase in altitudinal range for malaria, empirical evidence for this phenomenon is lacking and the attribution of trends to specific factors remains difficult because of multiple drivers, including drug resistance, land use change, human migrations and access to health facilities (Shanks *et al.*, 2005; Lindblade *et al.*, 2000). Increasing altitudinal range implies the potential for an increased burden of malaria with climate change, especially for countries of East Africa and South America with densely populated highlands, which have historically provided havens from this devastating disease (Pascual and Bouma, 2009). This is because colder temperatures at higher altitude in these tropical latitudes slow down and even halt the development of the parasite inside the mosquito vector, and also because low temperatures decrease the

reproduction and biting rate of the vector, reducing if not preventing transmission (Molineaux, 1988).

In recent decades (1970-2000) pronounced increases in malaria incidence have been documented at several locations in Africa (Hay *et al*., 2002a; Zhou *et al*., 2004; Loevinsohn, 1994) for which long term temporal records exist, and which precede the higher intervention efforts of the past decade (Otten *et al*., 2009). Disease trends, no less than climate warming trends in earlier studies (Pascual *et al*., 2006, Omumbo *et al.*, 2011; Alonso *et al.*, 2011), generate debate (Chaves and Koenraadt, 2010), but what has been missing is an analysis of spatio-temporal records that shift from looking at a single region over time towards examining changes both in space and time. Increasing incidence with altitudinal elevation in warmer years would be a clear signal of the response of highland malaria to changes in climate. Interestingly, although range shifts have been documented with empirical evidence for the distribution of several plant and animal species (Pounds *et al*., 1999; Lenoir *et al.*, 2008), similar patterns in vector-borne illnesses and infection agents of humans remain largely unexplored.

Hence, we looked for evidence of a changing spatial distribution of malaria with varying temperatures for over a decade in highland regions of Central Ethiopia (Fig. 1.4). To do so, we considered temperature variability at interannual time scales rather than long-term trends. Temporal associations between malaria and climate variability have been described for endemic regions of Colombia (Poveda *et al.*, 2001; Bouma and Dye, 1997), and for epidemic regions in highlands of Ethiopia and other East African countries (Zhou *et al.*, 2004; Abeku *et al.*, 2003; Bouma, 2003). Thus, we specifically asked how

temperature variability influences the spatial distribution of disease incidence along altitudinal gradients.

2.2 Data and methods

2.2.1 Description of study sites

The Debre Zeit study area borders the East African Rift Valley and includes parts of the Central highlands in Ethiopia. Its altitude ranges between 1600 meters above sea level (masl) in the South East to 2500 masl in the North Western highlands. The area is epidemic prone although there are pockets reporting cases year round. The main epidemic season occurs from September to December (SOND), following the long rainy seasons from June to August (JJA).

2.2.2 Epidemiological Data

The records consist of monthly *Plasmodium falciparum* cases for 159 administrative units, known as *kebeles*, in the Debre Zeit area from 1993 to 2005 (Fig. 2.2). Ethiopia: data from 159 subunits (*kebeles*) of Debre Zeit sector provided by the government malaria office in Debre Zeit town for the period 1993 to 2007 (see Introduction section). We added cases that were diagnosed in neighboring sectors (less than 2% of all cases). We have excluded malaria data after August 2005 because of the introduction of a new treatment (ACTs) for *P.falciparum* in September 2005, and a significant increase in vector control (indoor residual spraying, IRS) and prevention (Insecticide Treated Bednets, ITNs) in the aftermath of the severe epidemic years (2002-2003) in Ethiopia.

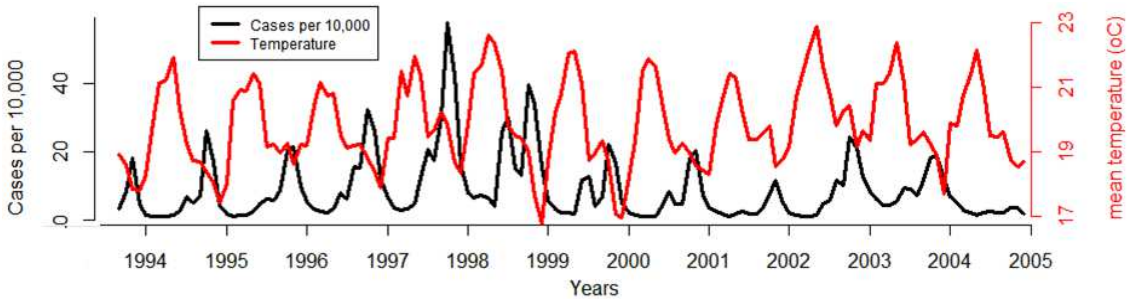

Figure 2.1: Time series of *P falciparum* prevalence obtained by aggregating cases and population data for all locations (black lines) calculated per 10,000 population; and monthly mean temperature records for Debre Zeit for the period between September 1993 and August 2004. A decline in overall cases in the last decade has been observed in other highland regions (Stern *et al.*, 2011) and reflects intensified vector control and the introduction of Artemisinin based Combination Therapy (ACT) for the treatment of *P. falciparum* cases. We show in Fig 2.12A, when we consider the aggregated longer time series (with no spatial information), the recent decline is preceded by an increasing trend in incidence from the 1970s to the end of the 1990s. This increasing trend is not apparent over the shorter time frame of our spatio-temporal analyses. Source: Siraj *et al*., 2014. Altitudinal changes in malaria incidence in highlands of Ethiopia and Colombia. *Science,*343, 1154-1158, fig. S2, A.

In addition to the spatially disaggregated data, we used a longer aggregate time series of monthly *P. falciparum* and *P. vivax* cases beginning in Jan 1980 for the entire Debre Zeit sector in Ethiopia. The pre 1993 monthly aggregated malaria data were reported by the same government malaria center in Debre Zeit, established in the late 1960's to aid Ethiopia's eradication efforts (Tulu, 1996). For compatibility reasons, we subtracted cases between 1993-2005 that were diagnosed in government clinics outside the sector not counted prior to 1993 and we added cases from 4 new clinics (not differentiated by *kebele*) that were opened after 1993 in Debre Zeit town, Mojo and Chefe Donsa.

These longer data sets for Ethiopia were included to examine the consistency of our findings on the changes in the spatial distribution of the disease, with the temporal

increase of cases from the beginning of the 1980s to the end of the 1990s (see below, Comparison of the change in cases for 1^{o}C). The study region is characterized by seasonal transmission with an alternation of non-epidemic and epidemic seasons, the latter taking place from the beginning of September to the end of December in Ethiopia (Fig. 2.2).

2.2.3 Cartographic and demographic data

Altitude data were obtained from the satellite based Advanced Spaceborne Thermal Emission and Reflection Radiometer (ASTER) Global Digital Elevation Model (GDEM) with a resolution of 30m x 30m (USGS, 2011). Population data were obtained from the Ethiopian Central Statistics Agency. In addition, coordinates of rural administrative units within each location in Ethiopia and maps of the locations were obtained from the Oromia Health Bureau. Finally, the altitude for each *kebele* was computed as a population-weighted average across the sub-location level populations (rural administrative units) within each *kebele*.

2.2.4 Climate data

Four meteorological stations in Ethiopia situated in close proximity to the study areas were selected. Monthly averages of daily minimum and maximum temperature data for the stations were obtained from the Ethiopian National Meteorological Agency (NMA). The four climate stations in Ethiopia (namely Addis Ababa (Bole), Addis Ababa (Obs), Adama and Debre Zeit) were selected based on their proximity to Debre Zeit town (within 50 km) and their high correlation with Debre Zeit's station readings. Missing data were filled by the lagged 5 year climatology (average for the same month in the

preceding five years). Data for the four stations were then averaged for the two variables, monthly mean temperature were generated by taking the average of the monthly minimum and maximum temperature.

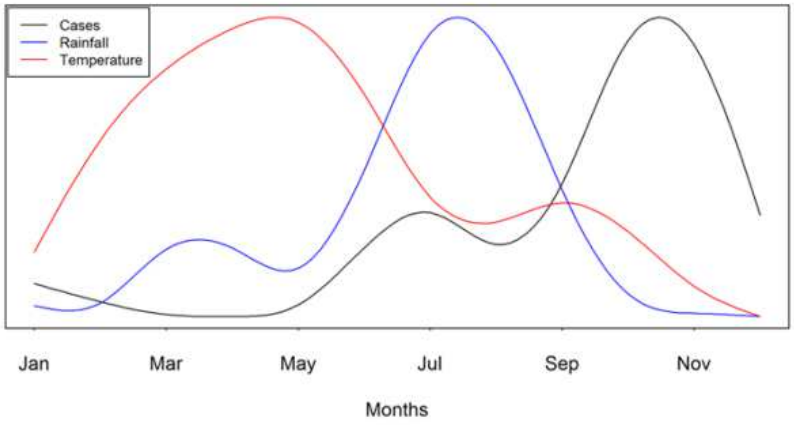

Figure 2.2: Annual cycle for cases (black line), rainfall (blue line) and temperature (red line) for our study area. Source: Siraj *et al*., 2014. Altitudinal changes in malaria incidence in highlands of Ethiopia and Colombia. *Science,*343, 1154-1158, fig. S4, A.

For the purpose of our analyses, we used average temperatures for the four months preceding the epidemic seasons (including a one month overlap with the epidemic season itself), i.e. June to September in Ethiopia (Fig. 2.3). These seasons were selected based on (1) their overlap with the main rainfall season, and (2) preliminary analyses which indicated a maximum lagged correlation between this period and the peak cases months. In the Ethiopian highlands, the significance of temperatures in the preceding 3 months for malaria forecasting purposes has been documented (Bouma, 2003).

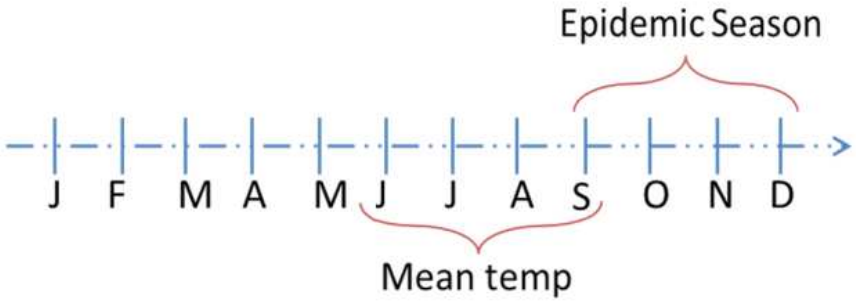

Figure 2.3: Schematic to show the main malaria seasons and the selected windows of time for mean temperatures for Debre Zeit. Source: Siraj *et al*., 2014. Altitudinal changes in malaria incidence in highlands of Ethiopia and Colombia. *Science,*343, 1154-1158, fig. S5, A.

2.2.5 Grouping Method

To identify groups of locations with similar dynamics, we employed a non-parametric Markov transition model in an empirical Bayesian framework (Baskerville *et al*., 2013; Reiner *et al.*, 2012). We used the epidemiological data from 159 *kebeles*. In this method the data is discretized into a set of finite levels. All zeros were put in one level since transition from no cases month to some cases month may involves a significant epidemiological process (invasion) and warrants representation in the Markov process. The remaining data was then divided into observed quantiles of cases per capita; transitions between levels over time are described by a Markov transition matrix (see Table 2.1, eg. Reiner *et al.*, 2012). Locations are assigned to different groups based on Metropolis Hasting Bayesian sampling algorithm (Metropolis *et al*., 1953; Hasting, 1970) and within a group each location's time series is assumed to follow the same transition matrix. Groupings thus have locations with similar dynamics assigned to the same groups. The goal is to identify the grouping that has the highest marginal likelihood of

the Markovian model given the data. Because of the large number of possible groupings, the best groups are inferred via a Markov-chain Monte Carlo method (Baskerville *et al.*, 2013). In this method, the desired number of groups is specified prior to running the algorithm to identify groups with higher marginal likelihood. The transition-matrix rows are assigned a non-informative Jeffrey's prior (Baskerville *et al.*, 2013; Jeffery, 1946).

Table 2.1
An illustrative transition matrix

	month t+1		
month t	**No malaria month**	**Low malaria month**	**High malaria month**
No malaria month	53	12	7
Low malaria month	13	8	8
High malaria month	5	10	27

The figures show the count of transitions from one month to the next based a 144-month long time series (total of 143 transitions per *kebele*)

The resulting three groups were significantly associated with altitude (***ANOVA, $p<<0.01$***), a pattern consistent with the altitudinal variation of disease severity with altitude.

2.2.6 Median analysis

To characterize the spatial distribution of the disease along the altitude gradient, we constructed cumulative distributions of cases for each year in the whole region and normalized these cases by the total cases for that year. Based on these cumulative proportions generated for each year of our study period, we calculated the altitude

corresponding to the median of the cumulative distribution. We refer to this quantity as the 'median altitude'. Finally, we considered the variation of the median altitude in relation to the mean temperatures of the critical window (see Fig. 2.3).

In order to have an estimate of the variance around the median value, we used bootstrap resampling from the set of individual altitude values attached to the location of each time series. We considered 1000 samples generated by resampling with replacement and computed the standard error deviation of the mean median value.

2.2.7 Statistical model

The association between temperature, altitude and malaria incidence was assessed with a regression analysis using a General Linear Model framework (GLM). Although count data, such as cases, are expected to follow a Poisson distribution, it is well established that observed disease cases often display substantial over-dispersion (Lawless, 1987). Preliminary analyses also showed that our monthly cases data exhibits this over-dispersion problem. Thus, we fitted a statistical model assuming a negative binomial distribution of monthly cases.

2.2.8 Selection of covariates

To select which of the explanatory variables are important, a negative binomial GLM with logarithmic link function was fitted to the *P. falciparum* cases with different covariates starting with a model that included all covariates (mean temperature with a 3 month lag, altitude, seasonality and their interactions).

Various models were considered, and comparisons were assisted by model selection algorithms based on the AIC stepwise regression, implemented in the MASS

package in R. A null model included only an intercept α, while a climate model included selected climate covariates x_{it}, where i is a given location and t is the time. We used a regional de-trended monthly mean temperature (x) and a seasonality factor common to all locations (n). We also tested a non-climate model which included only the altitude for each place centered at the average altitude of the meteorological stations (w) and population size (z). The combined model is an extension of the non-climate model, with the addition of the selected climate covariates and their interaction with geographical and temporal covariates. β, γ, δ, ξ, φ, ψ and η denote the regression coefficients.

The best model that emerged from this analysis in both study regions was the combined model with selected interactions among the variables (Eq. 2.2).

$$Y_{it} \sim NegBin(\mu_{it}, \theta) \quad (2.1)$$

$$\log(\mu_{it}) = \log(z_{it}) + \alpha + \beta_{it} w_i + \gamma_{it} x_t + \delta_{it} n_t + \xi_{it} x_t w_i + \varphi_{it} x_t n_t + \psi_i w_i n_t + \eta_{it} x_t w_i n_t \quad (2.2)$$

where Y counts the observed number of cases in a kebele of population z. The observed rate Y/z can then be modeled by using the negative binomial model, with a slight adjustment. Since the expected rate E(Y/z) = μ / z. When we apply logarithm to this expression we get log (μ) – log (z). Adding log (z) to both sizes of the traditional negative binomial model would cause inclusion of the first term in equation 2.4, i.e. log (zit). This term is called offset and its value is known before entering the regression model. The log-link allows comparison of point estimates to the Poisson model. Our model (equation 2.4) uses logarithmic link function and thus we applied exponential function to the

response variable log (μ) to convert it to fitted number of cases, with a dispersion factor θ.

2.3 Results

The importance of altitude to the spatial distribution of the disease was reflected in the typical decrease in malaria with increasing altitude that is expected from a concomitant decrease in temperatures (Fig. 2.4). This classic feature of the epidemiology of malaria was first reported in the 19th century (Hirsch and Creighton, 1883; Laveran, 1893). Furthermore, when we clustered *kebeles* or municipalities on the basis of similar spatio-temporal dynamics, the resulting communities exhibited significant differences in altitude (Fig. 2.5).

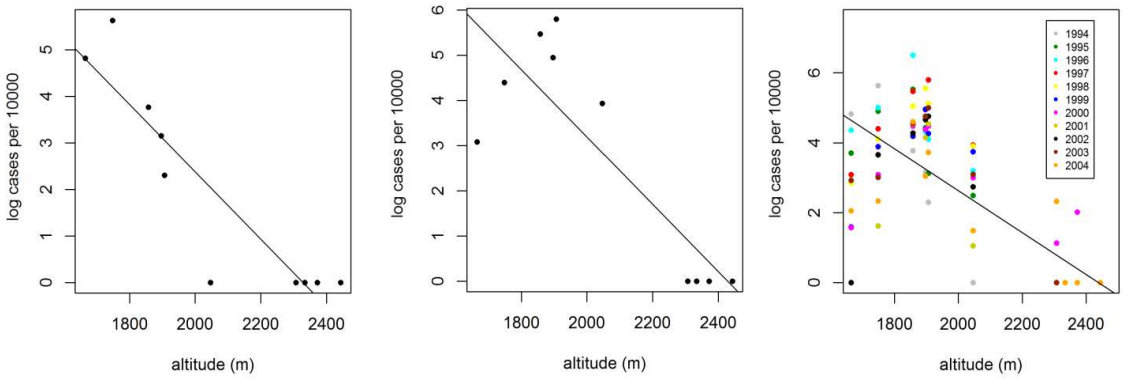

Figure 2.4: Log of cases per 10,000 population by altitude, also called the malaria lapse rate, for Debre Zeit in two different years, and all years combined (far right). The plots show patterns in 1994 (left) and 1997 (middle) with contrasting epidemic levels illustrating that the declining pattern of cases with altitude occurs not just in the overall data set (right) but also in individual years. Source: Siraj *et al*., 2014. Altitudinal changes in malaria incidence in highlands of Ethiopia and Colombia. *Science,*343, 1154-1158, fig. S6, upper panel.

We selected a north-south transect along the altitude gradient for Debre Zeit spanning 10 locations. We then extracted their annual number of cases for the main transmission season and plotted these as a function of their corresponding altitudes (Fig. 2.4). Results show the expected negative slope indicating lower altitude areas have a higher number of cases normalized by population.

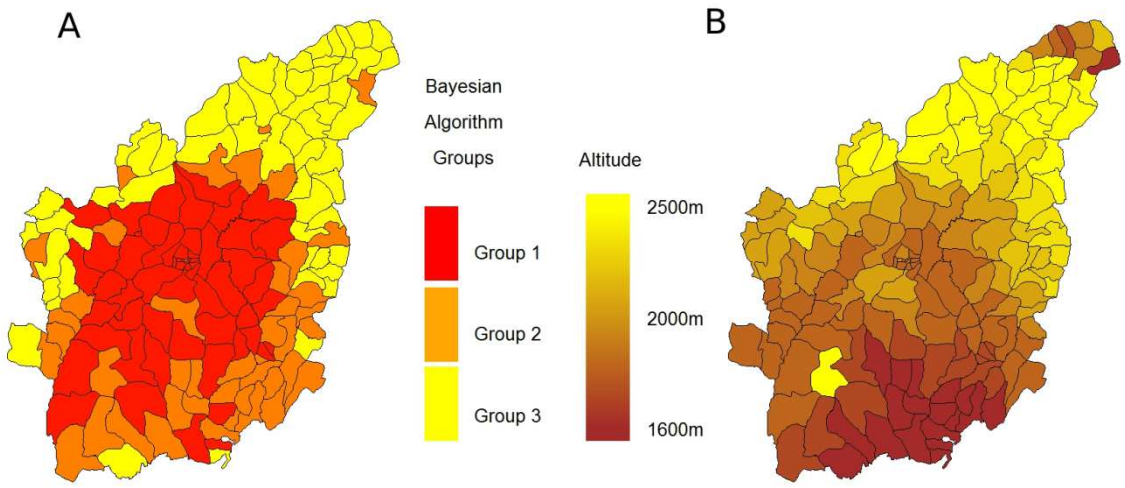

Figure 2.5: Geographic areas based on similar temporal dynamics of malaria cases correspond to different elevations. The first map shows the three different sets of administrative units categorized based on the temporal patterns of monthly cases for the study regions. These sets were obtained with a Bayesian grouping algorithm that identified locations based on similar temporal dynamics using a non-parametric Markov transition model (see section on grouping method). Figures B show corresponding elevation map, with elevation weighted by the population sizes within each location. The identified sets correspond to significant differences in altitude (ANOVA, $p<<0.01$ for A). Source: Siraj *et al*., 2014. Altitudinal changes in malaria incidence in highlands of Ethiopia and Colombia. *Science,*343, 1154-1158, fig. 1, A and B.

Because the absolute number of malaria cases from one year to the next can vary with a number of demographic and environmental factors, and we are interested in the spatial distribution of cases in a way that is independent from temporal variability including trends, we built cumulative distribution curves for yearly cases during the

epidemic season along the elevation gradient. The altitude corresponding to the median of this cumulative distribution is the 'median altitude'. The median altitude changed in time to reflect the movement of the distribution up or down the altitudinal gradient. Figure 2.6 illustrates these patterns for two given years and shows that the median altitude for case distribution changed across years as a function of the average temperature in a critical period preceding the epidemic season (Fig. 2.6, Fig. 2.3). Thus, the median altitude for case distribution increased with mean temperature (Fig. 2.6, B) and malaria cases occurred at higher elevation in warmer years, notably in 1997 and 2002 (Fig. 2.66, C). This phenomenon (Bouma *et al.*, 1994) may be related to above normal global temperatures that accompany El Niño events.

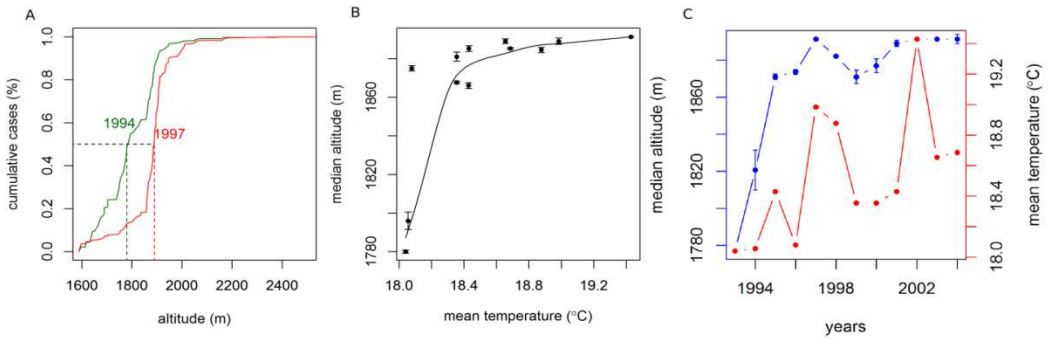

Figure 2.6: Changes in altitudinal distribution of malaria cases with mean temperature across years. Altitudinal cumulative distributions of cases for Debre Zeit are shown as a function of time, as well as mean temperatures preceding the transmission season. The left panels (A) illustrate the altitudinal cumulative curves generated with the incidence data in two given years, together with the location of the 50th percentile and its corresponding altitude. By definition, this is the altitude for which 50% of the cases occur below (and 50%, above) in the altitudinal gradient. A shift of this cumulative curve to the right indicates that more malaria cases have occurred at higher altitudes in a given year. This does not mean the number of cases has increased from 1994 to 1997, but that the distribution of the disease has moved towards a higher elevation. The center panels (B) show the corresponding scatter plots of the median altitude against these temperatures, demonstrating a movement of the distribution to higher altitudes in warmer years for the two highland regions. The right panels (C) show the yearly variation in the median altitude of cases (blue line), together with the mean temperatures in the critical 4-month window (red line) (Fig. 2.3). Uncertainty in the median value is estimated by bootstrap resampling (see median analysis) and is shown as one standard deviation in the plots. Source: Siraj *et al*., 2014. Altitudinal changes in malaria incidence in highlands of Ethiopia and Colombia. *Science,*343, 1154-1158, fig. 2, A, B and C.

In our 'median analysis', we focused on the median of the altitudinal cumulative distribution of cases to examine the elevation expansion in the spatial distribution of the disease. . Here, we show that similar changes, with temperature, have occurred in other quantiles of the cumulative distribution (Fig. 2.7).

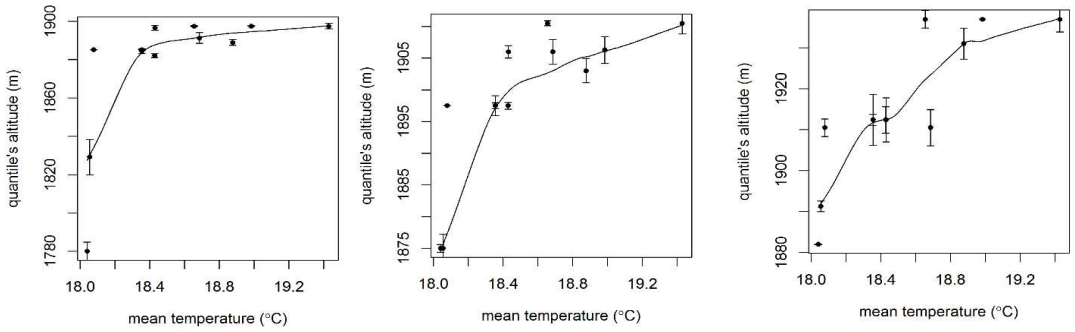

Figure 2.7: Altitudinal cumulative distribution of cases at different quantiles as a function of mean temperature for Debre Zeit. The plots are for quantile values of 60, 75 and 85% (from left to right) and the uncertainty bars correspond to one standard deviation. Source: Siraj *et al*., 2014. Altitudinal changes in malaria incidence in highlands of Ethiopia and Colombia. *Science,*343, 1154-1158, fig. S7, upper panel.

To examine the robustness of our results to a potential bias introduced by control efforts in Ethiopia, we repeated the analysis after excluding all locations in the Debre Zeit area that have experienced indoor residual spraying (IRS) during the study period. Results are similar to those obtained with all *kebeles* included (compare Fig. 2.6, with Fig. 2.8 below).

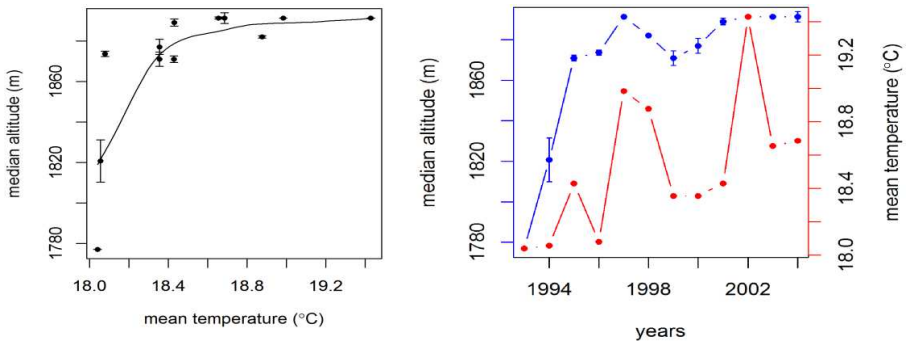

Figure 2.8: Scatter plots of the median altitude of SOND cases against JJAS mean temperatures for Debre Zeit excluding locations that experienced IRS operations during the study period. This demonstrates a movement of the median to higher altitudes in warmer years (left). On the right side is the yearly variation in median altitude of SOND cases (blue), together with JJAS mean temperature variation (red) for locations that experienced no IRS operations during the study period. Source: Siraj *et al*., 2014. Altitudinal changes in malaria incidence in highlands of Ethiopia and Colombia. *Science,*343, 1154-1158, fig. S8.

Based on altitudinal cumulative curves generated for annual cases in the main season, we considered all combination of two-year pairs, and computed the differences in their respective area under the cumulative curve (AUC). This difference allowed us to examine whether the distribution of cases moved towards a higher or lower altitude for positive and negative values respectively. We then considered the linear correlation between these differences and the corresponding mean temperature values (for the critical window), to get a quantitative measure of the AUC difference per given temperature change (Fig. 2.9).

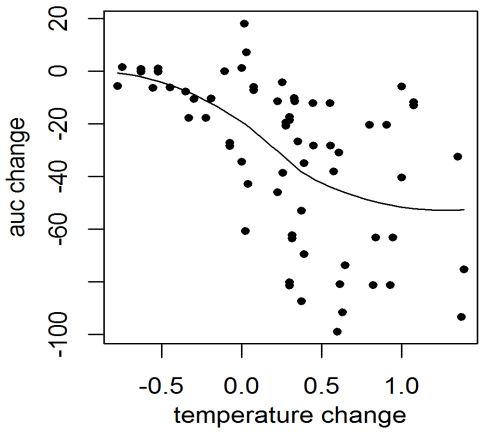

Figure 2.9: Changes in the area under the curve (AUC) for the cumulative distribution between two years as a function of the corresponding changes in mean temperatures in Debre Zeit. In these plots, warming temperatures are associated with a negative change in AUC displaying a shift to the right of the cumulative curve, a pattern representing an expansion upwards in the altitude of affected areas.

To analyze variation in incidence with temperature and altitude, we fitted a negative binomial regression to the monthly cases (see section on selection of covariates). Covariates included seasons, altitude, and linearly de-trended temperature (lagged by 3 months), where the latter represented a regional mean value. Model selection (based on

the Akaike Information Criterion, AIC) was used to compare models with different numbers of covariates and their interactions. The best model included temperature, seasons, and altitude, as well as a mix of the two-way and three-way interactions between these covariates (Table 2.2, Fig. 2.10). More importantly, the best statistical model showed a significant positive effect of mean temperature on the logarithm of malaria cases. This effect corresponded to a percent change in cases between 35 and 64% per 1^{o}C for *kebeles* in Ethiopia at the peak of the malaria season (Fig. 2.11, A).

Table 2.2
Parameter estimates for the negative binomial regression model with log malaria cases the dependent variable.

Covariates	Coefficient (std. error)
(Intercept)	-9.3348 (0.0402)***
Season factor	9.6623 (0.3509)***
Temperature	0.1880 (0.0316)***
Altitude	-0.0037 (0.0001)***
Temperature:Altitude	-0.0002 (0.0001)***
Temperature:Season	0.8437 (0.3919)*
Season:Altitude	-0.0091 (0.0010)***

***: significant at 0.001; ** significant at 0.01; * significant at 0.05
Source: Adapted from Siraj *et al*., 2014. Altitudinal changes in malaria incidence in highlands of Ethiopia and Colombia. *Science,* 343, table 2.

We used the statistical models to estimate rates of change in the response variable (log number of cases) for an increase in temperature of 1^{o}C, with all other explanatory variables set to constant values and for the different mean altitudes of the different administrative units (Fig. 2.11, A).

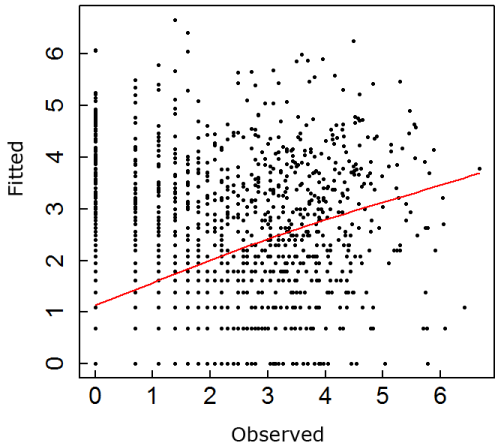

Figure 2.10: Observed versus fitted log cases for SOND based on the statistical model. The red curve is a local regression smoothing (Loess) curve.

To estimate the change in the number of cases associated with a given change in temperature, we considered a window of altitudinal range corresponding to locations associated with the long time series. Thus, for the overall Debre Zeit region, this included all locations in the study area. For each cumulative curve (representing cases in the main transmission season for one year), we computed the fraction of the distribution falling within the relevant altitudinal range, and converted this fraction to number of cases. We then considered all possible pairs of years and computed the corresponding differences in the number of cases within the altitudinal range of interest, as well as the differences in the corresponding temperatures within the critical window (Fig. 2.11, B). Results show an increase of 2600 cases in the epidemic seasons per 1^{o}C increase in temperature for the Debre Zeit region.

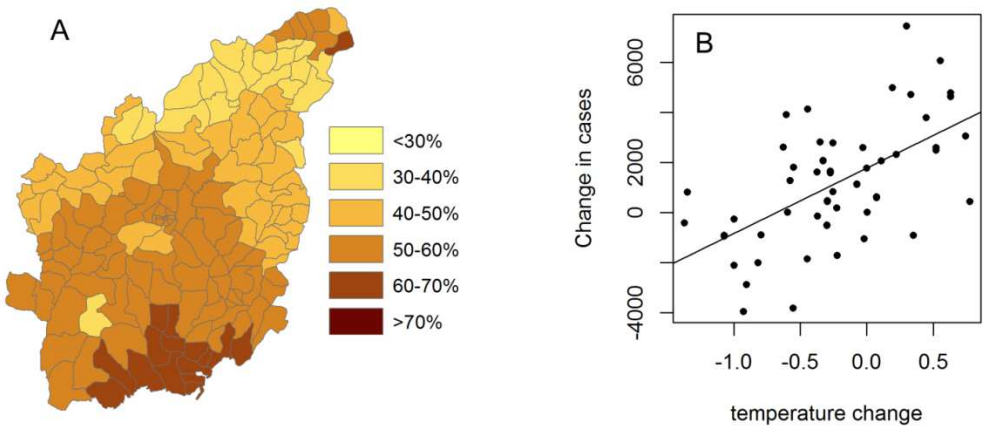

Figure 2.11: (A) Percent increase in number of cases at the peak season per 1°C increase in mean temperature in the critical window (JJAS). The plots include the effect of altitude and its interactions with temperature and seasonal effects- see regression model in equations (2.1) and (2.2); (B) Changes in the number of cases for the entire region and the corresponding changes in temperature for the critical window (JJAS) computed for all pairs of years. Source: Siraj *et al*., 2014. Altitudinal changes in malaria incidence in highlands of Ethiopia and Colombia. *Science,*343, 1154-1158, fig. S10,A and S11, A.

For the long time series of monthly *P. falciparum cases* and mean temperatures, we observed an increasing trend from 1980 to 1999 (Fig. 2.12). We estimated a general rate of increase by fitting a linear regression for cases as a function of time, as well as temperature as a function of time. This resulted in a temperature rate of 1°C for 378 months, and a corresponding increase in cases of 2310 for the main transmission season of SOND in Debre Zeit.

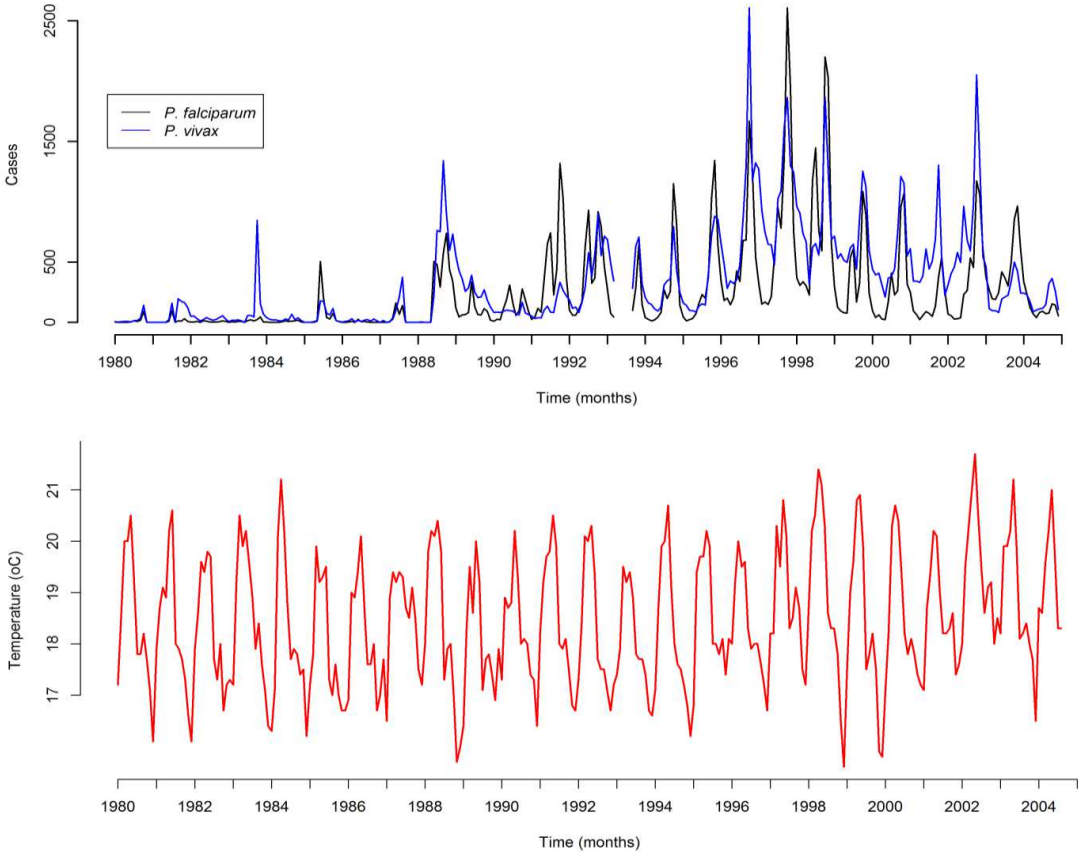

Figure 2.12: Temporal trends in temperature and malaria cases for the whole region of Debre Zeit (Ethiopia). The malaria cases for *P. falciparum* and *P. vivax* (top panel) are shown with the corresponding mean temperatures (bottom panel). Both *P falciparum* and *P. vivax* cases exhibit an increasing trend from the 1980s to the end of the 1990s. So does mean temperature at 1ºC in 378 months (estimated as a linear trend). An increase of 1ºC corresponds to an additional 2166 cases during the main transmission season (from September to December). This malaria increase over time is consistent with what is expected from the trend in temperature, given the described change in the altitudinal distribution of cases with the interannual variation of temperature over a shorter time period (Fig. 2.11, B). Source: Siraj *et al*., 2014. Altitudinal changes in malaria incidence in highlands of Ethiopia and Colombia. *Science,*343, 1154-1158, fig. 3.

2.4 Discussion

Our results showed that in this highland region increases in temperature across years extended the spatial distribution of malaria cases to higher elevations. The

implication is that global warming will increase the risk of contracting highland malaria in the future. The rapid climate variations associated with the pronounced topographic changes of highlands are poorly, if at all, captured by the coarse resolution of Global Circulation Models and their future projections (Price, 1994), and the intricacies of mountain climates may complicate local climate change predictions. Moreover, highlands tend to be poorly covered by the global network of meteorological stations (Barry, 1992). However, because of the potential attribution of rising malaria to warming, station temperature records in East African highlands have received much attention (Hay *et al.*, 2002a; Pascual *et al.*, 2006; Omumbo *et al.*, 2011). In particular, for the Debre Zeit station, significant trends in rising day and night time temperatures are uncontroversial (Hay *et al*., 2002b).

The spread of chloroquine resistance has been proposed as the main reason behind the increasing trends in malaria time series in the Kenyan highlands (Shanks *et al*., 2005). Interestingly, our retrospective data sets can be extended backwards in time to the early 1980s (albeit with no spatially explicit information) for the whole aggregated region of Debre Zeit in Ethiopia, and for both parasites, *P. falciparum* and *P. vivax* (Fig. 2.12). Although drug resistance to chloroquine almost exclusively applies to *P. falciparum*, also in the Debre Zeit region (Tulu *et al.*, 1996), the longer time series of cases show similarly increasing trends from the 1980s to the 1990s for both parasites. This increase occurred before the intensification of vector control and treatment of the past decade led to lower incidence (Otten *et al.*, 2009).

Climate change appears to have already influenced the burden of malaria in these regions. Specifically, the trend for malaria in Ethiopia since the 1980s (Fig. 2.12) is consistent with the rate of change we would expect from the inter-annual variation in the spatiotemporal data (Fig. 2.11, B). This expected change is approximately 2160 cases per degree Celsius over a season (September to December), and the value obtained from fitting linear trends to both the P. *falciparum* and temperature time series is of similar magnitude: 2310 cases. This means that the change expected from increasing temperatures alone can account for the retrospective temporal trend in cases observed in the recent past at both locations.

It has been argued that the effect of climate change on malaria globally will be negligible compared with the potential impact of intervention and improved socio-economic conditions (Gething *et al.*, 2010). However, in the East African highlands a strong temperature determined malaria lapse-rate persists (Bouma *et al.*, 2011). Importantly, a higher potential transmission intensity, driven by warmer temperatures, will require even greater control efforts, especially in countries such as Ethiopia with large populations at high elevation. In the altitude range of the Debre Zeit sector, between 1600 and 2400 m, approximately 37 million people live in rural areas at risk of malaria, which corresponds to 43% of Ethiopia's total population. Based on Ethiopia's current population size and the malaria lapse rate from pre-control mass survey prevalence data since the 1930s (Cox *et al*., 1999), we had previously estimated that a one degree rise in temperature would result, without mitigation, in an additional 410,000 infections per year due to malaria's territorial extension (Pascual and Bouma, 2009). An additional 2.8

million annual infections would occur in the population below the age of fifteen at altitudes where the disease would intensify, and where adults would have a degree of immunity (Pascual and Bouma, 2011). These estimates were based on the assumption of a temperature-dependent shift of the disease to higher altitudes (Lindsay and Martens, 1998; McCarthy *et al.*, 2001). By supporting this assumption, our findings here underscore the size of the problem and emphasize the need for sustained intervention efforts in these regions, especially in Africa where more highly anthropophylic vectors preclude extrapolation from the earlier and easier victories against malaria in latitudinal fringes of temperate climates (Bouma *et al.*, 2011).

Fortunately, the control of malaria at the edge of its altitudinal distribution is considerably easier than in highly endemic, lower-elevation regions. Despite Africa's exceptionally efficient vectors, an early eradication pilot scheme in highland regions shows that malaria transmission at altitudes in excess of 1130 m (3700 feet) can be fully interrupted (de Zulueta *et al.*, 1961). Public health policies should therefore be formulated that mitigate the effects of climate change on malaria in highland regions, including those policies that extend and sustain the network of diagnostic and monitoring facilities. These measures should further contribute to the early warning of epidemics and assist global malaria elimination.

CHAPTER THREE: THE ROLE OF TEMPERATURE AND POPULATION DENSITY IN THE PERSISTENCE OF HIGHLAND MALARIA

3.1 Introduction

Highland regions in East Africa are located at the edge of malaria's transmission range due to seasonal rainfall patterns and low average temperatures, which limit the development of the parasite and the abundance of the mosquito vector (MacDonald, 1957; Detinova 1962). In these regions of epidemiological transition, disease transmission is generally low, but exhibits intermittent seasonal outbreaks with high mortality and morbidity among large populations with low herd-immunity. Given that climate variables set the limits to the spatial distribution of the disease, changes in temperature and rainfall are expected to have clear, direct effects on malaria transmission in these regions (Lindsay and Martens, 1998). In particular, it has recently been shown that inter-annual variation in average temperatures can significantly expand and contract the spatial distribution of the disease following the main rainfall season, with implications for the impact of decadal warming trends (Siraj *et al*., 2014).

Spatial variation in incidence is also important at the seasonal scale in relation to the persistence of the disease during inter-epidemic periods when transmission is at its lowest. A better understanding of the spatial regions that act as spatio-temporal reservoirs of the pathogen is ultimately important to elimination strategies. Altitude, through its well know relation to temperature, is expected to influence spatial patterns of

persistence at regional levels. A dynamical understanding of persistence would require, however, consideration of spatial variation in demographic and environmental factors other than temperature at sufficiently high spatial and temporal resolution. Although among demographic factors, human mobility has recently attracted attention (Buckee *et al*., 2013, Stoddard *et al*., 2013; Tatem *et al*., 2014; Yukich *et al*., 2013; Alemu *et al*. 2014), the role of population density remains poorly understood in the population dynamics of malaria and other vector-transmitted diseases. In particular, host population size in mathematical models generally introduces a dilution effect by which larger numbers of hosts dilute the number of vector bites and in so doing also decrease transmission rates (Dobson, 2004). In only a few zoonotic pathogens, namely hantavirus and lymphocytic choriomeningitis virus, positive associations have been reported between host population density and infection prevalence (Mills *et al*., 1999; Tagliapietra *et al*., 2009). Despite the large spatial variations in population density and associated socio-economic conditions, the question of whether and how these factors interact with temperature to maintain disease transmission remains open. The fast population growth in highlands of East Africa makes questions on population density particularly pressing.

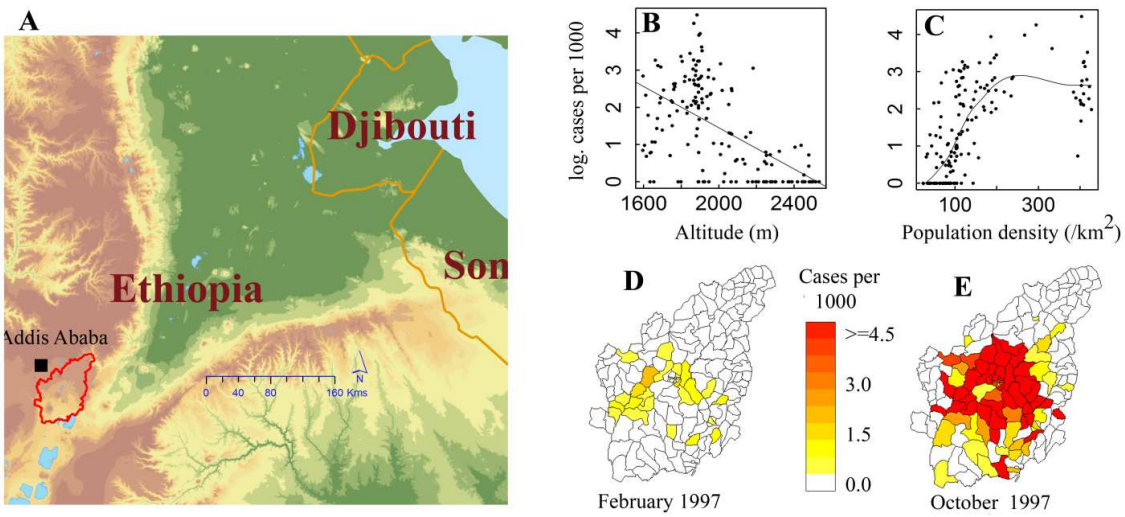

Figure 3.1: Location of study area (A), Log of number of *P. falciparum* cases per 1000 population in the low transmission season by altitude of *kebele* (B) and by population density of *kebele* (C). Illustration comparing the number of cases per 1000 population in two contrasting years - for the low (D) and high season (E). Source: Siraj *et al.*, 2015. Temperature and population density determine reservoir regions of spatial persistence in highland malaria. Submitted to *The Proceedings of the Royal Society – B*, fig. 1

By combining an extensive eleven-year long record of monthly cases of exceptional spatial resolution and a spatially-explicit statistical approach, we examine here the effects of demographic factors in concert with temperature. We specifically consider the influence of population density on malaria's variability during the low transmission season, as well as that of access to roads, as a main factor in human mobility. We also consider other environmental factors that could confound our results by affecting soil water content and moisture retention of relevance to the availability of breeding habitats for mosquitoes. These factors include land slopes, water holding capacity of the soils and their interactions, as well as proximity to perennial surface water bodies, since dams and rivers have been shown to provide breeding sites during the dry season when surface water availability is low (Ghebreyesus *et al*., 1999; Mouchet *et al*.,

1996). Our analyses identify population density, in addition to temperature, as having a significant role in the spatial distribution of disease incidence during seasonal troughs. This effect of population density is missing from current dynamical models of malaria transmission, despite its potential relevance to control efforts, which we discuss.

3.2 Material and methods

3.2.1 Epidemiological data

A monthly time series of *Plasmodium falciparum* cases confirmed through microscopy examination of blood slides from clinical (febrile) individuals is used in this study. The data is from 159 subunits (*kebeles*) surrounding the Debre Zeit sector, collected at the malaria examination and treatment center in Bishoftu town for the period from September 1993 to February 2007. We have excluded malaria data after August 2005 because of the introduction of a new treatment (ACTs) for *P. falciparum* in September 2005 in the aftermath of the severe epidemic years (2002-2004) in Ethiopia. In order to look at the dynamics at the seasonal level, we aggregated the monthly data for each *kebele* into four month seasonal blocks of January-March (JFMA), May-August (MJJA), September-December (SOND), representing the low, intermediate and high transmission seasons, for a total of 11 data points per *kebele* for each of JFMA, MJJA and SOND seasons.

3.2.2 Demographic and cartographic data

Each of the 159 *kebele* further encompasses up to 4 smaller administrative sub-units for which population data were obtained from the Central Statistical Agency of Ethiopia for 1994 and 2007 (CSA 1996, 2008). We interpolated these population data

temporally based on growth rates between the two censuses conducted in 1994 and 2007, separately considering changes in urban and rural populations at the district level. Spatial coordinates for these sub-units were obtained from the Oromia regional Bureau of Health. These coordinates, along with the population data, were used to weight all spatially explicit variables and obtain population weighted estimates aggregated at the *kebele* level.

We obtained digital elevation model (DEM) data at a 30-meters resolution from the Global Earth portal managed by United States Geological Survey (USGS 2011). By using ArcGIS software tools, we generated gridded slope from the high resolution DEM. For better data manageability, we resampled the high resolution DEM, averaged at a 0.5-arc-minutes resolution. Finally, we overlaid locations of our administrative sub-units on the DEM and slope gridded surfaces to obtain estimates for altitude and slope respectively at the sub-unit level.

As a measure of human mobility, we considered distance to roads adjusted for the type of roads, based on the notion that some surfaces are more difficult and costly to traverse than others. Thus, to account for differences in accessibility due to the type of roads, distances to gravel roads were multiplied by 1.5 when compared to alternative routes connecting to paved roads. After estimating the shortest distance to roads for each administrative sub-unit, population weighted aggregates were generated at *kebele* level.

3.2.3 Population density

Having spatially located the center of each of the 432 sub-unit in our study area along with their projected population sizes, we used this high resolution data to generate

our own estimate of population density. We drew circles of 5km radii around each sub-unit and summed the population that fell within each of these circles, giving the population in a buffer of 5km around each sub-unit. We divided the total population of each buffer by the area of the circle (~74.54sq. km for a circle of 5km radius) to generate an estimate of population density (population per square km). We finally averaged the sub-unit level population densities inside a *kebele* to aggregate them at the *kebele* level. We repeated the steps for a buffer size of 10km to generate a second measure of population density.

Note that the circles we drew around sub-units, for which population was summed, could overlap, and as could the population densities themselves. As such, our population density estimates cannot be multiplied by the area size to get the total population of a sub-unit or kebele, as is the usual case. This is a departure from the common method of generating population density where regions are subdivided before the population is aggregated within each region, and not across regions. Since the objective our estimating population density is to account for proximity of human to one another in the context of disease transmission, we assert that our method a more accurate account.

3.2.4 Climate Data

Daily readings of minimum and maximum temperature for Ethiopian stations were obtained from the National Meteorological Agency (NMA). Four meteorological stations in Ethiopia situated in close proximity to the study areas (namely Addis Ababa (Bole), Addis Ababa (Obs), Adama and Debre Zeit) were selected based on their

proximity to Bisoftu/ Debre Zeit town and their high correlation to Debre Zeit's station readings. Missing data were filled by estimating from the linear association of altitudes and temperature readings of the remaining station. We then developed regional minimum and maximum temperature lapse rates for each month of the year. This was done by pooling all four-station readings for a single month of the year (eg. January) and regressing the readings on the corresponding station altitude values to estimate a slope (change in temperature for a given change in altitude). These slopes were used to estimate the minimum and maximum monthly temperature at the altitude of each administrative sub-unit, by assuming the average of the four-station readings corresponds to the average altitude of the four stations (=2071 meters above sea level). Estimates at each administrative sub-unit were weighted by their respective population and averaged at the *kebele* level.

In addition, daily readings of rainfall from 13 stations in close proximity to Bishoftu town were obtained from the National Meteorological Agency (NMA). These stations are Addis Ababa (Bole), Addis Ababa (Obs), Aleltu, Chefe Donsa, Debre Zeit, Dertu Liben, Ejere, Guranda Meta, Hombole (had only 9 months of data), Koka Dam, Mojo, Nazeret and Sebeta. Missing data were filled by randomly selecting one reading from the same date of the year in the four nearby years: two years prior and two years after. If missing data were for Feb 29th of a leap year, we randomly selected from the Feb 28th data for the four years. Daily readings from these stations were then spatially interpolated by using ordinary Kriging (Krige, 1951). We cross-validate model estimates at each station by varying the type of variogram model and its parameters (sill, nugget

and range). We selected the best global parameters from a range of reasonable values by comparing the root mean square errors for all stations (Hofstra *et al*., 2008). The interpolated grids were made to have spatial resolution of 0.5 degrees covering the entire study region. Administrative sub-unit coordinates were then overlaid to obtain (drill down) daily estimates, which were then aggregated at the *kebele* level weighted by the sub-unit population.

Finally, all daily estimates of rainfall and temperature were aggregated at one, two and three month blocks to examine associations with cases in the low transmission season.

3.2.5 Other variables

Other climate related variables considered include Sea Surface Temperature (SST) anomalies for the Niño 3.4 region and monthly average Normalized Difference Vegetation Index (NDVI) at a resolution of 0.1 degrees. Monthly Sea Surface Temperature (SST) anomalies for the Niño 3.4 region were obtained from NOAA Optimal Interpolation SST Version 2 database (IRI, 2014b). Monthly average Normalized Difference Vegetation Index (NDVI) at a resolution of 0.1 degrees were obtained from the IRI analysis of USGS data for the period 1993 to 2004 (IRI, 2014a). For 2005, we obtained NDVI from the MODIS/Terra Vegetation Indices for the year 2005 (USGS, 2014) at a temporal resolution of 16 days and spatial resolution of 500m, which were aggregated to monthly average at a resolution of 0.1 degree, to match the resolutions before 2005.

In order to examine the role of other possible sources of mosquito breeding sites, we considered distances from subunits to perennial water bodies. In addition, we examined the ability of local soils to retain rain and flood water – water holding capacity as well as landscape slopes. All were aggregated at the *kebele* level in the same way as for the climate data. We used shape files of perennial rivers obtained from Food and Agriculture Organization (FAO, 2014), and lakes obtained from the Environmental Systems Research Institute (ESRI, 2013), and computed the distance between each administrative sub-unit and its closest perennial water body. This distance was considered to have a decay effect (the effect on malaria transmission decays exponentially as distance increases); thus we used the inverse-square distance, all weighted by sub-unit's population and aggregated at the *kebele* level.

We used the GAEZ soil database (FAO/IIASA, 2011) for the dominant soil type at a resolution of 5 arc minutes. We also obtained ISRIC-WISE soil water content data (in mm) at 30 arc minutes resolution (Batjes, 2005), which includes relative size of different soil types and their specific water capacities. By matching the higher resolution dominant soil types layer to the water capacity layer sorted by area size, we were able to obtain water capacity at higher resolution of 5 arc minutes. We then overlaid the administrative sub-units coordinates on the water holding capacity layer to estimate values at each subunit.

3.2.6 Control interventions

Our intervention data consists of indoor residual spraying (IRS) operations at the *kebele* level during the 11 year period spanned by the case data, obtained from the

Oromia Regional Bureau of Health. A categorical binary value of 1 was assigned to each month a *kebele* had an effective IRS and 0 other wise. A *kebele* is considered to have an 'effective' IRS for the duration of residual effect of the insecticide sprayed (6 months for DDT, 3 months for Malathion) (WHO, 1997).

3.2.7 Least cost distance estimates

A least-cost measure is based on the concept of minimizing the accumulated cost of a traveler in moving from point A to point B over a landscape. If the cost of traveling a certain distance is equal for all directions, then the least-cost distance is the Euclidean distance. The concept has been well developed in transportation, environmental economics and archeology where economic and social forces have a recognized influence on the spatial distribution of events (Stone, 1998; White and Surface-Evans, 2012). In relation to infectious disease dynamics, the concept applies to capturing connectivity between regions with consideration of the geographic space humans cover in their social and economic activities.

In this study, we assume cost of travel is contingent on the surface of travel corresponding to paved road, gravel road or walking trail. Studies have compared costs of travel on paved road and dirt roads (Stone, 1998), as well as on paved road and hiking trails (Pingel, 2010). We recognize that in addition to taking longer time, hiking is more laborious as compared to traveling on vehicles that utilize roads. While the cost of these transportation means is context specific (depending on availability, the quality of roads, the opportunity cost of walking etc.), we can use them as reference points for making our own assumptions. Thus, we assumed that for a given distance, travel on gravel roads is

1.5 times more costlier than that on paved roads, while hiking is two times costlier. This estimate seems conservative, but is most probably closer to reality than not using any concept of cost, which would imply equal cost per distance for all means of mobility.

3.2.8 Neighborhood Structures

We plotted all possible routes of connectivity between each administrative sub-units (n=342) using geographic information system (GIS) methods. We identified the least-cost routes for each pair of administrative sub-units using the ArcGIS‘s Network Analyst tool. Then neighborhood structures were implemented by considering 1) adjacent *kebeles* (2) *kebeles* with sub units at most 5km apart (3) *kebeles* with sub units at most 10km apart (least-cost distance estimates for paved-roads) .

3.2.9 Selection of explanatory variables

We started our analysis by defining a suite of explanatory variables to be assessed for their association with malaria cases during the low transmission season from January to April (JFMA), following the main transmission season from September to December (SOND). The low transmission season typically follows the coldest period of the year and receives the lowest rainfall accumulation (Fig.2.2). Because we expect the inter-annual variation in cases for this season to be associated with inter-annual climate variability, we included mean temperature and total rainfall at different aggregation windows, as well as NDVI and the Niño 3.4 SST anomalies, all at different lag periods. Land use change through deforestation was not considered here due to its small area impact, although it has been proposed to increase incidence in other regions (Stryker and Bomlies, 2012; Hahn *et al*., 2014; Vittor *et al*., 2006).

Because malaria represents a transmission system, the number of cases in one season should depend, in part, on the number of cases in prior seasons. Such temporal latent effects have been the basis for the temporal autoregressive terms used in statistical models for vector-borne diseases (e.g. Zhou *et al*., 2004; Lowe *et al*., 2013). We used here a lagged relative risk computed as the log-standardized ratio of observed SOND cases to the global expected seasonal malaria cases. The latter is the population in an area multiplied by a global estimate of the average seasonal malaria rate, a value estimated by dividing the total number of cases by the total population across all areas (Lowe *et al*., 2013, Zhou *et al*., 2004).

To select among these possible explanatory variables of the low season (JFMA) malaria cases, we used a generalized linear model (GLM) framework. Because observed count data, such as reported cases in infectious diseases, often exhibit significant over-dispersion (Lawless, 1987), and our exploratory analysis confirmed this pattern for our data, we used a negative binomial distribution of cases. We then tested different combinations of explanatory variables by step-wise model selection based on the Akaike information criteria (AIC).

The negative binomial model GLM used here has the following general form:

$$y_{it} \sim negBin(\mu_{it}, \theta) \tag{3.1}$$

$$log(\mu_{it}) = log(e_{it}) + \alpha + \sum_{j=1}^{5} \beta_j x_{jit} + \sum_{j=1}^{4} \delta_j w_{ji} + \gamma z_{it} + \tau S_t \tag{3.2}$$

where y_{it} is the number of JFMA cases for *kebele i* and year *t*, μ is the mean count of JFMA malaria cases, θ is a scale parameter (dispersion factor), e_{it} is the expected number

of cases , a known offset (the corresponding population multiplied by the global expected malaria rate), α is the intercept, β_j are coefficients of regression for x_j, the time and space varying factors including mean temperature and rainfall (with different lag periods), effective IRS status, population density and NDVI; δ_j are coefficients of regression for the w_j , non-time varying factors including slope, soil water capacity, water bodies, and distance to roads; γ is the coefficient of regression for z_{it}, the log ratio of prior season cases to the expected cases; and τ is the coefficient of regression for s_t, Sea Surface Temperature anomalies from the Niño 3.4 region.

We account for population in each *kebele* by using the offset term e_{it}, which is the global expected rate (a global constant k) multiplied by the population p at each *kebele*. For an expected number of cases of $e = k*p$ in a *kebele* i at time t, the expected rate $E(Y/p) = \mu / (k* p)$. When we apply logarithm to this expression we get $log (\mu) – log (k*p)$. Adding $log (k*p)$ on both sizes of the negative binomial model would cause inclusion of the first term in equation 3.2, i.e. $log (e_{it})$, serving as the population offset. The log-link allows comparison of point estimates to the Poisson model. Our *model* (equation 3.2) uses logarithmic link function and thus we applied exponential function to the response variable $log (\mu)$ to convert it to fitted number of cases, with a dispersion factor θ.

3.2.10 Generalized Linear Mixed Model

After identifying the variables that are significantly associated with the JFMA count of cases, we tested their significance in a negative binomial (Venables and Ripley,

2002) Generalized Linear Mixed Model (GLMM) framework that includes (i) a spatially-unstructured random effect and (ii) a spatially-structured random effect. Spatially structured random effects explicitly account for spatial autocorrelations and weight relative risks in regions according to the relative risks in their neighborhood. This is consistent with the latent effect of increased infectious disease risks from neighboring regions of high transmission recommended for both mathematical (Longini, 1988; Viboud *et al*., 2006, Bertuzzo *et al*., 2011) and statistical models (Kazembe, 2007; Lowe *et al*., 2011).

We tested three different neighborhood structures to represent the spatially-structured random effect: a) that of adjacency where neighborhood consists of *kebeles* with common borders (b) that of proximity within 5km (paved road distance equivalent) and (c) that of proximity within 10 km. The weighted proximity measure provides a means of incorporating different travel infrastructure types including trails, the latter being of particular importance during the dry seasons in this region (see section on least cost distance estimates) . A normal conditional autoregressive (CAR) prior distribution is assumed for these structured spatial effects (Baseg *et al,* 1995):

$$v_i | v_j \sim N\left(\frac{\sum_j a_{ij} v_j}{\sum_j a_{ij}}, \frac{\sigma_v^2}{\sum_j a_{ij}}\right) \qquad (3.3)$$

where σ^2 controls the strength of local spatial dependence, and a_{ij} are neighborhood weights for each *kebele* as defined above, with simple binary values of 1 when *kebele* i is a neighbor of *kebele* j, and 0 otherwise. Since the CAR distribution is improper, we applied a 'sum to zero' constraint on each v_i.

We chose a Bayesian Markov Chain Monte Carlo (MCMC) parameter sampling implementation in WINBUGS to estimate model parameters and their distributions (Lunn *et al*., 2000). We generated a sample of 10,000 parameters sets to form our posterior distributions. The general form of the Generalized Linear Mixed Model (GLMM) is as follows:

$$y_{it} \sim negBin(\mu_{it}, \theta) \tag{3.4}$$

$$log(\mu_{it}) = log(e_{it}) + \alpha + \sum_{j=1}^{5} \beta_j x_{jit} + \sum_{j=1}^{4} \delta_j w_{ji} + \gamma z_{it} + \tau S_t + \phi_i + \nu_i \tag{3.5}$$

where ϕ and v are the unstructured and structured random effects respectively. All other covariates and parameters are similar to those described above (in equation 3.2) except that, here all covariates are standardized to zero mean and unit variance to aid convergence in the MCMC sampling. Model selection was based on the Deviance Information Criterion (DIC), a goodness of fit measure for Bayesian models that penalizes for increasing model complexity (Spiegelhalter *et al*., 2002).

3.3. Results

A temporal pattern of expansion and contraction through the seasons is typically observed. It is exemplified in Figure 3.1E for the trough preceding the large peak of 1997. The documented changes suggest that a horseshoe-shaped area in the center of the study region accounts for the majority of cases during the low transmission season. As the main transmission season develops, increasingly more and more cases are reported from a larger area encompassing more *kebeles* at higher elevations. This temporal expansion is followed by a contraction in a seasonally-recurrent pattern (Fig. 3.1, D).

This pattern appears to be associated with elevation differences where lower altitude areas are generally those that contribute to the burden of cases in the low transmission season (Fig. 3.1, B). The contraction area during the low transmission season would serve as the reservoir of the pathogen from which disease transmission spatially expands in the main season. To examine the determinants of this area, we consider next the results from the statistical models.

The initial selection of significant explanatory variables revealed that rainfall and mean temperatures in December-February (DJF) are significantly associated with JFMA cases, as was the lagged malaria relative risk. Furthermore, our analysis showed that population density obtained from circles of 5 km radius around each sub-administrative units, was the most significant non-climatic factor associated with JFMA cases. Neither proximity to a road nor the other environmental factors (including NDVI, landscape slope, soil water holding capacity and proximity to a water body) were significant. Niño 3.4 anomaly lagged by 6 months was dropped from further consideration despite being significantly associated with JFMA cases, as it was highly collinear with DJF rainfall.

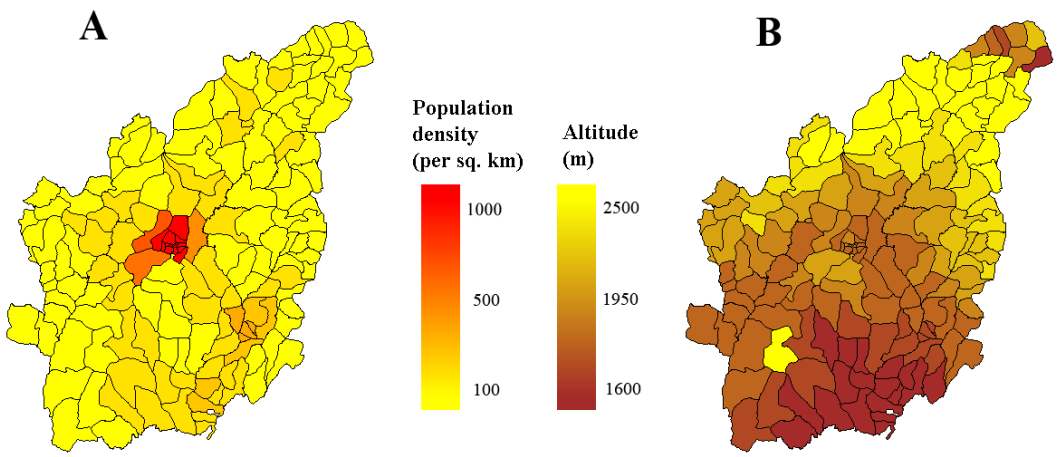

Figure 3.2: Figure A shows the population density obtained by adding all population within a 5km radius around each administrative sub-unit (up to 4 per *kebele*) and by dividing the value by the area of the circle (see text for details). The high-density area at the center is Bishoftu/ Debre zeit town (A). Figure B shows the elevation map, with elevation weighted by the population size of the administrative sub-units within each *kebele* (see text for details). Source: Siraj *et al.*, 2015. Temperature and population density determine reservoir regions of spatial persistence in highland malaria. Submitted to *The Proceedings of the Royal Society – B*, fig. S2.

Table 3.1
Comparison of goodness of fit for the different models based on the Deviance Information Criterion (DIC) with log JFMA malaria cases the dependent variable.

	Model	Deviance Information Criterion (DIC)
I.	**Fixed effect only**	
A.	climate factors only	4346
B.	climate factors and population density	4333
C.	climate factors, population density and IRS status	4324
II.	**Fixed effect and unstructured random effect**	
A.	climate factors only	4277
B.	climate factors and population density	4275
C.	climate factors, population density and IRS status	4272
III.	**Fixed effect, unstructured and structured random effect**	
A.	climate factors only	4256
B.	climate factors and population density	4256
C.	climate factors, population density and IRS status	4258

Source: Adapted from Siraj *et al*., 2015. Temperature and population density determine reservoir regions of spatial persistence in highland malaria. Submitted to *The Proceedings of the Royal Society – B,* table 1. Smaller DIC values signify better fit.

Inclusion of the random effects (both structured and unstructured) resulted in the best model. Moreover, neighborhood structure based on 10 km least-cost distance proximity (equivalent to 10 km paved roads and 5km trail distance) proved to be best in capturing the random effects around each *kebele*. Population density also contributed significantly when considered together with structured and unstructured random effects (see Table 3.1). During the low malaria season, the residual effect of IRS was not significant in all three models (the coefficients' posterior distributions included zero), despite a slight improvement of DIC over the models with non-structured random effect.

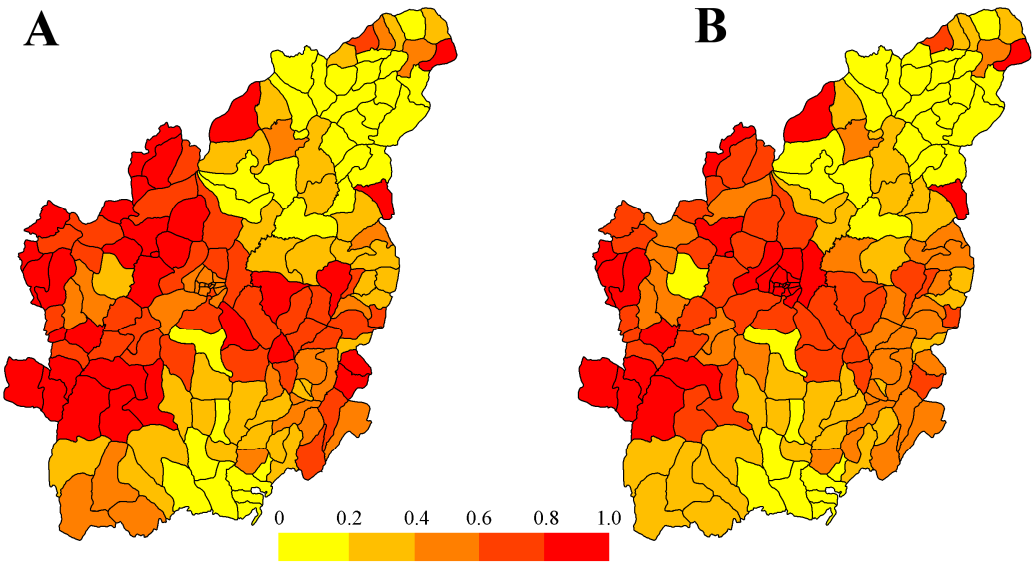

Figure 3.3: Structured random effect from model III-A (with no population density) (A), and the sum of structured random effect and population density from model III-B (with population density) (B), both normalized to range between 0 and 1 for the median parameter values. The two random variables have high partial correlation (r-value = 0.9), indicating the importance of population density in explicitly defining the model's structured random effects. Source: Siraj *et al.*, 2015. Temperature and population density determine reservoir regions of spatial persistence in highland malaria. Submitted to *The Proceedings of the Royal Society – B*, fig. 4.

Importantly, population density and the spatial random effect seem to explain similar variation in JFMA cases, where the spatial random effect would compensate for population density when the latter is not included. Consistent with this observation, the spatial random effect alone in model III-A (with no population density) has high partial correlation with the sum of the spatial random effect and population density in model III-B (with population density) (Fig.3.3; Table 3.1). This pattern is largely due to the fact that population density and the neighborhood structure, which is defined through proximity measures, are closely related. Indeed, *kebeles* that have several population centers in their neighborhood are also likely to fall in a region with high population density. The inclusion of population density in our model helps to explicitly define part of what would have been otherwise incorporated as structured random effects.

Table 3.2
Coefficients of the best GLMM model in the low transmission season with log JFMA malaria cases the dependent variable.

Covariate		Median	95% CI*	R-hat
Total DJF rainfall	$\beta 1$	0.2001	[0.117, 0.280]	1.005
Mean DJF temperature	$\beta 2$	0.5299	[0.345, 0.723]	1.008
Population density	$\beta 3$	0.1055	[0.003, 0.204]	1.001
Lagged malaria relative risk	γ	1.4270	[1.340, 1.518]	1.002
Spatial unstructured hyper-parameter	σ^2_ϕ	0.3257	[0.134, 0.632]	1.001
Spatial structured hyper-parameter	σ^2_ν	0.0026	[0.000, 0.042]	1.001
Over dispersion parameter	θ^{-1}	2.5190	[2.062, 3.098]	1.001

* Credible Intervals (CI) obtained from the 2.5% and 97.5% quantiles of each parameter's distribution.
Source: Adapted from Siraj *et al*., 2015. Temperature and population density determine reservoir regions of spatial persistence in highland malaria. Submitted to *The Proceedings of the Royal Society – B*, table 2. R-hat is the potential scale reduction factor on split chains. Values close to 1.0 indicate convergence.

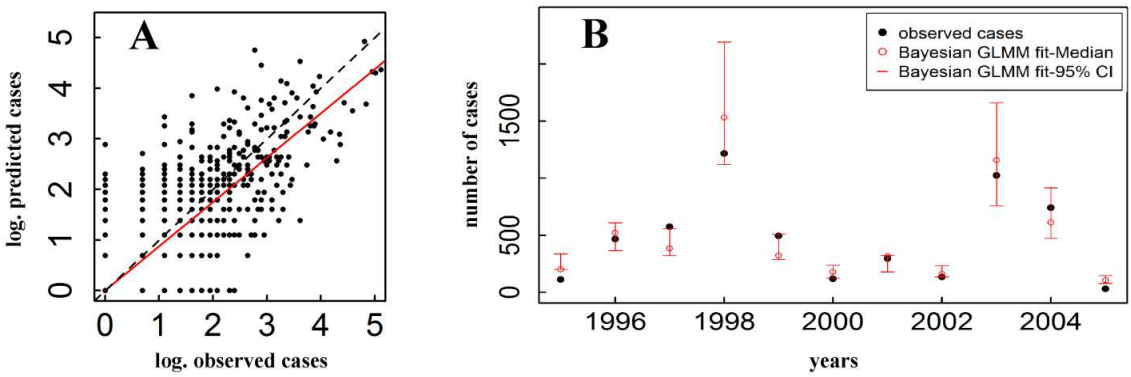

Figure 3.4: Observed versus fitted JFMA log cases with the best GLMM model (smooth curve computed by loess, in red) (A). Comparison in time of observed and fitted total JFMA cases from the best GLMM model (that includes structured and unstructured random effects) (B). The 95% Credible Intervals (CI) are obtained from the 2.5% and 97.5% quantiles of the distribution. The GLMM 95% CI includes the observed cases in more than 80% of the time. Source: Siraj *et al.*, 2015. Temperature and population density determine reservoir regions of spatial persistence in highland malaria. Submitted to *The Proceedings of the Royal Society – B*, fig. 3.

All parameters in the best model (with population density and both unstructured and structured random effects) are significantly different from zero, with posterior distributions from the two chains well mixed and converged (see Table 3.2). Model fits are reasonably good (Fig. 3.4, A and B), with JFMA incidence (in quantiles) correctly predicted 65 percent of the time for the all quantiles, while for the zero-case quantile we get 82 percent correct predictions. Similarly, for the highest-incidence quantile, we get 63 percent correct predictions (Fig. 3.5; Table 3.3).

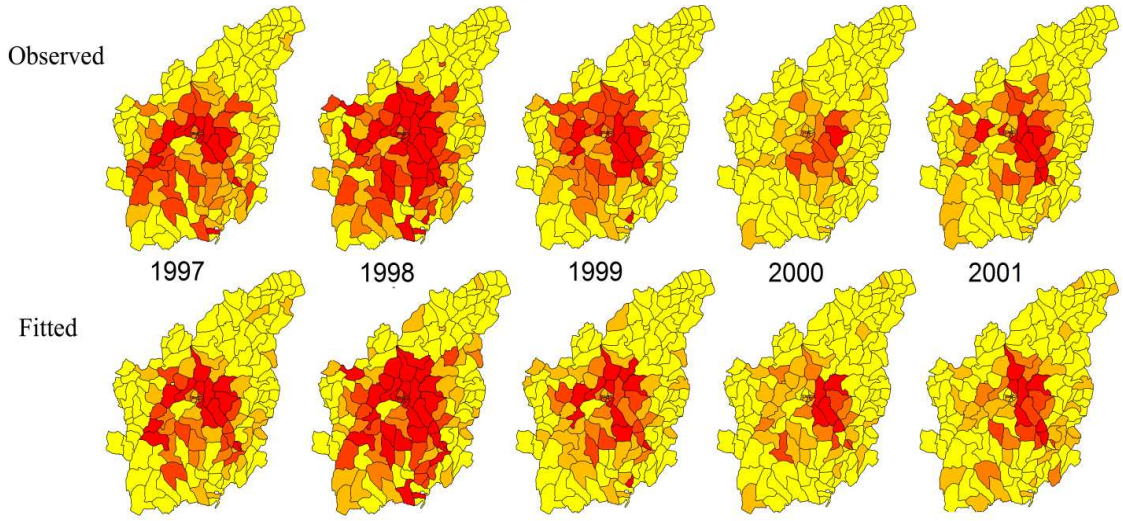

Figure 3.5: Observed (first row) and fitted quantiles of JFMA cases for five years (1997-2001). These quantiles are generated by considering zero cases in one class, and by subdividing all nonzero JFMA cases into five equally-sized quantiles, with the resulting categories representing respectively no cases, very low, low, high and very high cases, with colors ranging from yellow to red. Source: Siraj *et al.*, 2015. Temperature and population density determine reservoir regions of spatial persistence in highland malaria. Submitted to *The Proceedings of the Royal Society – B*, fig. 4.

Table 3.3
Counts of observed versus predicted quantiles of JFMA cases.

		Observed				
		No case	Very low	Low	High	Very High
predicted	No case	883	113	27	13	2
	Very low	163	85	47	35	16
	Low	23	32	26	28	7
	High	6	15	16	43	26
	Very high	5	10	8	32	88

Source: Adapted from Siraj *et al*., 2015. Temperature and population density determine reservoir regions of spatial persistence in highland malaria. Submitted to *The Proceedings of the Royal Society – B*, table S1.

Table 3.4
Median Coefficients of the best GLMM model for the high transmission season with log SOND malaria cases the dependent variable

Covariate		Median	95% CI	R-hat
Total JJA rainfall	$\beta 1$	-0.1188	[-0.1654, -0.0729]	1.001
Mean JJAS temperature	$\beta 2$	0.6750	[0.5853, 0.7665]	1.001
Population density	$\beta 3$	-0.1681	[-0.4000, 0.0738]	1.009
Indoor Residual Spraying	$\beta 4$	-0.2810	[-0.4727, -0.0806]	1.001
Lagged malaria relative risk	γ	0.2934	[1.3400, 1.5183]	1.001
Spatial unstructured hyper-parameter	σ^2_ϕ	0.0115	[0.0003, 0.1419]	1.163
Spatial structured hyper-parameter	σ^2_ν	4.1288	[2.9638, 5.7176]	1.003
Over dispersion parameter	θ^{-1}	1.9180	[1.7000, 2.1600]	1.001

Credible Intervals (CI) obtained from the 2.5% and 97.5% quantiles of the distribution.
Source: Adapted from Siraj *et al*., 2015. Temperature and population density determine reservoir regions of spatial persistence in highland malaria. Submitted to *The Proceedings of the Royal Society – B*, table S2. R-hat is the potential scale reduction factor on split chains. Values close to 1.0 indicate convergence.

3.4 Discussion

The spatial distribution of malaria expands and contracts as we transition from high to low seasons in a way that at first sight might appear simply related to altitude (or equivalently, to temperature). Our results indicate however that while climate factors play an important role, it is their combined effect with population density that maintains a reservoir of disease transmission and explains the spatial heterogeneity of persistence during the troughs between transmission seasons. Thus, our analyses reveal that the spatial variation in malaria incidence in the low transmission season is explained not just by lagged temperature and rainfall values during critical windows, but also by the more densely populated and spatially interconnected population centers. Population density helps explicitly define the spatial effects identified in the statistical models. In particular, areas of persistence, where malaria transmission continues in the low season, are largely

confined to a stretch of land adjacent to the town of Bishoftu with a considerably high population density ranging from 150 to 700 persons (30-80 households) per sq. km. (Fig. 3.2).

Our results also indicate that human mobility as represented by a simple proximity to roads is not significantly associated with the number of cases in the low season. This could be due the fact there are only a few roads in the region, and trails rather than roads tend to have wider use, especially in the dry season. Reliance on weighted proximity (as opposed to adjacency) as a basis for neighborhoods appears effective in capturing human movement patterns that influence disease transmission in a way that is independent from the adjacency of geographic regions. This observation is consistent with other studies that used proximity measures as opposed to adjacency measures (Longini, 1988; Viboud *et al*., 2006, Bertuzzo *et al*., 2011). Moreover, our results confirm significant spatial autocorrelation as expected for vector-borne infections from similar studies (Low *et al*., 2013; Kazembe, 2007).

Increases in mean temperature during the period between December and February have a delayed prompting effect on transmission in the low transmission season (Jan - Apr). Since this period includes the coldest months of the year, our results imply that higher DJF temperatures can limit the seasonal inhibition on the development of parasites, the population growth of vectors and their biting frequency (Craig *et al*., 1999; Detinova 1962, Moulneux 1988). This finding is consistent with the demonstrated temperature effects on malaria transmission in highland regions, where warmer years

contribute to increases in the intensity of the disease (Siraj *et al*., 2014, Pascual *et al*., 2006; Zhou *et al*., 2004).

Higher DJF rainfall also aids malaria transmission during the low season, a period of low precipitation where vector breeding continues during these colder months. Conversely, we observe a reverse effect of rainfall in the main transmission season (SOND), where more rainfall in the preceding wet months of JJA decreases malaria incidence in SOND, most likely due to a wash-out effect on mosquito habitats.

Although indoor residual spraying was not identified here as significant for the low season, it is found to be a major factor in the main transmission season (Table 3.4). Because IRS operations in our study area exclusively target the main season 90% of the time, they provide no protection in the low transmission season, which can account for the poor association with disease incidence.

The use of host population size as the only demographic factor in malaria transmission models may be insufficient for low intensity regions (and seasons) with high spatial heterogeneity in incidence levels. A spatially-resolved dynamical model would require a more explicit characterization of differences in demographic factors, especially population density to capture its heterogeneity. Our results imply that incorporating population density in dynamical models of malaria and similar vector transmitted diseases would account for fine-scale differences in incidence.

Along these lines, a recent study on the spatial heterogeneity of malaria risk in a region of low transmission with similar seasonal patterns suggests the importance of

considering risk 'hot spots' at different spatial scales (Bejon *et al*., 2014). For highland regions, which represent the highly populated low transmission regions, our results show that these 'hotspots' are associated with both temperature and population density. With the efficacy of the African vectors diminishing in urban areas with higher population densities (Trape and Zoulini, 1987; Robert *et al*., 2003; Hay *et al*, 2005; Keiser *et al*., 2004), the significance of population density identified here is counter intuitive. People who settle in densely populated, peri-urban areas are often met however with underdeveloped programs, personnel, and resources to combat infectious diseases, a situation exacerbated by poverty, low levels of education, and poor infrastructure (Robert *et al*., 2003). They are also involved in economic activities (agriculture, in our case) that demand higher mobility which together with the higher population density elevate the risk of infection. Higher population numbers in a given area may also alter the agricultural landscape in ways that create additional recruitment sites for the vector (Bomblies *et al*, 2008).

Moreover, higher human density may facilitate vector aggregation, and in so doing, increase the probability of a vector biting clusters of hosts. As climate conditions supporting widespread malaria transmission dwindle during the low transmission season, the vector is expected to take every little comparative advantage it has for it survival – in this case concentration in areas with higher human population density where other limiting factors are also tolerable for the vector. By contrast, we should not necessarily expect any particularly strong correlations between malaria incidence and population

density during the main transmission season which covers larger geographic areas and affects a larger fraction of the population.

The results presented here make a case to strengthen control during the low transmission season in rural areas with higher population densities. Such control measures would consist of targeting the spatial reservoir of the pathogen in humans (finding and treating symptomatic and non-symptomatic carriers) and/ or the vector (additional rounds of IRS). These measures would improve cost effectiveness and aid existing initiatives to eliminate malaria from African highlands. Our findings could be relevant to other locations with seasonal malaria.

CHAPTER FOUR: CLIMATE WARMING AND MALARIA SUITABILITY IN ETHIOPIA

4.1 Introduction

Malaria transmission is greatly influenced by environmental and climatic factors. Temperature affects the transmission cycle of the malaria parasite *Plasmodium falciparum* in many ways. Within a certain range, increasing temperature shortens the time required for the parasite to develop inside the vector (sexual reproduction or sporogony), during which time the parasite matures and is ready for transmission to a healthy human host (Detinova, 1962; Molineaux, 1988). At the same time, an increase in temperature increases the probability that a mosquito survives the sporogony period, shortens the larval stage of mosquito, which increases the abundance of adults, and increases the vector's feeding frequency (Molineaux, 1988).

Similarly, rainfall provides breeding habitat for the aquatic stage of mosquito development. It also increases relative humidity, which in turn boosts the survival rate of the vector (Pampana, 1969). Climate therefore plays a critical role in the epidemiology of malaria, particularly before the active human control of the disease (Gething *et al.*, 2010), but still obvious in endemic dryland and highland areas in endemic countries (Bouma *et al*., 2011). This provides an opportunity for using climate to develop a malaria suitability

index that takes into account both rainfall and temperature suitability for the vector as well as the parasite.

Historically, altitude has been used to differentiate regions by their risk of malaria transmission. In the early 20th century, European researchers documented the altitudinal pattern of malaria transmission in Ethiopia ranging from stable to seasonal, to malaria-free regions along altitude gradients. Based on parasitological and entomological surveys, Corradetti (1938, 1940) observed seasonality becoming more pronounced as altitude increases. For instance, between 1000 and 1500m elevations, transmission was widespread in the wet season, but only isolated cases appeared in dry seasons. Also, between 1500 and 1900m transmission was completely absent during the dry season and rose gradually after the onset of the wet season, reaching its altitude limits of 2000m at the end of the rainy season (Corradetti,1940). This altitudinal upper limit for stable malaria transmission was further confirmed in an era that saw limited human interventions (Melville *et al.* 1945),

In Chapter 1 we showed that the distribution of malaria shifts to higher altitudes during warmer years, with the implication that this is likely to occur too in a warmer world (Siraj *et al*., 2014). This would permanently introduce malaria to populations not previously exposed, and intensify malaria where low temperatures mitigate transmission (Bouma and Pascual, 2014). With its large population living at high altitudes, Ethiopia seems particularly vulnerable to global warming. Malaria in the Ethiopian highlands appears, contrary to most malaria endemic regions, a relative simple disease with temperature as main determinant because rainfall due to “orographic lifting” does not

appear to constrain transmission in many highland regions such as in our study area in Chapter 1 (Siraj *et al*., 2014). In addition, Ethiopia's malaria epidemiology has only one (dominant) vector, *An. arabiensis*, and therefore a less complicated epidemiology than in many other endemic countries. In this chapter the hypothesis of malaria as a mainly temperature driven disease in Ethiopia is further explored. Confirming the limited complexity of the epidemiology of malaria in Ethiopia would allow more robust estimates of the changes in malaria's public health burden for the country that may have occurred since the warming trend commenced in the 1980s, and projections for the 21th century if warming continues.

The true burden of malaria in is notoriously difficult to establish in any malarious region, but particularly countries with limited diagnostic facilities. This is further complicated by difficulties to estimate malaria as a co-factor in other health problems and mortality, and to differentiate new infection (transmission) from disease in endemic regions (Snow, 2003).

To assess the implication of climate change for the epidemiology of malaria not only a reliable assessment of the current burden of malaria, but also a realistic extrapolation based on climate sensitivities of the disease is fundamental. Indirect country estimates for malaria's disease burden can be obtained from extrapolations of surveys (establishing the prevalence of the parasite in the surveyed population, usually children), which is not necessarily representative of the whole country (Bouma and Pascual, 2014). Potentially, more comprehensive estimates could be obtained from high

resolution weather and climate parameters if these parameters can be shown to accurately reflect malaria risk, and taking into account the distribution of the population.

For continental Africa a climate based suitability index for *P.falciparum* was developed based on rainfall and temperature, generating values between 0 and 1 for every grid point (Craig *et al*., 1999). On a continental scale this *Falciparum* Climate Suitability (FCS) corresponded well to the high and low endemic regions and the latitudinal and altitudinal fringes of the disease. However, this approach did not find much following by national programs to assess malaria burdens or assist in planning control efforts. Attempts to validate the method on country level have been limited. In Kenya with extensive highlands this climate suitability approach was shown to predict classes of endemicity as measured by parasite prevalence accurately (Snow *et al.*, 1998), and for the East African highlands, including Ethiopia, a striking relation was uncovered between historical prevalence surveys and MARA's climate suitability index (Cox *et al*., 1999). Kenya's study also identified that the duration of months suitable for transmission, using similar climate criteria, was a very good predictor of prevalence.

To assess impact of climate change for the countries of Africa, both the FCS and the length of the season (malaria suitable months) have been used subsequently by co-authors of the (Snow *et al*., 1998) paper, but with very different conclusions (Tanser *et al*., 2003; Hay *et al*., 2006). Tanser (2003) identified the high altitude regions of Africa as most vulnerable to climate change with striking rises of malaria risk with climate change. For Ethiopia an increase in "person-months malaria exposure" of 149 %, 231% and 349% was predicted, for increase in temperature of 1.9, 2.2 and 3 ^{o}C respectively compared to

the 1920-1980 baseline corresponding to the 2070-2099 climatology under different climate change scenario's (Tanser *et al*, 2003). Hay *et al.* (2006) used the *Falciparum* suitability for an all Africa estimate under the A2 high emission and HADCM3 circulation model for 2015 and 2030, with 1960-1990 and the 2005 climatology as baseline. Their continental results suggest that the effect of population growth outstrips those of climate change in the absolute increases of population at risk, downplaying the impact of climate change. They dismissed their results on country level (provided in an electronic annex), particularly for the highlands despite striking rises observed (Bouma and Pascual, 2014), because of the resolution of their climatologies centered on 2015 and 2030 (2.5 by 2.5 degrees, corresponding to 275 x 275 km) introduced bias when "up-sampled" to higher resolutions similar to the 1960-1990 base-line historical climatology at higher definition (55 x 55km) base line climatology.

In this chapter we aim to validate the MARA suitability index for Ethiopian conditions, improve the index if desirable, and repeat the procedures of Hay *et al* (2006) without the use of coarse climate resolutions that could overestimate malaria suitability. Ethiopia has 3 regions with strikingly different rainfall patterns which may compromise conclusions for the whole country. Analysis is therefore also conducted for each separate region. As Ethiopia also has a significant proportion of *P.vivax* cases, which is unusual in the African context (Duffy antigen with genetic resistance), we added the VCS (Vivax Climate Suitability) to this investigation. We used the pre-control survey data (Cox *et al.*, 1999; Tulu, 1996; and Melville *et al.*, 1945) and the consensus that around 1/3 of the population in Ethiopia resided in malaria free territory prior to the 1990s (Tulu, 1993), as

reference points to validate the FCS and VCS, and create a high resolution (5 x 5 km) baseline climatology using records of 146 meteorological stations in Ethiopia. To this improved climatology 1, 2 and 3 ^{o}C were added to simulate warming in the 21th century without changing the high resolution to assess the associated changes in malaria risk. Populations depending on their residence and accompanying malaria climate suitability can be classified in 4 categories, from malaria free (CS=0) to CS is between .75 and 1, corresponding with stable endemic malaria (Snow *et al.*, 2003). Results from changes in the suitability are then used to estimate the changes in the disease burden in Ethiopia, based on the established estimates of mortality under malaria stable (endemic) conditions.

4.1.1 The MARA model

The Mapping Malaria in Africa (MARA) project uses monthly temperature and rainfall from gridded climate surfaces to estimate and plot malaria climate with values between 0 and 1 (Craig *et al*, 1999; Hay *et al.*, 2006). The model is based on the perceived effects of mean rainfall and temperature on the biology of one of Africa's main vectors, *An.gambiae (*including *An.arabiensis*), and Africa's most important malaria species, *Plasmodium falciparum* (Craig *et al*, 1999). The suitability estimate depends on 3 components: 1) The temperature range suitable for the parasite to develop in the vector (the sexual stage of the parasite or sporogony), 2) suitable amounts of rainfall concomitant with the first component, and 3) suitable temperatures for the vector population to survive the coldest month of the year. The last component was added to account for the South African latitudinal boundary (of *An. Arabiensis*), and malaria, as this vector species appears unable to maintain itself in regions where frost occurs (at any

time of the year). However, for the African highlands, where *An.arabiensis* is an important vector too, this factor apparently was not considered.

The MARA climate suitability model relied on the mean monthly temperature and total monthly rainfall based on 1961-1990 climatology, for each location on a grid system covering the entire African continent. For each grid cell and each month of the year (Jan, Feb, etc), a suitability value was assigned with respect to the mean temperature first. This assumed a lower limit of 18°C and an upper limit of 40°C, beyond which mean temperature was considered unsuitable (FCS=0) for the *P. falciparum* parasite and the vector respectively. The model then included an ascending suitability curve between the mean temperature values of 18°C and 22°C; and a descending one between 32°C and 40°C, while for the range between 22°C and 32°C, mean temperature was assumed maximally suitable (FCS=1). The ascending and descending curves of temperature suitability follow the equation given in (4.1) and (4.2) respectively and are described in Table 4.1 (Craig *et al.*, 1999).

$$FCS = 1 - \cos^2\left(\frac{x-l}{u-l} \cdot \frac{\pi}{2}\right) \quad \text{for ascending curve and} \quad (4.1)$$

$$FCS = \cos^2\left(\frac{x-l}{u-l} \cdot \frac{\pi}{2}\right) \quad \text{for descending curve} \quad (4.2)$$

where x is the particular climate variable being considered, l is the lower limit and u is the upper limit of the range for which fuzzy logic is applied.

Table 4.1
Lower and upper limits of climatic ranges where fuzzy logic is applied based on the MARA climate suitability model for P. falciparum.

Mean monthly temperature (°C)	Ascending	$l = 18$, $u = 22$
	Descending	$l = 32$, $u = 40$
Monthly total rainfall (mm)	Ascending	$l = 0$, $u = 80$
Coldest month's minimum temperature (°C)	Ascending	$l = 4$, $u = 6$

Similarly for rainfall, the MARA model assumed a single ascending curve for the total monthly rainfall amount between 0 and 80mm, which follows the equation given in (equation 4.1). MARA model acknowledges that flooding often causes destruction of breeding sites and a temporary reduction of vectors. Nonetheless, very high rainfall was considered optimal for transmission as it never eliminates the vector (Craig *et al.*, 1999).

These temperature and rainfall cutoff points were determined by examining patterns of mean climatic conditions in different sites across Africa as they relate to different epidemiological settings. These sites (n=20) were selected from regions where malaria transmission has traditionally been regarded as perennial (annual, for more than six months), seasonal (annual, for less than six months), epidemic (transmission not recorded every year) and malaria-free (malaria never recorded). Results confirmed 18°C to be the approximate cutoff between epidemic and no-malaria zones, and that 22°C allows stable transmission (Craig *et al*, 1999).

The analysis by MARA also showed that a single month of 80mm rainfall was not sufficient to sustain stable malaria transmission. In regions where temperature is high but

rainfall is limiting, such as the fringes of the North African deserts, mosquito populations increase rapidly at the onset of rain, because of short developmental cycles. Thus, three months of rain was considered sufficient to constitute one transmission season. In regions where temperature is limiting during the colder season, as is the case in large parts of southern Africa and highland areas, mosquito populations increase slowly at the onset of rain, and thus is where five months of rain was considered necessary to constitute one transmission season (Craig *et al.,* 1999). Consequently, the composite suitability index (based on both mean temperature and rainfall suitability indices) each month of the year were aggregated per grid cell into a single value determined calculating the maximum fuzzy values that persisted for five months (three months if north of 8^{o}N).

Once the two climate factors were converted into suitability indices, a composite index was generated by taking the minimum of the mean temperature and rainfall suitability indices for each grid cell and each month of the year; resulting in suitability for malaria *Plasmodium falciparum* transmission in each month of the average year for each grid cell.

At the same time, the MARA suitability index considered the effect of frost in the coldest month of the year. A single ascending suitability curve was modeled for monthly minimum temperature of the average year between 4^{o}C and 6^{o}C, where suitability follows equation (4.1) and described in Table 4.1. With respect to the effect of frost alone, temperature below 4^{o}C temperature was considered completely unsuitable (FCS=0), while above 6^{o}C it was considered maximally suitable (FCS=1). Finally, the MARA suitability index for a grid cell was determined by considering the minimum of

the aggregated composite suitability and the frost related suitability index, with values ranging between 0 – representing areas completely unsuitable, and 1 – representing areas maximally suitable (Craig *et al.*, 1999)

4.1.2. Malaria climate suitability assessment for Ethiopia

The climate suitability index for Ethiopia calculated for the areas where the historical surveys were conducted suggested a good match between the prevalence values (between 0 and 100%) and the FCS values (between 0 and 1) (Cox *et al.*, 1999). Hay *et al.* (2006) has used the FCS to estimate present and projected populations at risk of malaria in different categories of epidemiological settings for all countries in Africa, including Ethiopia. They dismissed the validity of results for individual countries however, particularly for fringe areas such as the highlands due bias introduced by "up-sampling" of the low resolution of the climate scenarios (275 x 275km at the equator), to the base-line climatology (55 x 55km). The scale sensitivity of climate surfaces for establishing the FCS was indeed confirmed, showing an overestimation of the suitability (and malaria population at risk for malaria) using lower climate resolutions (Bouma and Pascual., 2014).

A climate suitability model that utilizes high resolution climate surfaces can greatly reduce the difficulty of disentangling the real and potential effect of climate change by enabling the resolution of subtle (fuzzy) differences in the biological constraints of climate on parasite and vector development. Thus, while malaria risk model can benefit from insight gained by including high resolution risk modifiers including demographic and land use/ land cover, improving the resolution should further

aid resolving malaria's fringe areas that are more sensitive to the effects of climate change.

The MARA climate suitability index can also be further refined in view of the Ethiopian climatic and epidemiological conditions. Firstly, due to its exclusive design targeting suitability for *P. falciparum,* it is expected to have excluded a large portion of the country that might be suitable for *P. vivax*. Secondly, owing to its design targeting the African continent, in an attempt to generalize for the entire continent, the MARA model might have included constraints not relevant to the Ethiopian climatic conditions.

In this study, we made use of a high resolution (5 x 5 km) climate surface data that we developed from a maximum of 146 stations across Ethiopia Fig. 1.2) for the period 1961 to 1990. We analyze the effect of different climate constraints included in the FCS model by using results of historical malaria prevalence surveys across Ethiopia (Cox *et al*., 1999; Melville *et al.*, 1945). Further we enhance its results by include suitability for *P. vivax* which account for estimated 40% of clinical cases in Ethiopia (MOH, 2001). Based on the best estimate of malaria suitability measures, we make further inference on the population at risk at present both now and in the future, assuming mean global temperature changes based on IPCC scenarios, and projecting temperature rises of 1, 2 and 3^{o}C.

4.2 Data and methods

4.2.1 Climate data

Data on monthly total rainfall and. monthly average minimum and maximum temperature readings for a maximum of 146 stations across Ethiopia was obtained from

the Ethiopian National Meteorological Agency (NMA) for the period 1961 to 1990 (see Fig. 1.2 for location of stations). The initial number of stations in 1961 was only 26 with others joining in later years. Missing data were filled by the lagged 5 year climatology (average for the same month in the preceding five years).

A Digital elevation model (DEM) at a 1 arc second resolution was obtained from the Global Earth portal managed by USGS (USGS 2011). To match the resolution of the gridded population, we reduced the resolution of the DEM, to a 2.5' x 2.5' spatial resolution by averaging values in the same larger grid.

A thin plate spline interpolation model was trained by using rainfall readings from all stations for each month as the response variable and their coordinates and altitude values as covariates (Fields Development Team, 2015). The gridded altitude obtained from DEM was then used as a linear covariate to generate a rainfall surface based on the thin plate spline model. The result is a gridded rainfall surface for each month at a resolution of 2.5-arc minutes. (4.6km x 4.6km)

Similarly, we used a thin plate spline model using monthly minimum temperature (or maximum temperature) station readings as the response variable with station coordinates, rainfall reading and altitude as covariates. A gridded altitude value obtained from DEM and a gridded rainfall value obtained by interpolation were then used as a linear covariates to generate a minimum temperature (or maximum temperature) surfaces based on the thin plate spline model. This resulted in monthly gridded minimum and maximum temperature surfaces at 2.5' x 2.5' spatial resolution (equivalent to 0.0417^{o} x

0.0417^{o}). Monthly mean temperature surfaces were generated by simply taking the average of the monthly minimum and maximum temperature surfaces.

4.2.2 Population data

We used population data from the Gridded Population of the World (GPW) version 3.0 (CIESIN/ CIAT, 2005). At a 2.5' x 2.5' spatial resolution, each grid cell represents the residential population count for the year 2000, based on the census of 1994. We started by calibrating the gridded population count for Ethiopia by multiplying by a factor to match it to the historical record of total Ethiopian population obtained from the World Urbanization Prospects: The 2014 Revision. For comparison with at risk population done by others, we projected population after classifying grids into urban and rural classes.

We obtained population size for Ethiopia, separated by urban and rural, for the years 2000 and 2005 from the World Urban Prospect (UNPD, 2014). We then computed population growth for urban and rural between the two years. In order to apply differential population growth rates to the 2000 gridded population of Ethiopia (GPW3) and obtain a projected population estimates for 2005, we used the corresponding 2000 GPW3 gridded population density of Ethiopia (CIESIN/ CIAT, 2005) and tested different population density based urban-rural cutoffs in the range between 120 and 1500 persons per km (at every 20 steps), applying the population growth rates to the grids according to which side of the cut-off they are, and aggregating the population in all grid cells to get a national estimate for 2005. The candidate cutoff that produced a projected 2005

population closest to the UNPD figures was selected as the best cutoff between urban and rural. That cut off was 320 persons per sq.km.

After applying different growth rates for urban and rural (separated by using 320 persons/ km as the cutoff population density), the total Ethiopian population for 2005, 2015 and 2030 were all within 0.01% of records and estimates of the UN data and estimated (UNPD, 2012) [also could be downloaded at http://esa.un.org/unpd/wpp/].

For the classification of populations at risk in different epidemiological classes we only used the rural population. Urban populations are exposed to a reduced risk of malaria (1 to 2 orders of magnitude), because breeding conditions for the vector in an urban environment are severely restricted (Kaiser *et al.*, 2003; Hay *et al.*, 2005).

Finally, while the main objective of this study is to estimate the effect of climate warming on future population at risk of malaria, using projected population and applying it to the changes of climate suitability would add an uncertainty that would make interpretation our results difficult. Moreover, a comparison of the proportion of population at different altitude ranges based on two gridded population products for the years 1990 and 2000 (GPW3), revealed that there is no significant difference between the 1990 and 2000 proportion of population living at the altitude ranges of above 2600m, 2200-2600m, 1800-2200m, 1400-1800m, 1000-1400m and below 1000m, with all differences within 0.3 percentage points. Consequently, except for comparison with other works, all future population proportions are based on constant 2015 population.

4.2.3. Climate models

We used 20 Global Circulation Models (GCMs) included in the Model for Greenhouse gas Induced Climate Change (MAGICC) and SCENGEN software application (Hulme *et al.* 2000). The GCMs are consistent with the IPCC Fourth Assessment Report (AR4) and generate projected global-mean surface air temperature changes for a specified year at a resolution of 2.5^{o} x 2.5^{o} spatial resolution [http://www.cgd.ucar.edu/cas/wigley/magicc/]. To enable comparison with previous works, we chose the high A2 emission scenario. We also chose HadCM3 coupled atmosphere-ocean general circulation model (AOGCM), to ensure our results are comparable with those of Hay *et al.* (2006). Since model simulations for individual years can be noisy MAGICC/ SCENGEN provides 30 year averages for future climate. We chose outputs centered on 2015 (2000-2030) and 2030 (2015-2045). To match the spatial resolution of population density we resampled all temperature change projections using cubic-spline interpolation to get a spatial resolution of 0.0417^{o} x 0.0417^{o} from the GCM resolution of 2.5^{o} x 2.5^{o}.

4.2.4 Fuzzy climate suitability and disease burden.

We implemented the FCS (Craig *et al*, 1999) based on the 1961-1990 climatology that we developed from the interpolated monthly surfaces for minimum temperature (Tmin), mean temperature (Tmean), and rainfall based on station data obtained from the Ethiopian Meteorology Agency . In addition we generated a climate suitability surface for *P. vivax* (VCS) by using the lower limit for parasite development to be 16^{o}C (as opposed to the current 18^{o}C for *P. falciparum*) due to its tolerance to develop at lower temperatures (Molineaux, 1988). To examine future changes to FCS and VCS surfaces

as well as the population that will be at risk as a result of potential changes we test the effect of adding 1ºC, 2ºC and 3ºC to the mean temperature while setting the population constant (extrapolated for 2015).

Finally, we added the temperature change surface (low resolution) obtained from GCM (both for HADCM3 and ensemble) to the baseline climatology (therefore maintaining its resolution) and generated FCS values based on the new mean temperature surfaces. We examined changes over time of population that reside in each region falling under areas with stable malaria transmission (FCS>=0.75), seasonal malaria transmission (FCS between 0.25 and 0.75), epidemic prone (FCS< 0.25) and no malaria transmission (FCS=0). Malaria burden estimates have been generated in recent decades for these epidemiological classes, particularly for the "stable" endemic malaria class with fuzzy climate suitability index greater than 0.75 and corresponding 25 percent malaria prevalence among children (Snow *et al.,* 2003). We used these to estimate the impact of climate change for rural Ethiopia. These estimates build on extensive efforts in the last decades to establish the health burden of malaria. For estimating malaria specific mortality, a demographic surveillance system (DSS) was developed, to monitor prospectively births, deaths and migration of populations between 20,000 and 100,000 people in West Africa (Smith and Morrow, 1996). The established malaria specific mortalities are summarized below (Snow *et al*., 2003).

Based on twelve independent estimates for malaria related mortality of children (0-4) living in areas of endemic malaria in Africa (prevalence rates >= 25%) provide a median malaria specific mortality rate amongst these communities of 9.33 per 1000 per

year (Interquartile range of 7.38 to 14.57), 52.2% of all deaths in this age group. Amongst children in 10 communities between 5 and 14 this was 1.58 (IQR 0.66-2.77), and amongst those over 15, the median rate in 15 samples amounts to 0.6/1000 per year (IQR 0.37-0.94).

We used the median mortality rates to estimate the Ethiopia's country burden using and the age distribution based of the last census (CSA, 2008). We only used the rural population because the urban population is at strikingly lower malaria risk due to unfavorable breeding conditions for the vector (Keiser et al., 2004), and for the mortality estimates we excluded the relatively small population in region C as the malaria dynamics in this arid part of Ethiopia are much less temperature (change) dependent.

4.3 Results

Based on the distinctly different rainfall regimes in Ethiopia Fig. 1.2), in timing, intensity and associated differences in population density, we computed the malaria climate suitability for each region separately. In the southern part of Ethiopia (Fig. 1.2, C), with (semi) arid sections, low rainfall is likely to limit malaria suitability. Not surprisingly, temperature is strongly related to altitude in all regions Fig. 4.1, lower panel), the physical lapse rate (for the mean annual temperature) being similar for regions A and B (respectively 0.59 ^{o}C and 0.53 ^{o}C degree per 100m and 0.99 ^{o}C per 100 m in the dryer region (seasonal precipitation dependent lapse rates not shown). In all regions there is an increase of rainfall with altitude related with orographic lifting, most pronouncedly in the most populated region A Fig. 4.1, upper 3 panels).

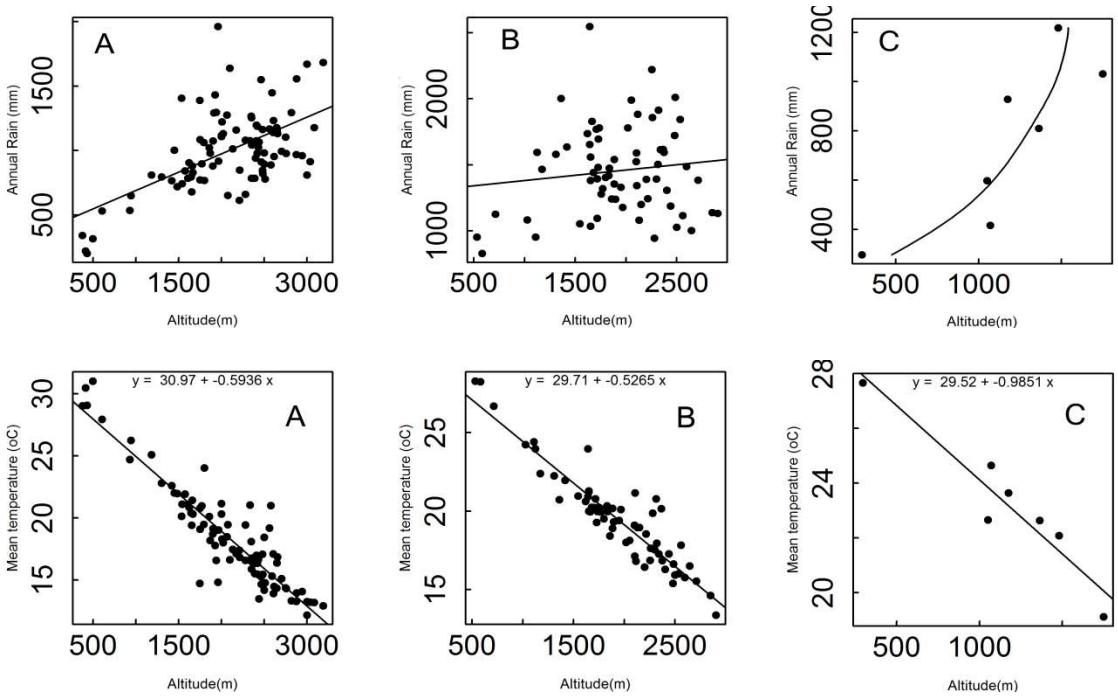

Figure 4.1: Average annual rainfall (mm) by altitude for regions A, B and C (Panel 1); annual mean temperature (in degree Celsius) by altitude in rainfall regimes A, B and C (Panel 2) for 146 stations.

The standard *Falciparum* Climate Suitability (FCS) computed for Ethiopia using a high resolution climate surface of 4.6 x 4,6 km (See methods), and based on the 1961-1990 climatology is shown in Figure 4.2 for *P.falciparum* (FCS) and for *P.vivax* (VCS). It reveals a far larger area with suitability index for *P. vivax* than for *P. falciparum* in the higher altitudes. With its tolerance to develop at lower temperatures (16 instead of 18 C), *P.vivax* would in theory be able to occupy much higher altitudes than *P.falciparum*, and the population in the zero suitability class would shrink to 11.8% when this higher tolerance for lower temperatures is applied in the VCS (results not shown). This is not consistent with historical or recent observations. The territory on high altitudes where *P.vivax* appears at an advantage over *P.falciparum* is trivial (Tulu *et al.*, 1996). With the

very low vector densities encountered at higher altitudes in East African highlands (e.g. Bodker *et al.*, 2003), it appears most likely that vectors are not present in sufficient densities to provide the *P. vivax* parasite with its genetic advantage over *P.falciparum*.

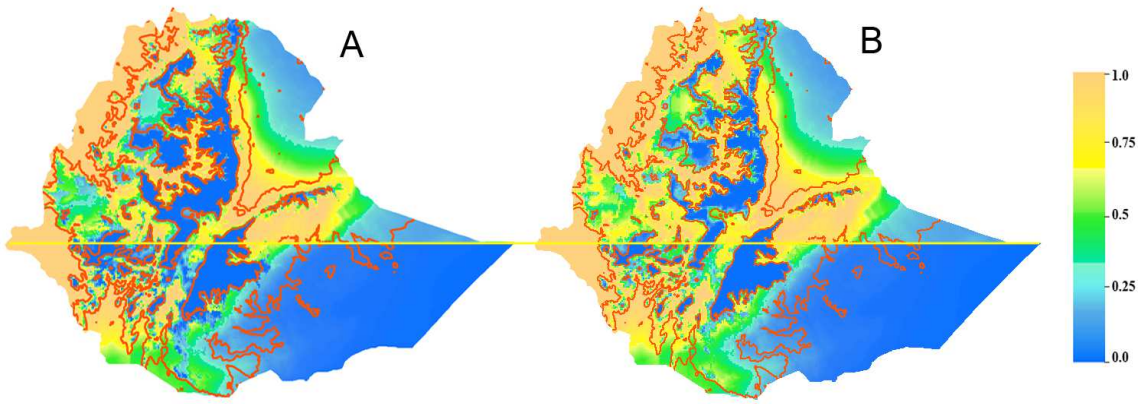

Figure 4.2: Fuzzy suitability index for *P. falciparum* malaria (A) and *P. vivax* (B), developed based on temperature and rainfall suitability for any 3 months of the year (5 months if south of 8ºN). Of the total area of the country 34% (or 29%) falls in regions with *P falciparum* (or *P. vivax*) climate suitability below 0.1. Suitability of Pv exceeds Pf because of the parasite's lower temperature requirement (16ºC vs 18º C). Yellow horizontal line marks the 8ºN latitude. The altitude range between 1000m and 2100m, shown in red, is historically associated with steady decrease in malaria prevalence from the highest levels at the lower end to zero at the high end (Melville *et al*., 1945).

In the standard MARA model, the vector in Southern Africa, *An.arabiensis*, the same as the main vector in Ethiopia, is curtailed by the frost-line (corresponding with Tmin of 4ºC in the coldest month of the year). In Figure 4.3 we show that in Ethiopia this vector "niche isotherm" does not limit the suitability for the parasite *P.falcipum*. The same is the case for *P.vivax* (not shown). With its proximity to the equator and its high altitude, there is less seasonal variation in the Tmin, but more pronounced diurnal

temperature variation. Therefore the lowest Tmin in the coldest month is not likely to apply to Ethiopia.

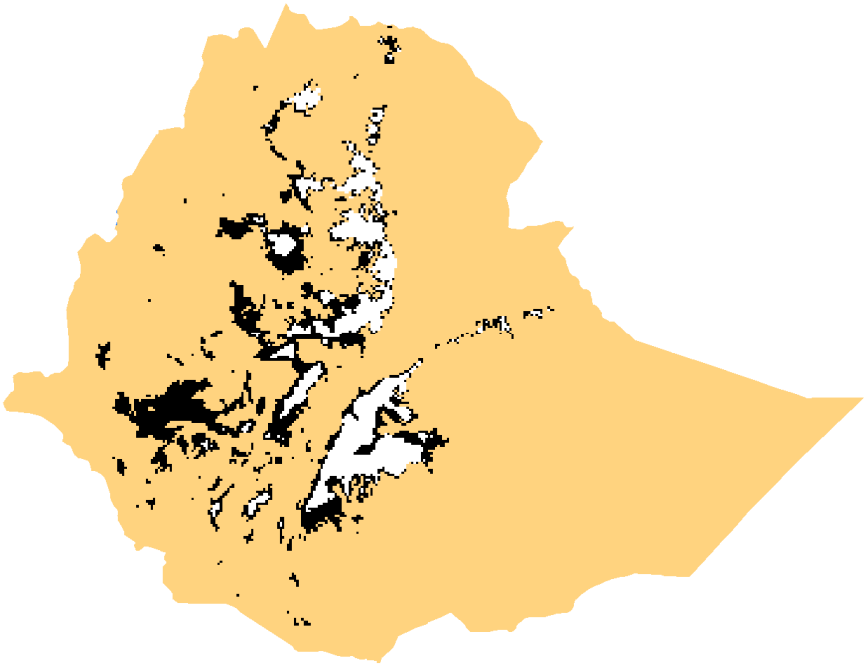

Figure 4.3: Malaria suitability exclusion zones based on suitability threshold for the vector (minimum temperature of coldest month below 6ºC) (white), and for the parasite development in the vector (mean temperature below 18º C) (black). This shows that the critical frost temperature for the vector does not lower the standard FCS in Ethiopia.

When we increase, empirically, the requirement of the Tmin for the vector from 4 to 10 degrees, the high altitude distribution *of P.vivax* is reduced, as visible from the percentage of the population living in *P.vivax* free territory Table 2). A value of 8 ºC for Tmin of the coldest month in the year appears to reduce the vivax territory without much affecting the *falciparum* suitability, and the historical malaria free fraction of the population (around 1/3, e.g. Tulu, 1993) is retained. In table 2 we also show that a 3 month window of consecutive suitable months North of 8º Latitude and 5 months for the region south of this meridian (in the standard MARA model) when replaced by a 3 month

window for all Ethiopia is not changing much in view of the share of both parasites over the different suitability classes (see also Fig 4.6).

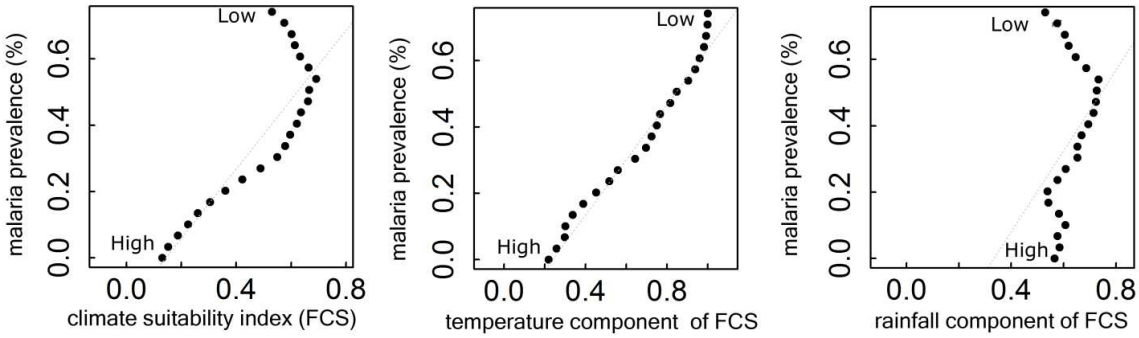

Figure 4.4: Historical malaria prevalence (Melville *et al.*, 1945, see Fig. 4.10) by climate suitability and its separate components. Each point represents a constant 50m altitude bin ranging from 1000 (low) to 2100m (high), and correspond to the average malaria prevalence at the that altitude (y-axis). On the x axis are malaria suitability indices generated from three different combinations: suitability based on both mean temperature and rainfall (A), based on mean temperature only (B) and based on rainfall only (C). We note that, the point where prevalence gets to 0.0 corresponds with 0.2 suitability based on temperature alone, and that rainfall appears restrictive on lower altitudes.

By using the historical association between altitude and malaria prevalence (Melville *et al.*,1945) we examined the significance of the three components of the FCS, namely monthly mean temperature's lower limit for parasite sporogony length (18ºC for *P. falciparum* and fuzzy increase up to 22ºC). We show in Figure 4.4 that, for the altitude range associated with steady decrease in malaria prevalence (1000-2100m), the FCS based on temperature alone explains 97% of the variance in malaria prevalence (Fig. 4.4, B), and support the hypothesis of temperature (and altitude) as main determinant of malaria suitability in the highlands. When the prevalence gets to 0.0 at the altitude of around 2100m, Tmean based suitability also goes to around 0. 2, significantly below the

value of 0.25 often used to separate areas with no stable malaria (epidemic outbreaks) and those suitable for seasonal malaria transmission (Craig *et al.*, 1999).

Matching the FCS zero value with the zero value for the prevalence (Melville, 1945) would also be possible by increasing the Tmean for *falciparum* parasite from 18 to 19 C (see Fig. 4.10), We further tested the effectiveness of models with different combinations of climate parameters and temperature cut-off's and compared proportions of population falling in different classes of malaria stability with the proportions we get when using the standard one – based on temperature and rainfall suitability.

Our results reveal that, while suitability based on temperature alone captures the proportions at the malaria free regions, it poorly reflects the proportions of population in regions of stable malaria transmission (Fig. 4.5). The reduced (rainfall related) suitability at lower altitudes seems also supported by the (limited) survey prevalence values (Fig 4.10). This supports the view that, rainfall, although on its own not predictive for malaria (suitability) on higher altitudes, is indeed an important co-factor at the lower part of the 1000-2000 m range. Rainfall was therefore retained in our "modified" suitability index.

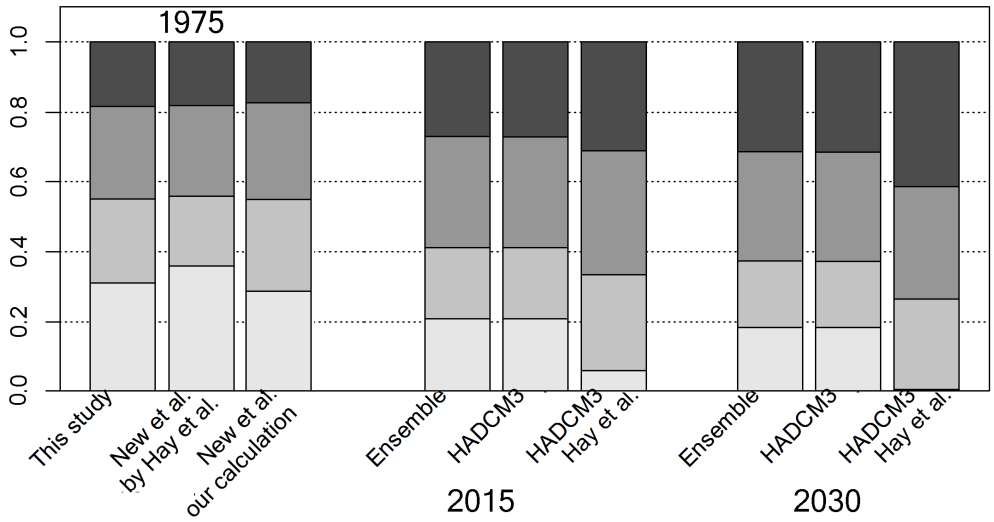

Figure 4.5: Comparisons of changes in the distribution of Ethiopian population (urban and rural) over different suitability classes using the standard MARA's FCS as a result of climate change projected for 2015 (2000-2030) and 2030 (2015-2045) under HADCM3 and an ensemble of 20 GCMs (A2) scenario's. Baseline climatologies centered on 1975 (1961-1990) from New *et al*. and our climatology (this study). The four epidemiological classes are (from top to bottom) stable (FCS greater than or equal to 0.75), seasonal (FCS between 0.25 and 0.75), epidemic prone (FCS greater than 0 and less than 0.25) and malaria free (FCS equal to 0). HADCM3 estimates by Hay (2006) based on "up-sampled" low resolution forecasts using temperature and rainfall. This is compared to anomalies of the HADCM3 temperature forecasts with the IPCC 1960-1990 climatology added to my high resolution 1960-1990 climatology (this study).

As a result of our examinations of different combinations of climate factors, temperature cut-off's and required length of the transmission season, we chose the model which is based on both temperature and rainfall, with Tmin limits of 8ºC, and requiring suitability that lasts 3 consecutive months. These modifications more accurately reflect the distributions of both *P. falciparum* and *P. vivax* for Ethiopia. The changes in the malaria suitability are visually displayed in Figure 4.6.

We applied the standard FCS (Craig *et al.*, 1999) to our climatology surfaces so that our results are comparable with those of Hay *et al.* (2006) and help investigate the effects of up-sampling, which allegedly biased the suitability forecasts in fringe areas

(Hay *et al.*, 2006). In subsequent analyses, however, we used the modified suitability index for Ethiopia "FCSmod" and "VCSmod".

Table 4.2
Proportion of population in the malaria free class under different minimum temperature lower limits for the vector's niche.

	Temperature and rainfall based				**Temperature based**			
Lower limits	**3 months**		**3 (or 5) months**		**3 months**		**3 (or 5) months**	
	Pf [a]	***Pv*** [b]	***Pf*** [c]	***Pv*** [d]	***Pf*** [e]	***Pv*** [f]	***Pf*** [g]	***Pv*** [h]
4 ºC	27.81%	11.79%	30.21%	13.44%	27.81%	11.79%	30.49%	13.46%
5 ºC	27.81%	11.79%	30.21%	13.44%	27.81%	11.79%	30.49%	13.46%
6 ºC	27.81%	12.28%	30.21%	13.91%	27.81%	12.28%	30.49%	13.93%
7 ºC	27.82%	17.53%	30.22%	18.27%	27.82%	17.53%	30.50%	18.33%
8 ºC	**31.06%**	**28.44%**	**33.26%**	**28.44%**	**31.06%**	**28.44%**	**33.59%**	**28.73%**
9 ºC	40.12%	39.44%	40.74%	39.16%	40.12%	39.44%	41.08%	39.51%
10ºC	53.65%	53.48%	53.49%	53.03%	53.65%	53.48%	53.94%	53.48%

By raising the Tmin lower limit for the coldst month to 8ºC the malaria free population remains around the observed histroic malaria free zone 30%, and the suitability for *Pv* is reduced to realistic values as compared to *Pf*. The columns in the table correspond to FCS and VCS based on the standard climate variables and requiring 3 consecutive months of suitability (columns a and b), reqiuring 3 month in the north and 5 in the southern part (column c and d); FCS and VCS based on suitable temperature only and requiring 3 consecutive months (columns e and f), and reqiuring 3 month in the north and 5 in the southern part (column g and h).

The striking difference between the HADCM3 from Hay *et al.* (2006), and from our study is shown in Figure 4.5. In the coarse resolution from the HADCM3 and other climate change scenario's (275 x 275 km) Ethiopia consists of less than 20 pixels. Even in the high resolution surface Hay *et al.* (2006) used as their climatology, Ethiopia has only 768 pixels, compared to over 100.000 in the climatology we developed. In the "up-sampled" results from Hay *et al*. (2006), Ethiopia's malaria suitability is greatly overestimated, with scarcely any population remaining in the malaria free territory. This

further demonstrates the inadequacy of the methods Hay *et al*. (2006) selected to assess the impact of climate change in highland areas Fig. 4.5).

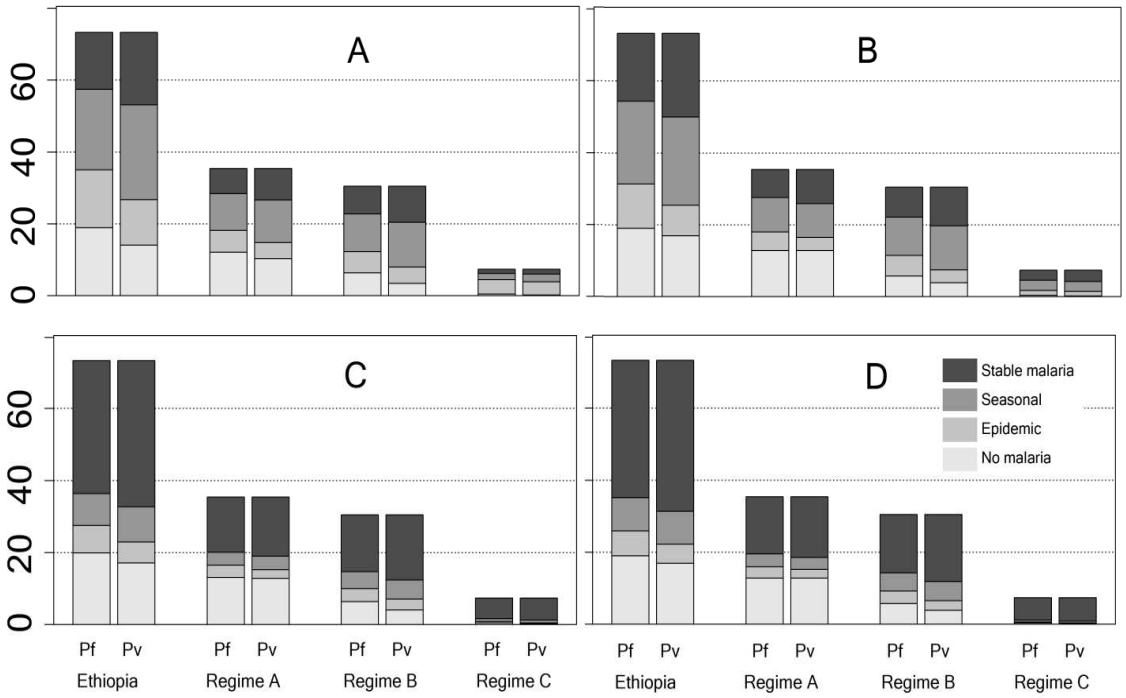

Figure 4.6: 2015 (rural) population distributed in the four *P. falciparum* (*Pf*) and *P. vivax* (*Pv*) epidemiological classes based on the 1961-1990 climatology for Ethiopia and the three rainfall regimes; based on (A) temperature and rainfall suitability in 3 (or 5 if south of 8^{o}N) consecutive months, (B) temperature and rainfall suitability in 3 consecutive months, (C) temperature only in 3 (or 5 if south of 8^{o}N) consecutive months, (D) in 3 consecutive months; all with minimum temperature limit set at 8^{o}C. The four epidemiological classes represent (from top to bottom) areas with FCS greater than or equal to 0.75, between 0.25 and 0.75, greater than 0 and less than 0.25, and equal to 0.Proportion of population in regions with stable malaria seems too high in plot C and D, indicating temperature suitability index's struggles to capture malaria suitability in dry, low altitude regions without rainfall complementing.

We have by-passed the up-sampling problem by adding anomalies to our fine scale climatology, thus retaining the information on the sharp altitudinal variations of the Ethiopian landscape. These anomalies were calculated from the scenario outputs of the coarse scale scenario's (HADCM3 and the ensemble of 20 GCM's) with the base-line

climatology (See methods). Our "local" baseline climatology (Fig 4.5) shows higher levels of FCS compared to New *et al*. climatology for the 1960-1990 baseline calculated by Hay *et al.* (2006). This is possibly due to the differences in resolution (of the order of 10).

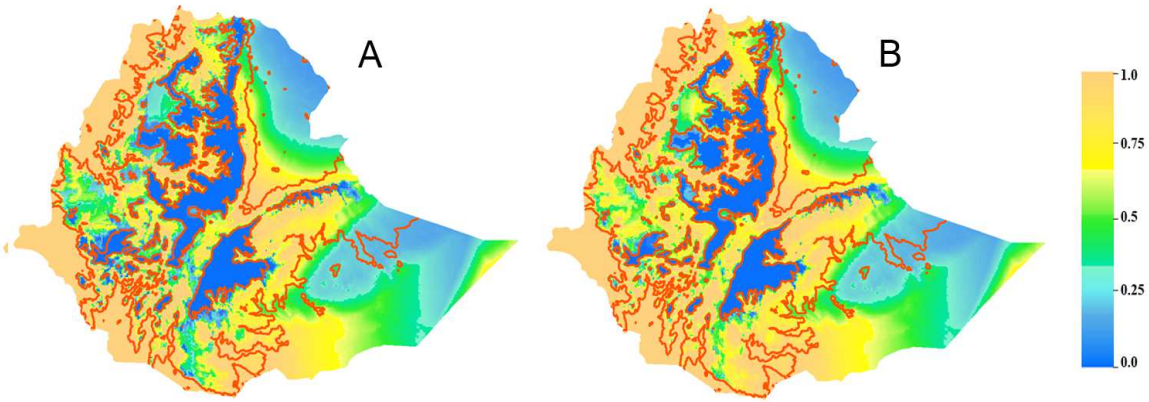

Figure 4.7: Improved fuzzy suitability index for *P. falciparum* malaria (A) and *P. vivax* (B), lasting for 3 consecutive months for all of Ethiopia and of the Tmin for the coldest month increased to 8^{o}C.

We estimated changes to population living in the four suitability classes based on *P. falciparum* and *P. vivax* suitability (FCSmod and VCSmod) by applying constant increases of local temperature at 1, 2, and 3^{o}C and same amount of increase in global mean temperatures Fig. 4.8). For the global climate change projections we tested an ensemble of 20 GCM 's models and HADCM3. Our results show a consistent shift to populations living under higher stability of malaria transmission. This is the case for both parasites and in all scenarios.

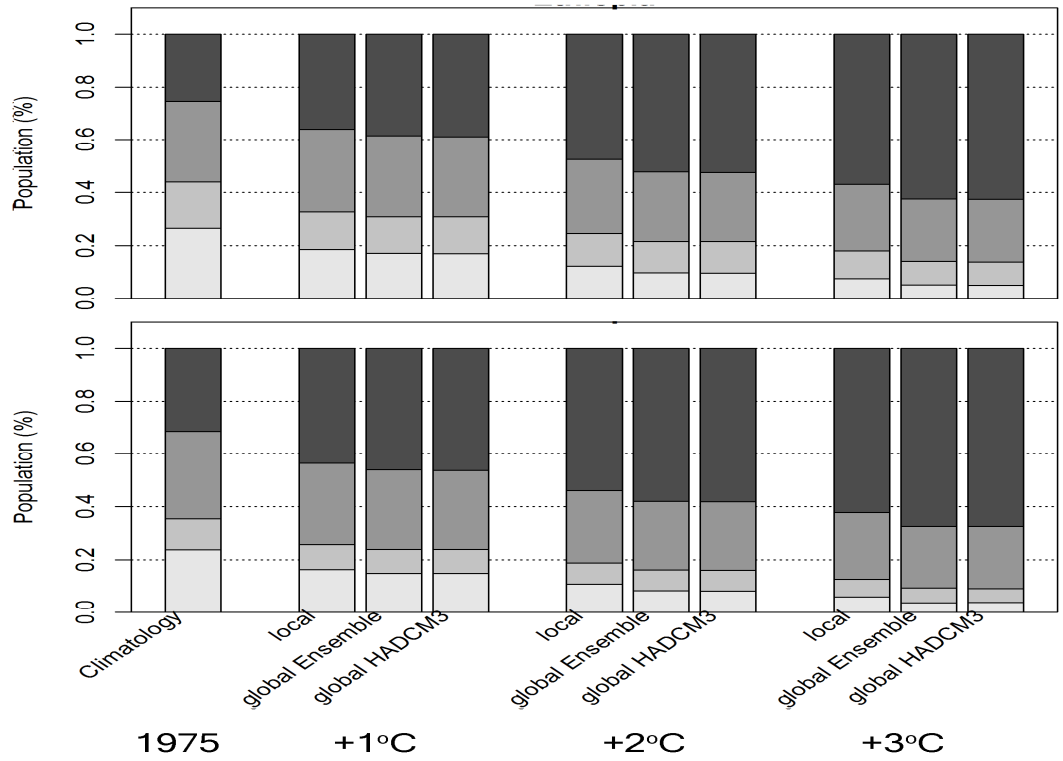

Figure 4.8: Comparisons of changes in population distribution (rural) over different epidemiological classes based on *P. falciparum* suitability index (panel 1) and *P. vivax* suitability index (panel 2) due to climate change assuming increases in the mean local and global (change in the global mean) air temperature of 1ºC, 2ºC and 3ºC. Both HADMC3 and the ensemble mean projection have the years 2036, 2065 and 2087 as the years of global mean temperature increase (over the those centered on 1975) by 1ºC, 2ºC and 3ºC respectively. The global climate projection results were up-sampled from 2.5º x 2.5º resolution before being applied to our base climate suitability based on the 1961-1990 climatology at 2.5' x 2.5'.

Effects of the lower resolution projections are still visible in the observed slightly higher suitability estimates compared to our "local" climatology. With a 3ºC increase in the HADCM3 based climate projection, of the 30 million people who are in malaria free areas based on the 1061-1990 climatology (centered on 1975), an estimated 26 million people (84%) will become exposed to malaria, with more than 40 million additional people living in areas of stable malaria transmission (see Figure 4.8).

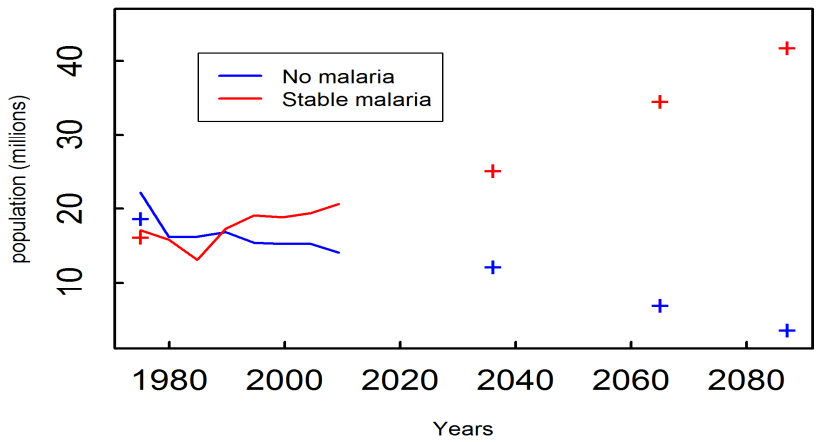

Figure 4.9: Population (rural 2015 estimates) residing in areas that are free of malaria (blue line) and stable malaria (red line) for *P. falciparum* by years in a five-year sliding window on every five year step between 1973 and 2008 (146 stations), based on combined population of the two larger rainfall regimes A and B. Climatology (centered at 1975) and future population in malaria-free territory (blue cross), and stable malaria territory (red cross) under climate change scenario A2 (HADCM3) with temperature rises of 1, 2 and 3°C projected for 2036, 2065 and 2087 respectively.

Finally, to assess the impact of warming that has already occurred, we used the rural populations of the two large rainfall regimes (see Fig. 1.2, A and B) in Ethiopia to generate suitability index values for five year sliding windows beginning in 1971 and ending in 2010, and computed population falling in the different epidemiological classes (Fig. 4.9). Compared to the climatology of 1975, an estimated 8 million new rural people were exposed to malaria risk in the period up to 2010. At the same time, 3.5 million new people (rural) shifted into the highest (stable) malaria risk class. Table 4.3 gives the numbers of people entering the "stable" malaria class, and the associated mortality (See section 4.2.4 in methods section), since 1975. Projections for 2036, 2065 and 2087 relate to warming of 1, 2 and 3°C under the HADCM3 (with A2 scenario of high emissions) projections for Ethiopia.

Table 4.3
Rural population in regimes A and B, transitioning to endemic (stable) malaria transmission class for in the 21 century, and the corresponding annual death associated with the shifts by age groups.

	Persons shifting to the stable malaria condition (x 1000)				Annual deaths by age group			
Year	0 to 4	5 to 14	>15yr	All ages	0 to 4	5 to 14	>15 yr	All ages
2010	524	949	2,081	3,554	1,371	892	1,478	3,741
2036	1,314	2,381	5,224	8,919	3,441	2,238	3,708	9,387
2065	2,705	4,901	10,752	18,358	7,083	4,607	7,633	19,322
2087	3,769	6,829	14,981	25,580	9,869	6,419	10,635	26,924

The years 2036, 2065 and 2087 are years at which global mean temperature is projected to increase by 1ºC, 2ºC and 3ºC from those centered in 1961-1990 (centered on 1975) respectively, based on HADCM3 under high A2 emission scenario.

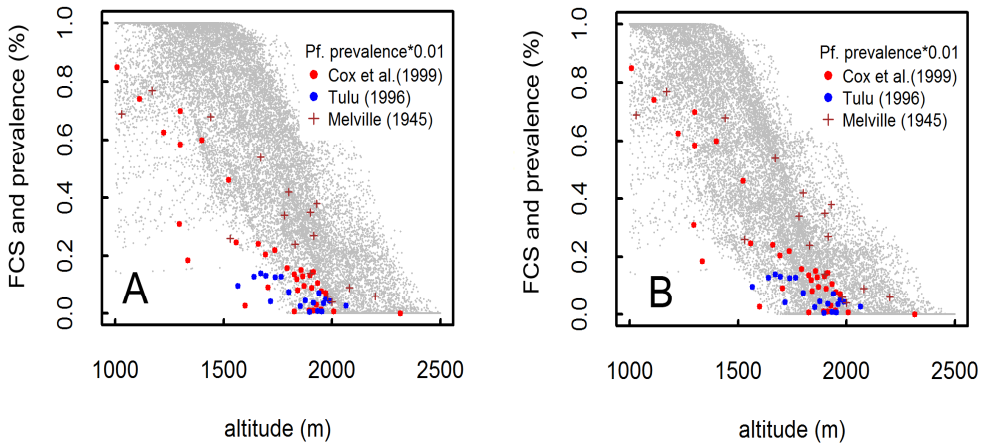

Figure 4.10: The 1975 centered climatology based FCS by altitude at each grid between 1000 and 2500m in altitude, and prevalence survey results compiled by Cox *et al*. (1999) (red), Tulu (1996) (blue) and Melville *et al*. (1945) (cross) by taking lower and upper mean temperature limits of (A) 18ºC and 22ºC (standard) and (B) 19ºC and 23ºC for the fuzzy suitability for parasite inside the vector; based on the two larger regimes A and B.

Recognizing that climate suitability has both lower and upper limits of temperature, we examined the effect of increasing temperature on areas already near the upper limits of temperature. Regime C, in the South East of Ethiopia provides a good case where increasing temperature by 2 and 3oC causes suitability to stabilize and start

reversing. This is due to the (see Fig. 4.11, A). This is due to part of the regime being pushed out of the suitable temperature range above the higher limit which we have lowered for this experiment to 33ºC, and fuzzy decrease starting at 28ºC (Mordecai *et al*., 2013).

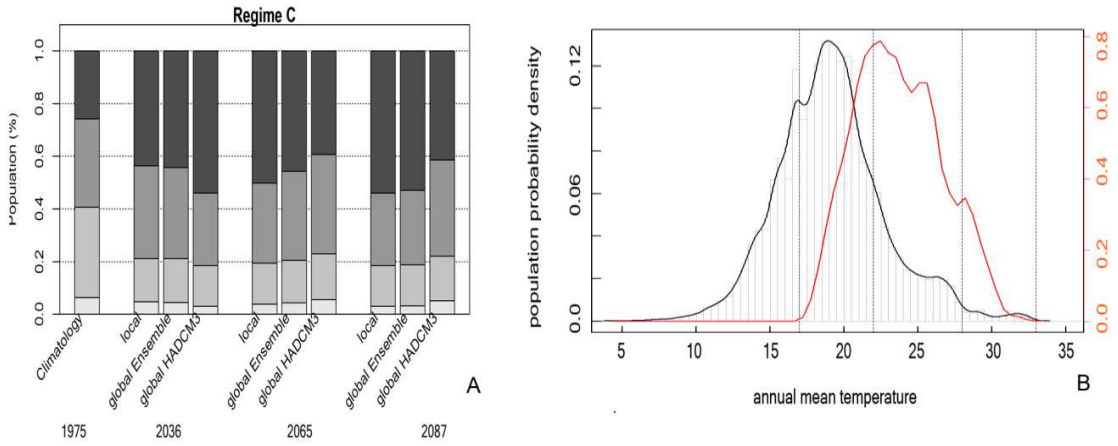

Figure 4.11: (A) Distribution of population in the regime C, hot dry part of Ethiopia, in 21st century based on a modified FCS using mean temperature limit of 33ºC and fuzzy decrease starting at 28ºC (Mordecai et al., 2013). Suitability stabilizes at 2ºC and 3ºC increases after a sharp increase for 1ºC increase. (B) Distribution of Ethiopia's population by mean annual temperature gradients binned at every 0.5ºC. Dotted vertical line show the increasing and decreasing fuzzy temperature limits, the latter modified based on Mordecai *et al.* (2013). This graph clearly shows with increase of 1, 2, 3, 4, 5ºC mean annual temperature, the Ethiopia's population niche and that the malaria niche are coming together, causing dramatic increases in population at risk of malaria.

At the national level, however, the net effect of climate warming is clearly increasing malaria risk, even with the modified lowered upper limit of temperature (see Fig. 4.11, B). Comparison of population entering and leaving the suitable temperature range shows that, at 3oC increase in the mean annual temperature, an additional 26 million will enter while only .75 million will leave the malaria suitable temperature range (between 18 and 33ºC) (see Table 4)..

Table 4.4
Ethiopian population entering and leaving the lowered malaria suitable temperature range of 18 to 33ºC (in millions)

		Climatology	+1oC	+2oC	+3oC
Leaving	Population	0	0.208	0.551	0.751
18-33ºC	Change	0	0.207	0.551	0.751
Entering	Population	61.391	71.606	81.262	88.119
18-33ºC	Change	0	10.215	19.871	26.728
Net			10.008	19.32	25.977

4.4 Discussion

Unstable highland malaria with fulminant epidemics in Ethiopia have been documented since the 1950s (e.g. Fontaine *et al*., 1962), with a pause during the era Ethiopia attempted eradication in the 1960 and 70s. Since 1992 a trend of more frequent epidemic episodes have occurred in some parts of the country, some localized, and in other parts with sustained higher transmission rates (Kiszewski and Teklehaimanot, 2004). This echoes the findings of a dramatic rising trend with intermittent interannual exacerbations in the Debre Zeit region of Oromia (Tulu, 1996), located in region A of this study, and our study region described in chapter 1. Kiszewski and Teklehaimanot (2004) offer no explanation for their observation that "a transition appears underway to higher levels of endemicity" in Ethiopia, whereas Tulu (1996) has pointed to rising temperatures, particularly for the mean minimum temperatures. Findings of Abeku *et al.* (2003) that epidemics were significantly more frequent preceded by high minimum temperatures supports this finding.

Warming for the Ethiopian highlands since the 1980 has indeed been undisputed (see Siraj *et al*., 2014), and we have now shown that warming pushes malaria's distribution to higher altitudes (Siraj *et al.,* 2014). In this chapter we provide further evidence that raised temperatures provide the most likely explanation for the rise of malaria, and that persistent global warming threatens the privileged position of a large fraction of the Ethiopia population that live at malaria free altitudes.

Ethiopia is not the only country where highland malaria has become a serious public health problem. Highlands in Kenya, Uganda, and Tanzania all had their share of attention after the first serious climate change related malaria concerns were voiced from Madagascar (de Zulueta, 1988) and Ruanda (Loevinsohn, 1994). However, Ethiopia has the largest highland population on the continent, has the most reliable records with a large fraction of microscopically diagnosed cases, and the co-existence of *P.falciparum* with *P.vivax* that has shown a similar ascent. Serious drug resistance in *P.falciparum*, frequently blamed for Africa's malaria woes, does not apply to *P.vivax*. For these reasons, a thorough case study for Ethiopia is of significant importance, also for countries with less prominent highlands. Suitable methods to assess impact of climate change on vector borne disease could play an important role in guiding public health in mitigating populations at risk for the impacts of climate change.

Climate driven suitability models can be used to measure shift in malaria risk and disease burden for the country. GIS have played a great role in the last decades to map vector borne diseases, their vectors and help to study their environmental determinants (Thomson, 1996; Hay *et al.*, 1998). The standard climate suitability index for Africa was

here applied to Ethiopia, and adjusted to match the country's epidemiology. As the suitability index does not take into account the levels of malaria control, the historical prevalence survey data that predate most human intervention provided an important component in this validation process.

A three month window of successive suitable transmission months was adopted, instead of a three month window for the northern and a five month window for the southern part of the country. This division in the standard FCS to account for continental differences in the length of the transmission season between the parts of Africa N and South of 8 degrees introduced an unwarranted artificial jump in suitability. The critical minimum temperature for the coldest month was raised from 4 to 8 degrees to account for the limited altitudinal extension of *P.vivax* (more permissive for low temperatures than *P.falciparum*) that appeared greatly exaggerated when MARA's suitability model was applied. We infer that the vector (and its temperatures required to colonize an area), is the restrictive factor on high altitude, rather than the critical temperature for the *P. vivax* malaria parasite. Whether the empirical isotherm of 8 degrees in Ethiopia's corresponds with the frost-line (for which this parameter was designed) remains to be explored.

The validity of MARA's climate suitability index had been established in its extended HIMAL program (Cox *et al*., 1999) in African highland countries. However, the continental application of climate suitability (including Tanser *et al*, 2003; Hay *et al.*, 2006) generated serious interpretation difficulties and much acrimonious debate. It has probably discouraged others to pursue this method in regions where malaria is a relative simple disease such as in arid regions and highlands. In this study we have not included

the possible effects of changes in rainfall resulting from climate change. Changes in rainfall are part of the climate change scenario's, but contrary to the predictions for temperature there is considerable variation between these scenario's. Rainfall also modulates local temperatures, and changes in seasonal (physical) lapse rates may arise from changes in air moisture without actual rainfall. However, we do not foresee that changing in the seasonality of rainfall (rather than total rainfall) that are reported in response to climate change in East Africa, are likely to modify malaria risk. The relation between the FCS and parasite rates appears to have changed over the last century.

It has been argued that warming climate may also improve condition in areas near the higher limit of temperature suitability (Lafferty, 2009). By using a 30 year gridded monthly rainfall and temperature data for Africa, we show that increasing temperature has a net increasing effect on risk of malaria (see Figure 4.12, Table 4.5).

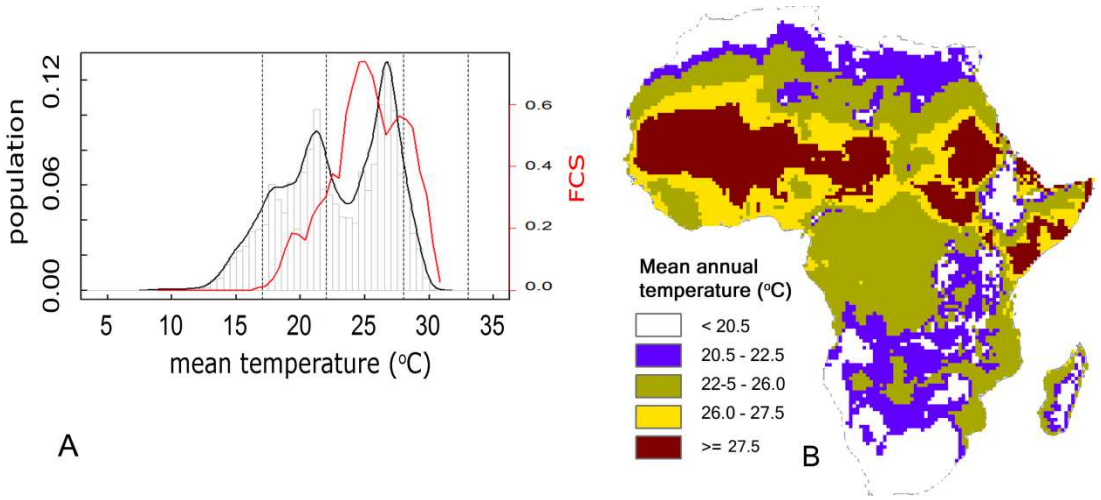

Figure 4.12: (A) Distribution of Africa's population by mean annual temperature gradients binned at every 0.5°C. Dotted vertical line show the increasing and decreasing fuzzy temperature limits, the latter modified based on Mordecai *et al.* (2013). (B) Map of annual mean temperature (°C) for Africa. The first graph clearly shows with increase of 1, 2 and 3 °C mean annual temperature, malaria niche seems to be coming closer to Africa's population niche especially for the lower peak, which includes regions in the East and Southern Africa (blue in B). Even for the larger peak, no net decrease occurs in the population at risk with increases of 1 and 2°C. the larger peak population includes regions in West Africa with temperature in the range of 26-27.5°C. Source: Climate data for Africa obtained from Harris *et. al.* (2014) at a resolution of 0.5° x 0.5°.

The effect of mean temperature increases in Africa is not much different from what we concluded for Ethiopia, with net increase in the number of people at risk of malaria (see Fig. 4.12, Table 4.5). . These results confirm that the effect of climate change is not limited to highland regions and it affects all regions in Africa. Two processes are believed to explain this result. First, as the mean annual temperature increases, malaria transmission may shift its seasonality by moving to mildly warm months causing regions to maintain their suitability for transmission. Second, despite the larger population peak happening in temperatures near the higher limit of malaria niche, African population also comprises of a significantly broad population to the left of the malaria niche curve that is poised to come closer to the malaria niche temperature ranges

as a result of increasing global temperature (Fig. 4.12, A). Table 4.5 further confirms the net effect of climate change on the population at risk of malaria, where an additional 95 million people will be exposed to the risk of malaria with 3ºC increase in the mean annual temperature.

Table 4.5
African population entering and leaving the lowered malaria suitable temperature range of 18 to 33ºC (in millions)

		Climatology	+1oC	+2oC	+3oC
Leaving	Population	0	0	0	0.193
18-33ºC	Change	0	0	0	0.193
Entering	Population	642.771	686.011	717.447	738.471
18-33ºC	Change	0	43.24	74.676	95.7
Net			43.24	74.676	95.507

The slope of the malaria lapse rate, apparent from surveys in the 1940 (de Melville *et al.*, 1945) with a very good match between suitability (0 to1) and prevalence (0 to 100%), gradually flattened in the later part of the century. This is visible Fig. 4.10) from the prevalence survey's between 1950 and 1980 uncovered by Cox *et al*. (1999) from the WHO archives, and the even "flatter" altitude related prevalence figures from the surveys of Tulu (1996) in the 1980s in the Debre Zeit area. The altitudinal malaria slope described by the malaria pioneers of the 19th century is still present in Ethiopia's most recent surveys (Bouma *et al.*, 2011). Interestingly, whereas the slope of the malaria lase rate has changed in the 20th century, most likely reflecting improved control of the

disease, the altitude a which malaria disappears has changed in the 20th century Fig. 4.10).

Our study in Chapter 1 (Siraj *et al.*, 2014) suggests that this is likely to change with global warming. Our finding of a dramatic shift in malaria risk under the high emission scenario's for the 21th century is likely, without breakthroughs in malaria control, to expose tens of millions of people to malaria for the first time. Warmer high risk malaria years in the East African highlands are associated with the years of El Nino (Bouma *et al.*, 1995), the climate system that periodically changes the global ocean and air circulation. An early warning system in Ethiopia based on this climate system can aid epidemic warning and timely intervention in conjunction with close monitoring of cases (e.g. Abeku *et al*., 2003; Teklehaimanot *et al*., 2004). It has been difficult to establish reliable mortality figures for regions at risk of epidemics (Cox *et al*., 2007), but epidemic mortality in Ethiopia in unprepared populations without adequate medical facilities may suffer mortalities exceeding 20% during a single epidemic event (Fontaine *et al*., 1962). Malaria early warning should therefore be a cornerstone of adaptation to climate change in East Africa.

Malaria is easiest to control and prevent where the disease in unstable as it is in the highland fringes. Effective intervention could therefore prevent most of the dramatic mortality associated with epidemic malaria. However, as warming increases the malaria exposure to those on lower altitudes intensifies. The burden of stable endemic malaria is most difficult to alleviate, but perhaps most accurate to establish. Child mortality, the most prominent feature of endemic malaria has remained rather stable during the 20th

century. Greenwood *et al* (1987) reported a mortality of 10.4 per 1000 per year in infants (1-4 year), a figure similar to that quoted 30 years earlier (Greenwood *et al.*, 1987). The more recent multi center (median) estimates for Africa we here used (described by Snow *et al*., 2003) are 9.3 per 1000 per year in areas with parasite prevalence rates over 25%. Perhaps the recent efforts and advances in controlling African malaria, that has seen mortality rates drop sharply since the beginning of this century, suggest that we could cautiously halve the mortality rates and the burden predicted for Ethiopia's warming in the 21th century.

CHAPTER FIVE: CONCLUSIONS

The Sub-Sahara African highlands are home for more than 165 million people (19% of sub-Saharan population below 15ºN), of which about 60 million live in areas higher than 2000m[3]. Historically, these highland regions have avoided stable malaria transmission due to their low mean temperature, which negatively effects parasite sporogony and vector development. Our results have shown that in highland regions of Ethiopia, inter-annual increases in temperature extend the spatial distribution of malaria cases to higher elevations. The implication is that global warming will increase the risk of contracting highland malaria, in regions among the most densely populated regions in Africa.

Based on the evidence from Ethiopian highlands, climate change appears to have already influenced the burden of malaria in these regions. We have shown that the change expected from increasing temperatures alone can account for the retrospective temporal trend in cases observed in the recent past. In the East African highlands, in particular, a strong temperature determined malaria lapse-rate persists. As the global temperature

---

[3] Our estimates based on GPW3 and GDEM calibrated and projected to 2015 using Ethiopia's data and growth rate for all locations south of 15ºN). Highlands in this case are areas with altitude higher than 1500m.

increases, countries such as Ethiopia with large populations at high elevation will have to deal with increased spread and intensity of malaria in areas that used to have no or little incidence.

Projected temperature changes for 2015 based on the IPCC global circulations models (MAGICC, 2014) seems to underestimate observed warming even under the high emission scenario A2. Despite that, our estimates based on these projections show a dramatic shift in malaria risk for the 21th century, where tens of millions of people in Ethiopia will be exposed to malaria for the first time.

With its two co-existing parasites, *P. falciparum and P. vivax*, showing similar patterns, Ethiopia also offers an opportunity to isolate the effect of drug resistance, which is frequently blamed for Africa's malaria woes, and is only applicable to *P. falciparum* (Tulu, 1996). In addition, the availability of most reliable records with a large fraction of microscopically diagnosed cases, Ethiopia is well positioned to provide significant lesson to other countries.

The suitability index we have improved in this project can easily be adapted to other regions especially in Africa where similar parasite and vector species exist. We have seen how, aided by artificially decreased maximum thermal limits, further warming could start slowing the observed worsening condition in areas where it is already hot. In Ethiopia, where very small proportion of its population lives in areas near the higher end of temperature suitability, this phenomenon could be negligible in the 21st century even

assuming a lowered maximum temperature limits. Similar effect can be expected in countries with large population living at high altitude.

The hypothesis that increasing temperature could improve conditions in areas already hot warrants careful study and rigorous evaluation, since increase in the mean temperature could also result in changes to the seasonality of the disease, where the vector, along with the disease transmission, shifts its niche to seasons that are mildly hot. However, even with no considerations of such changes, our results have demonstrated that, climate change will have a worsening effect on malaria, with far larger population being exposed to the risk of disease than those supposed to have lesser risk, both in Ethiopia and the entire African continent.

Recent decline in malaria incidence in many African countries in the last decade have been associated with intensive control measures including distribution of insecticide treated bed nets and provision of efficacious drugs (Otten *et al.*, 2009; Karema *et al.,* 2012). The evidences that the suppression of the disease was only possible with significant scaling up of interventions suggest that consolidation of these results through sustained interventions is imperative in order to avoid a possible resurgence, as has happened in the past (Sharma & Mehrotra 1986; Mouchet, 1998).

Elimination of malaria from countries where the intensity of transmission is high and stable such as in tropical Africa will require more potent tools and stronger health systems than are available today (Mendes *et al.*, 2009). In addition, malaria control and elimination are under the constant threat of the parasite and vector developing resistance

to medicines and insecticides, which are the cornerstones of current antimalarial interventions (Mendes *et al.*, 2009). In the absence of alternative tools, therefore, global malaria control and eradication will remain elusive.

As public health continues to witness significant reductions in malaria transmission through intensified control measures, the role of reservoirs of the pathogen will become more prominent in low transmission regions and seasons. Our findings have shown population density, along with temperature, as the main risk factors associated with pathogen reservoirs, through their contribution towards the persistence of the disease. Control measures would consist of targeting the spatial reservoir of the pathogen in humans (finding and treating symptomatic and non-symptomatic carriers) and/ or the vector (additional rounds of IRS). Such measures would improve cost effectiveness and aid existing initiatives to eliminate malaria from African highlands. These findings are believed to be relevant to other locations that are dealing with low intensity transmission in general, and those with seasonal malaria transmission as well as those affected by intermittent epidemic outbreak, in particular.

Future works

Implementation of climate based suitability is expected to inform countries with significant population at high altitude on what the potential effects of climate change could be. Since changes in the risk levels to population primarily concern population living at the fringes of climate suitability, which exhibit large variations within small geographic area, the required data on population distribution and climate factors need to

be at an appropriate spatial resolution. Geographic Information Systems (GIS) have played a great role in the last few decades in mapping vector borne diseases, their vectors and help to study their environmental determinants. Analysis of spatially coexisting natural and demographic factors, is essential in assess impact of vector borne disease in the face of changing global climate. GIS approaches to the analysis of climate and population distribution will continue to be useful. The lessons learned from Ethiopia, as a result of the availability of good quality data at high resolution, will serve as a springboard to implement similar studies in other malaria affected countries with significant population at risk of malaria.

Process-based models are increasingly confronted by retrospective temporal data to address specific hypotheses on the population dynamics of infectious diseases and the feasibility of their predictions. With the possibility of non-climatic factors confounding the effect of climate variability and climate change, in order to disentangle the effects of individual factors, process based models that couple human population dynamics and their vector counterpart will be in high demand in regions of rapidly changing topography. With the availability of large computational power improving by the day, the feasibility of process based models is no more in question.

Spatial factors of disease transmissions are poorly understood in the context of vector-borne diseases especially malaria. Movement of the pathogen among communities, through humans as well as the vectors, is greatly influenced by how close the communities are to each other, not just in physical distance but also in their social and economic interactions. These factors need to be considered when climatic and other

spatially explicit factors are examined in process based models as well as in more general spatio-temporal statistical models.

REFERENCES

Abeku TA, van Oortmarssen GJ, Borsboom J, de Vlas SJ, Habbema JDF 2003 Spatial and temporal variations of malaria epidemic risk in Ethiopia: factors involved and implications. *Acta Tropica* **87**, 331-340.

Alemu K, Worku A, Berhane Y, Kumie A. 2014. Men traveling away from home are more likely to bring malaria into high altitude villages, Northwest Ethiopia. *PLoS ONE*. **9**, e95341

Alonso D, Bouma MJ, Pascual M 2011 Epidemic malaria and warmer temperatures in recent decades in an East African highland. Proc. Biol. Sci. 278, 1661–1669.

Anderson RM, May RM, Anderson B. 1992. *Infectious diseases of humans: Dynamics and Control*. Oxford Science Publications.

Barry RG 1994 *Mountain Weather and Climate*. 2nd revised Edition. Routledge, London. pp. 206–298.

Baskerville EB, Bedford T, Reiner RC, Pascual M 2013 Nonparametric Bayesian grouping methods for spatial time-series data. http://arxiv.org/abs/1306.5202.

Batjes NH 2005 ISRIC-WISE Global dataset of derived soil properties on a 0.5 by 0.5 degree grid (version 3.0). Report 2005/ 05, ISRIC – World Soil Information, Wageningen (with dataset).

Bauleni A, Wong J, Wiegand R, Howell P, Zoya J, Chiphwanya J, Mathanga DP. 2015. A cohort study of the effectiveness of insecticide treated bed nets to prevent malaria in an area of moderate

Bayou MN, Lindsay SW 2003. Effect of temperature on the development of the aquatic stages of Anopheles gambiae sensu stricto (Diptera: Culicidae). *Bulletin of Entomological Research* 2003. 93,375-381.

Bejon P, Williams TN, Nyundo C, Hay SI, *et al*. 2014 A micro-epidemiological analysis of febrile malaria in coastal Kenya showing hotspots within hotspots. *eLIFE*. **3**, e02130.

Bertuzzo E,Mari L, Righetto L, Gatto M, Casagrandi R, Blokesch M, Rodriguez-Iturbe I, Rinaldo A. 2011 Prediction of the spatial evolution and effects of control measures for the unfolding Haiti cholera outbreak. *Geophysical Research Letters*. **38**, L06403.

Besag J, Green P, Higdon D, Mengersen K 1995 Bayesian Computation and Stochastic Systems. *Statistical Science*. **10**, 3-66.

Bomblies A, Duchemin JB, Eltahir EAB 2008 Hydrology of malaria: Model development and application to a Sahelian village. *Water Resour. Res.*, **44**, W12445.

Bouma MJ 2003 Methodological problems and amendments to demonstrate effects of tempera-ture on the epidemiology of malaria. A new perspective on the highland epidemics in Madagascar, 1972-89. Trans. R. Soc. Trop. Med. Hyg. 97, 133–139.

Bouma MJ, Baeza A, ter Veen A, Pascual M 2011Global malaria maps and climate change: A focus on East African highlands. *Trends Parasitol.* **27**, 421–422.

Bouma MJ, C. Dye 1997. Cycles of malaria associated with El Niño in Venezuela. *JAMA* **278**, 1772–1774.

Bouma MJ, Pascual M 2014 Global warming and malaria in tropical highlands – An estimation of Ethiopia's "unmitigated" annual malaria burden in the 21th century.. In Ed. Butler CD. *Climate change and global health*, CABI, Wallingford/Boston.

Bouma MJ, Sondorp HE van der Kaay HJ 1994 Climate change and periodic epidemic malaria. Lancet **343**, 1440.

Bradley J, Rehman AM, Schwabe C, Vargas D, Monti F, Ela C, Riloha M, Kleinschmidt I. 2013. Reduced Prevalence of Malaria Infection in Children Living in Houses with Window Screening or Closed Eaves on Biko Island, Equatorial Guinea. *PLoS ONE.* **8**, e80626

Bruce-Chwatt LJ. 1987 Malaria and its control: Present situation and future prospects. *Ann. Rev. Public Health.* 8, 75-110

Buckee CO, Wesolowski A, Eagle N, Hansen E, Snow RW 2013 Mobile phones and malaria: modeling human and parasite travel. *Travel Med Infect Dis*. **11**: 15–22.

Chaves LF, Koenraadt, CJM 2010 Climate change and highland malaria: Fresh air for a hot debate. *Q. Rev. Biol.* **85**, 27–55.

Choi HW, Breman JG, Teutsch SM, Liu S, Hightower AW, Sexton JD. 1995 The Effectiveness of Insecticide-Impregnated Bed Nets in Reducing Cases of Malaria Infection: A Meta-Analysis of Published Results. *Am J Trop Med Hyg.* 52, 377-382

CIESIN (Center for International Earth Science Information Network), Columbia University; and CIAT (Centro Internacional de Agricultura Tropical). 2005. Gridded Population of the World Version 3 (GPWv3): Population Density Grids. Palisades, NY: Socioeconomic Data and Applications Center (SEDAC), Columbia University. Available at http://sedac.ciesin.columbia.edu/gpw. (Accessed on April 05, 2014)

Clements AN. 1992. *The Biology of Mosquitoes.* Chapman & Hall.

Corradetti A. 1938. Richerche epidemiologiche sulla malaria nella regione di Oullo-Jeggui durante la stagione delle pioggi. *Riv malar.* **17**, 101

Corradetti A. 1940. L'epidemiologia de la malaria nella regione Uollo Jeggui (A.O.I) *Riv.Malar*. 19: 1

Cox J, Craig M, le Sueur D, Sharp B 1999 Mapping Malaria Risk in Africa/Highland Malaria Project (MARA/HIMAL) Technical Report (Mapping Malaria Risk in the Highlands of Africa, MARA, Durban, South Africa; and the London School of Hygiene and Tropical Medicine, London).

Cox J, Hay SI, Abeku AA, Checchi F, Snow RW. 2007. The uncertain burden of *P.falciparum* epidemics in Africa. *Trends Parasit* **23**, 142-148.

Craig MH, Snow RW, le Sueur D 1999 A climate-based distribution model of malaria transmission in Sub-Sahara Africa. *Parasitology Today*. **15**, 105-111.

CSA, Central Statistical Authority 1996 The 1994 population and housing census of Ethiopia. Results for Oromia Region. Volume I. Addis Ababa, Ethiopia: *Central Statistics Authority*.

CSA, Central Statistical Authority 2008 The 2007 population and housing census of Ethiopia. Statistical Report for Oromia Region. Addis Ababa, Ethiopia: *Central Statistics Authority*.

De Zulueta J, Kafuko GW, Cullen JR, Pedersen CK 1961 The results of the first year of a malaria eradication pilot project in Northern Kigezi (Uganda). East Afr. Med. J. 38, 1–26.

De Zulueta J. 1988. Rapport de mission effectuee a Madagascar, 28 Julliet-13Sept 1988. Geneva, World Health Organization.

Detinova TS 1962 *Age-grouping methods in Diptera of medical importance, vol. 47. World Health Organization Monograph Series*. Geneva, Switzerland: World Health Organization.

Diro GT, Grimes DIF, Black E. 2010. Teleconnections between Ethiopian summer rainfall and sea surface temperature: part I—observation and modelling. *Clim Dyn,* **37**,103–119

Diro GT, Black E, Grimes DIF. 2008. Seasonal forecasting of Ethiopian spring rains. *Meteorol. Appl*. **15**: 73–83

Dobson A 2004 Population dynamics of pathogens with multiple host species. *The American Naturalist*, **164**, S64-S78.

ESRI (Environmental Systems Research Institute). 2013. *World Lakes. Data & Maps for ArcGIS.* ESRI. Redlands, USA.

FAO (Food and Agriculture Organization of the United Nations). 2014. FAO GEONETWORK. Perennial Water Courses (Rivers) of the World (Vmap0) (GeoLayer). (Latest update: 18 Feb 2014) (accessed on April 13, 2015). http://data.fao.org/ref/c0c0dfa0-88fd-11da-a88f-000d939bc5d8.html?version=1.0

FAO/IIASA 2011 Global Agro-ecological Zones (GAEZv3.0). FAO, Rome, Italy and IIASA, Laxenburg, Austria.

Fontaine RE, AE Najjar, JS Prince. 1962. The 1958 malaria epidemic in Ethiopia. Am J *Trop Med Hyg*. 10: 795-803.

Gething PW, P Van Boeckel T, Smith DL, Guerra CA, Patil AP , Snow RW, Hay SI. 2011 Modelling the global constraints of temperature on transmission of Plasmodium falciparum and P. vivax. *Parasites & Vectors 2011,* **4**, 92

Gething PW, Smith DL,Patil AP, Tatum AJ, Snow RW, Hay SI. 2010. Climate change and the global malaria recession. *Nature*, 465: 342-345.

Ghebreyesus TA, Haile M, Witten KH, Getachew A, Yohannes AM, Yohannes M, Teklehaimanot HD, Lindsay SW, Byass P 1999 Incidence of malaria among children living near dams in northern Ethiopia: community based incidence survey. *BMJ*. **319**, 663–666.

Gill CA. 1923. The prediction of malaria epidemics. *Indian Journal of Medical Research,* 10, 1136-1143.

Gissila T, Black E, Grimes DIF, Slingo JM 2004 Seasonal forecasting of the Ethiopian summer rains. *Int. J. Climatol*. **24**, 1345–1358

Greenwood BM, Bradley AK, Greenwood AM, Byass P, Jammeh K, Marsh K,Tulloch S, Oldfield FSJ, Hayes R. 1987. Mortality and morbidity from malaria among children in a rural area of The Gambia, West Africa. Transaction Roy Soc Trop Med Hyg. 81:478-486.

Hahn MB, Gangnon RE, Barcellos C, Asner GP, Patz JA 2014 Influence of Deforestation, Logging, and Fire on Malariain the Brazilian Amazon. *PLoS ONE*. **9**, e85725

Harris I, Jones PD, Osborn TJ, Lister DH. 2014. Updated high-resolution grids of monthly climatic observations – the CRU TS3.10 Dataset. *Int. J. Climatol*. **34**, 623-642

Hastings W. 1970. Monte Carlo sampling methods using Markov chains and their applications. *Biometrika*. **57**, 97- 109.

Hay SI, Cox J, Rogers DJ, Randolph SE, Stern DI, Shanks GK, Myers MF, Snow RW 2002a Climate change and the resurgence of malaria in the East African highlands. *Nature* **415**, 905–909.

Hay SI, Rogers DJ, Randolph SE, Stern DI, Cox J, Shanks JD, Snow RW. 2002b. Hot topic or hot air? Climate change and malaria resurgence in East African highlands. *Trends Parasitol*. 18, 530–534

Hay SI, Guerra CA, Tatem AJ, Atkinson PM, Snow RW. 2005. Urbanization, malaria transmission and disease burden in Africa. *Nat Rev Microbiol* **3,** 81-90.

Hay SI, Snow RW, Rogers DJ. 1998. Prediction of malaria seasons in Kenya using multi-temporal meteorological satellite sensor data. *Trans. R. Soc. Trop. Med. Hyg*. **92**, 12–20

Hay SI, Tatem AJ, Guerra CA, Snow RW. 2006. Population at malaria risk in Africa: 2005, 2015 and 2030. Foresight publication, Infectious diseases: preparing for the future. Office of science and innovation. Department of trade and industry, UK.

Hirsch A, Creighton C 1983 *Handbook of Geographical and Historical Pathology. Vol. 1 Acute Infective Diseases*. The New Sydenham Society, London, First edition.

Hofstra N, Haylock M, New M, Jones P, Frei C 2008 Comparison of six methods for the interpolation of daily, European climate data. *Journal of Geophysical Research*, **113**, D21110

Hulme M, Wigley TML, Barrow EM, Raper SCB, Centella A, Smith SJ, Chipanshi AC. 2000. Using climate scenario generator for vulnerability and adaptation assessments: MAGICC and SCENGEN Version 2.4. Workbook. *Climate Research Unit*, Norwich, UK, 52pp.

IRI (International Research Institute for Climate and Society) 2014a Data Library. http://iridl.ldeo.columbia.edu/SOURCES/.Indices/.nino/.EXTENDED/.NINO34/ (accessed on March 15, 2014).

IRI (International Research Institute for Climate and Society) 2014b Data Library. http://iridl.ldeo.columbia.edu/expert/SOURCES/.IRI/.Analyses/.USGS/.ADDS/.NDVI/.NDVIg/.deg0p1/.monthly/.c8204/.avgNDVImonavg/ , (accessed on March 15, 2014).

Jeffreys H. 1946. An invariant form for the prior probability in estimation problems. *Proc. R. Soc. London A Math. Phys. Sci*. **186**, 453–461

McCarthy JJ, Canziani OF, Leary NA, Dokken DJ, White KS, Climate Change. 2001: Impacts, Adaptation and Vulnerability – Contribution to Working Group II to the Third Assessment Report of the Intergovernmental Panel on Climate Change (Cambridge Univ. Press, Cambridge).

Karema C, Aregawi MW, Rukundo A, Kabayiza A, et al. 2012 Trends in malaria cases, hospital admissions and deaths following scale-up of anti-malarial interventions, 2000–2010, Rwanda. *Malaria Journal*. **11**.

Karunaratne SHPP, Hemingway J. 2001. Malathion resistance and prevalence of the malathion carboxylesterase mechanism in populations of mosquito vectors of disease in Sri Lanka. *Bulletin of the World Health Organization*. 79, 1060-64

Kazembe LN 2007 Spatial modelling and risk factors of malaria incidence in northern Malawi. *ActaTropica*. **102**, 126-137.

Keiser J, Utzinger J, de castro MC, Smith TA, tanner M, Singer BH. 2004 Urbanization in sub-Saharan Africa and implication for malaria control. *Am. J. Trop. Med. Hyg.*, **71**, 118–127

Kirby MJ, Lindsay SW. 2004. Responses of adult mosquitoes of two sibling species, Anopheles arabiensis and A. gambiae s.s. (Diptera: Culicidae), to high temperatures. *Bulletin of Entomological Research*. 94, 441-448.

Kiszewski AE, Mellinger A, Spielman A, Malaney P, Sachs SE, Sachs J 2004 A global index representing the stability of malaria transmission. *Am. J. Trop. Med. Hyg.* **70**, 486-498.

Kiszewski AE , Teklehaimanot A 2004. A review of the clinical and epidemiological burden of epidemic malaria. *Am. J. Trop. Med. Hyg*. **71**, 128-135.

Korecha D, Sorteberg A. 2013. *Construction of Homogeneous Rainfall Regimes for Ethiopia.* In Characterizing the Predictability of Seasonal Climate in Ethiopia, PhD Thesis: University of Bergen.

Krige, DG 1951 A statistical approach to some basic mine valuation problems on the Witwatersrand, *J. Chem. Metall. Min. Soc. S. Afr.* **52**, 119–139.

Lafferty, KD. 2009. The ecology of climate change and infectious diseases. *Ecology.* **90**, 888-900

Laveran A 1893 Paludism The New Sydenham Society, London.

Lawless JF 1987 Negative binomial and mixed Poisson regression. *The Canadian Journal of Statistics*. **15**, 209-225

le Sueur D et al .1988 The breeding requirements of three members of the Anopheles gambiae (Giles complex in the endemic malaria area of Natal South Africa. Bull Entomol Res, 78, 549-560.

Lenoir J, Gégout JC, Marquet PA, de Ruffray P, Brisse H 2008 A significant upward shift in plant species optimum elevation during the 20th century. *Science* **320**, 1768–1771

Lindblade KA, Walker ED, Onapa AW, Katungu J, Wilson ML 2000 Land use change alters malaria transmission parameters by modifying temperature in a highland area of Uganda. *Trop. Med. Int. Health* **5**, 263–27.

Lindblade KA, Mwandama D, Mzilahowa T, Steinhardt L, Gimnig J, Shah M, 2015. Pyrethroid resistance, Malawi. *Malaria Journal*. **14**, 31

Lindsay SW, Birley MH 1996 Climate change and malaria transmission. *Ann. Trop. Med. Par-asitol.* **90**, 573–588.

Lindsay SW, Emerson P, Charlwood JD. 2002. Reducing malaria by mosquito-proofing Houses. *Trends in Parasitology*. **18**,510-514.

Lindsay SW, Martens WJM 1998 Malaria in African highlands: past, present and future. *Bulletin of the World Health Organization*. **76**: 33-45

Loevinsohn ME 1994 Climatic warming and increased malaria incidence in Rwanda. *Lancet* **343**, 714–718.

Longini IM, Jr. 1988 A mathematical model for predicting the geographic spread of new infectious agents. *Math Biosci* **90**, 367-383.

Lowe R, Bailey TC, Stephenson DB, Graham RJ, Coelho CAS, Carvalho MS, Barcellos C. 2011 Spatio-temporal modelling of climate-sensitive disease risk: towards an early warning system for dengue in Brazil. *Computers & Geosciences*, **37**, 371–381.

Lowe R, Bailey TC, Stephenson DB, Jupp TE, Graham RJ, Barcellos C, Sá Carvalho M 2013 The development of an early warning system for climate-sensitive disease risk with a focus on dengue epidemics in Southeast Brazil. *Statist. Med*. **32**, 864–883.

Lunn DJ, Thomas A, Best N, Spiegelhalter D. 2000. WinBUGS - A Bayesian modelling framework: Concepts, structure, and extensibility. *Statistics and Computing*. **10**, 325-337.

Mabaso MLH, Sharp B, Lengeler C. 2004. Historical review of malarial control in southern African with emphasis on the use of indoor residual house-spraying. *Tropical Medicine and International Health*. **9**, 846–856

MacDonald G 1957 *The Epidemiology and Control of Malaria*. Oxford, UK: Oxford University Press.

MAGICC (Modeling for the Assessment of Greenhouse-gas Induced Climate Change). 2014. A regional climate scenario generator. http://www.cgd.ucar.edu/cas/wigley/magicc/ (Accessed on March 07, 2014).

Maheu-Giroux M, Castro MC. 2013. Impact of community-based larviciding on the prevalence of malaria infection in Dar es Salaam, Tanzania. PLoSONE. 8,e71638.

Martins PH, Lefebvre MG. 1995. Malaria and Climate: Sensitivity of Malaria Potential Transmission to Climate. *Ambio.* **24,** 200-207.

Martens WJM, Jetten TH, Focks DA. 1997. Sensitivity of malaria, schistosomiasis and dengue to global warming. *Climatic Change*. 35, 145-156

McMichael, AJ. 1996. *Human population health. Impacts, adaptations, and mitigation of climate change*. New York: Cambridge University Press, 1996:559-84.

Melville AR, Bagster Wilson D, Glasgow JP, Hocking KS. 1945. Malaria in Abyssinia. *East African Medical Journal*. **22**: 285-294.

Mendis K, Rietveld A, Warsame M, Bosman A, Greenwood B, Wernsdorfer WH. 2009. From malaria control to eradication: The WHO perspective. Trop Med Int Health, **14**, 802-809

Metropolis N, Rosenbluth A, Rosenbluth M, Teller A, Teller E. 1953. Equations of state calculations by fast computing machines. *Journal of Chemistry and Physics*. **21**, 1087-1092.

Mills JN, Ksiazek TG, Peters CJ, Childs JE 1999 Long-Term Studies of Hantavirus Reservoir Populations in the Southwestern United States: A Synthesis. *Emerging Infectious Diseases*. **5**,135-142.

MOH (Ministry of Health) 2001 *National Five-Year Strategic Plan for Malaria Prevention and Control in Ethiopia*.

MOH (Ministry of Health). 1999. *Guidelines for malaria epidemic prevention and control in Ethiopia.*

Molineaux L 1988 The epidemiology of malaria as an explanation of its distribution, including some implications for its control. In *Malaria: Principles and Practice of Malariology*. ed. WH Wernsdorfer, SI McGregor. Edinburgh, Churchill Livingstone. **2**, 913-998.

Montoya-Lerma J . Solarte YA, Giraldo-Calderón GI, Quiñones, F. Ruiz-López, RC. Wilkerson, R. González 2011 Malaria vector species. In *Colombia: A review. Mem. Inst. Oswaldo Cruz* 106 (suppl. 1), 223–238.

Mordecai EA, Paaijmans KP, Johnson LR, Balzer C, Ben-Horin T, Moor E, McNally A, Pawar S, Ryan SJ, Smith TC, Lafferty KD. 2013. *Ecology Letters*, **16**, 22–30.

Mouchet J, Faye O, Julvez J, Manguin S 1996 Drought and malaria retreat in the Sahel, West Africa. The Lancet. **348**, 1735-1736.

Mouchet J. 1998 Origin of malaria epidemics on the plateaus of Madagascar and the mountains of East and South Africa. *Bull Soc Pathol Exot.*. **91**, 64-6.

Murphy GS, Basri H, Purnomo, Andersen EM, Bangs MJ, Mount DL, Gorden J, Lal AA, Purwokusumo AR, Harjosuwarno S. 1993 Vivax malaria resistant to treatment and prophylaxis with chloroquine. *Lancet,* **341**, 96-100.

Najera JA, Gonzalez-Silva M, Alonso PL. 2011 Some Lessons for the Future from the Global Malaria Eradication Programme (1955–1969). *PLoS Med,* **8**, e1000412.

Negash K, et al. 2005. Malaria epidemics in the highlands of Ethiopia. *East African Med J*. 82, 186-192.

New M, Hulme M, Jones P. 1999. Representing 20th century space-time climate variability Part 1: Development of a 1961-90 mean monthly terrestrial climatology. *Journal of climat*e, **12**, 829-856.

NMSA (National Meteorological Services Agency). 2013. Climate Data observation, climate monitoring and long range forecast methods in Ethiopia. A paper presented at the World Meteorological Organization Workshop on Climate Monitoring with focus on Eastern and Southern Africa. http://www.wmo.int/pages/prog/wcp/wcdmp/documents/Ethiopia.pdf (accessed January 30, 2015)

NMSA (National Meteorological Services Agency) 2001. Initial National Communication of Ethiopia to the United Nations Framework Convention on Climate Change (UNFCCC).

Omumbo JA, Lyon B, Waweru SM, Connor SJ, Thomson MC 2011 Raised temperatures over the Kericho tea estates: Revisiting the climate in the East African highlands malaria debate. *Malaria Journal,* 10, 12.

Otten M, Aregawi M, Were W, Karema C, Medin C, Bekele W, Jima D, Gausi K, Komatsu R, Korenromp E, Low-Beer D, Grabowsky M 2009 Initial evidence of reduction of malaria cases and deaths in Rwanda and Ethiopia due to rapid scale-up of malaria prevention and treatment. *Malaria Journal,* **8**, 14.

Pampana E. 1969. *A textbook of malaria eradication*. London, Oxford University Press.

Parry ML, Canziani OF, Palutikof JP, van der Linden PJ, Hanson CE. 2007. *Contribution of Working Group II to the Fourth Assessment Report of the Intergovernmental Panel on Climate Change*, 2007. Cambridge University Press. Cambridge UK. New York USA

Pascual M, Bouma MJ, 2009 Do rising temperatures matter? *Ecology* **90**, 906–912.

Pascual M, Ahumada JA, Chaves LF, Rodo X, Bouma M 2006 Malaria resurgence in the East African highlands: temperature trends revisited. *Proc. Natl. Acad. Sci.* **103**, 5829–5834

Patz, JA, Campbell-Lendrum D, Holloway T, Foley JA. 2005. Impact of regional climate change on human health. *Nature*, **438**, 310-217.

Patz, JA, Hulme M, Rosenzweig C, Mitchell TD, Goldberg RA, Githeko AK, Lele S, McMichael AJ, Le Sueur D, 2002: Regional warming and malaria resurgence. *Nature*, 420, 627-628

Patz, JA, Olson SH 2006. Malaria risk and temperature: Influences from global climate change and local land use practices. *Proc. Natl. Acad. Sci. U.S.A.* **103**, 5635–5636.

Phillips EJ, Keystone JS, Kain KC. 1997. Failure of Combined Chloroquine and High-Dose Primaquine Therapy for Plasmodium vivax Malaria Acquired in Guyana, South America. *Clinical Infectious Diseases.* **23**,1171-3.

Pingel, TJ. 2010 Modeling Slope as a Contributor to Route Selection in Mountainous Areas. *Cartography and Geographic Information Science*, **37**, 137-148.

Pounds JA, Fogden MP, Campbell JH 1999 Biological responses to climate change on a tropical mountain. *Nature,* **398**, 611–615.

Poveda G, Rojas W, Quiñones ML, Vélez ID, Mantilla RI, Ruiz D, Zuluaga JS, Rua GL 2001 Coupling between annual and ENSO timescales in the malaria-climate associa-tion in Colombia. Environ. *Health Perspect.* **109**, 489–493.

Price MF 1994 Should mountain communities be concerned about climte change? In *Mountain Environments in Changing Climates,* Beniston M, Ed. Routledge, London, pp. 431–451.

Reiner Jr. RC, King AA, Emch M, Yunus M, Faruque AS, Pascual M 2012 Highly localized sensitivity to climate forcing drives endemic cholera in a megacity. *Proc. Natl. Acad. Sci. U.S.A*. **109**, 2033–2036.

Robert V, Macintyre K, Keating J, Trape JF, Duchemin JB, Warren M, Beier JC. 2003 Malaria transmission in urban sub-Saharan Africa. *Am J Trop Med Hyg*. **68**, 169–176

Shanks GK, Hay SI, Omumbo JA, Snow RW 2005 Malaria in Kenya's western highlands. *Emerg. Infect. Dis.* **11**, 1425–1432 (2005).

Sharma VP, Mehrotra KN. 1986. Malaria resurgence in India. Soc Sci Med. 1986.22,835-45

Sinka ME, Bangs MJ, Manguin S, Coetzee M, et al. 2010 The dominant Anopheles vectors of human malaria in Africa, Europe and the Middle East: occurrence data, distribution maps and bionomic précis. *Parasites and Vectors*. **3**, 117

Siraj AS, Santos-Vega M, Bouma MJ, Yadeta D, Ruiz Carrascal D, Pascual M 2014 Altitudinal Changes in Malaria Incidence in Highlands of Ethiopia and Colombia. *Science*, **343**, 1154-1158.

Siraj AS, Bouma MJ, Santos-Vega M, Yeshiwondim AK, Rothman DS, Yadeta D, Sutton PC, Pascual M. 2015. Temperature and population density determine reservoir regions of spatial persistence in highland malaria. Submitted to *The Proceedingss of the Royal Society – B*.

Smith PG, Morrow RH 1996 *Field trials of health interventions in developing countries: A toolbox*, 2nd Edition Macmillan Education Limited, London.

Snow RW, Craig MH, Newton, Steketee RW. 2003. The public health burden of Plasmodium falciparum malaria in Africa: Deriving the numbers. Working Paper No. **11**, Disease Control Priorities Project. Bethesda, Maryland: Fogarty International Center, National Institutes of Health.

Snow RW, Gouws E, Omumbo J, Rapuoda B, Craig MH, Tanser FC, le Sueur D, Ouma J. 1998. Models to predict the intensity of P.falciparum transmission: applications to the burden of disease in Kenya. *Transaction Roy Soc Trop Med Hyg*. **92**, 601-606.

Spiegelhalter DJ, Best NG, Carlin BP, van der Linde A. 2002 Bayesian Measures of Model Complexity and Fit (with discussion), *Journal of the Royal Statistical Society, Ser. B*. **64**, 583–639.

Stern DI, Gething PW, Kabaria CW, Temperley WJH, Noor AM, Okiro EA, Shanks GD, Snow RW, Hay SI 2011 Temperature and malaria trends in highland East Africa. *PLOS One* **6**, e24524

Stoddard ST, Forshey BM, Morrisson AC , Paz-Soldan VA, Vazquez-Prokopec GM, Astete H, Reiner RC, Vilcarromero S, Elder JP Halsey ES, Kochel TJ, Kitron U, Scott TW 2013. House-to-house human movement drives dengue virus transmission. *Proceedings of the National Academy of Sciences*, **110**: 994-999

Stone, S.W. 1998 Using a geographic information system for applied policy analysis: the case of logging in the Eastern Amazon. *Ecological Economics*. **27**, 43–61.

Stryker JJ, Bomlies A 2012 The Impacts of Land Use Change on Malaria Vector Abundance in a Water-Limited, Highland Region of Ethiopia. *EcoHealth*. **9**, 455–470

Tagliapietra V, Rosa R, Hauffe H, Laakkonen J, Voutilainen L, Vapalahti O, Vaheri A, Henttonen H, Rizzoli A 2009 Spatial and Temporal Dynamics of Lymphocytic Choriomeningitis Virus in Wild Rodents, Northern Italy. *Emerging Infectious Diseases*. **15**, 1019-1025**.**

Tanser FC , Sharp B, le Sueur D 2003 Potential effect of climate change on malaria transmission in Africa. *The Lancet*, **362**, 1792-1798.

Tanser FC, Pluess B, Lengeler C, Sharp BL. 2007. Indoor residual spraying for preventing malaria. (Protocol) *Cochrane Database of Systematic Reviews*. **3**, CD006657.

Tatem AJ, Huang Z, Narib C, Kumar U, Kandula D, Pindolia DK, Smith DL, Cohen JM, Graupe B, Uusiku P, Lourenço C 2014 Integrating rapid risk mapping and mobile phone call record data for strategic malaria elimination planning. *Malaria Journal*, **13**:52

Teklehaimanot A. 1999 *Travel Report to Ethiopia*. Geneva, World Health Organization, (unpublished document).

Teklehaimanot HD, Schwartz J, Teklehaimanot A, Lipsitch M.. 2004. Weather-based prediction of *P.falciparum* malaria in epidemic-prone regions of Ethiopia II. *Malaria Journal* 3: 44.

Trape J. 2001. The Public Health Impact of Chloroquine Resistance in Africa. In The Intolerable Burden of Malaria: A New Look at the Numbers: *American Journal of Tropical Medicine and Hygiene*. Supplement to 64 (1).

Trape JF, Zoulani A 1987 Malaria and urbanization in Central Africa: the example of Brazzaville. Part III: Relationships between urbanization and the intensity of malaria transmission. *Transactions of the Royal Society of Tropical Medicine and Hygiene* **81**, 19-25

Tulu AN, Webber RH, Schellenberg JA, Bradley DJ 1996 Failure of chloroquine treatment for malaria in the highlands of Ethiopia. Trans. R. Soc. Trop. Med. Hyg. 90, 556–557.

Tulu AN. 1993. Malaria In: The ecology of health and disease in Ethiopia. Eds. Kloos H, Zein ZA. Westview Press, Boulder.

Tulu, AN. 1996. Determinants of malaria transmission in the highlands of Ethiopia: the impact of global warming on morbidity and mortality ascribed to malaria. PhD thesis, London School of Hygiene and tropical medicine.

UNPD 2012 World Population Prospect: The 2012 revision http://esa.un.org/unpd/wpp/ (accessed on January 14, 2015)

UNPD 2014 World Urban Prospect: the 2014 revision http://esa.un.org/unpd/wup/ (accessed on January 14, 2015)

USGS (United States Geological Survey) 2014 Modis Vegetation Indices 16-day L3 Global 500m. obtained from site https://lpdaac.usgs.gov/data_access maintained by the NASA Land Processes Distributed Active Archive Center (LP DAAC), USGS/Earth Resources Observation and Science (EROS) Center, Sioux Falls , South Dakota, (accessed on September 12, 2014).

USGS 2011 USGS's Earth Explorer Online System, http://earthexplorer.usgs.gov/ (accessed on March 14, 2011) (ASTER GDEM is a product of METI and NASA).

Venables WN, Ripley BD. 2002. *Modern Applied Statistics*. S. Springer: New York. 1–495

Viboud C, Bjørnstad ON, Smith DL, Simonsen L, Miller MA, Grenfell BT 2006 Synchrony, waves, and spatial hierarchies in the spread of influenza. *Science*. **312**, 447-451.

Visser BJ, Wieten RW, Kroon D, Nage IM, Bélard S, van Vugt M, Grobusch MP. 2014. Efficacy and safety of artemisinin combination therapy (ACT) for non-falciparum malaria: a systematic. *Malaria Journal.* 13, 463.

Vittor AY, Gilman RH, Tielsch J, Glass G, Shields T, Lozano WS, Pinedo-Cancino V, Patz JA 2006 The effect of deforestation on the human-biting rate of anopheles darlingi, the primary vector of falciparum malaria in the peruvian amazon. *Am. J. Trop. Med. Hyg*. **74**, 3–11

White GB 1980 Malaria vector capacity of Anopheles arabiensis and An. quadriannularis in Ethiopia: Chromosomal interpretation after 6 years storage of field preparations. *Trans. R. Soc. Trop. Med. Hyg.* **74**, 683–684.

White, DA; Surface-Evans, SL (2012 *Least Cost Analysis of Social Landscapes: Archaeological Case Studies*. University of Utah Press.

WHO (World Health Organization) 2005 *World Malaria Report 2005.* World Health Organization and UNICEF. Geneva. Switzerland.

WHO (World Health Organization). 2013 *World Malaria Report 2013.* World Health Organization. Geneva. Switzerland.

WHO (World Health Organization). 2014 *World Malaria Report 2014*. World HealthOrganization. Geneva. Switzerland.

WHO, 1997. Jay A. Rozendaal.Vector control: Methods for use by individual communities. World HealthOrganization. Geneva. Switzerland.

Yohannes M , Haile M, Ghebreyesus TA, Witten KH, Getachew A, Byass P, Lindsay SW. 2005. Can source reduction of mosquito larval habitat reduce malaria transmission in Tigray, Ethiopia? *Tropical Medicine and International Health*. **10** ,1274–1285.

Yukich JO, Taylor C, Eisele TP, Reithinger R, Nauhassenay H, Berhane Y, Keating J. 2013. Travel history and malaria infection risk in a low-transmission setting in Ethiopia: a case control study. *Malaria Journal,* **12**:33

Zhou G, Minakawa N, Githeko AK, Yan G, 2004 Association between climate variability and malaria epidemics in the East African highlands. *Proc. Natl. Acad. Sci. U.S.A.* **101**, 2375–2380.